CLASS VI PERMIT APPLICATION NARRATIVE
40 CFR 146.82(a)

One Earth CCS

Project Background and Contact Information

The One Earth CCS project entails the capture of carbon dioxide (CO_2) from the One Earth Energy, LLC, ethanol plant in Gibson City, IL, transport of the CO_2 by pipeline approximately 5 miles west, and geological storage of the CO_2 in strata of the Mt. Simon Sandstone. The One Earth Energy ethanol facility annually produces about 460,000 metric tonnes (Mt) of CO_2 associated with the fermentation of corn to produce ethanol, all of which will be captured for storage.

One Earth CCS is designed as a carbon storage hub for the region and can accept additional CO_2 from sources to be determined. Three CO_2 injection wells are planned for One Earth CCS, each capable of storing 30 Mt of CO_2 with injection taking place over 20 years or longer.

Construction of capture and compression equipment for the One Earth Energy plant is expected to commence in late 2022 to early 2023. Injection activities would commence upon completion and approval of all UIC Class VI permit requirements.

One Earth Sequestration, LLC, will own and operate and be the permit holder of the three injection wells: Injection well OES #1, OES #2, and OES #3.

Contact for the One Earth CCS project is:

Mark Ditsworth, VP of Technology and Special Projects
One Earth Sequestration, LLC
202 N Jordan Drive, Gibson City
(217) 784-5321 ext. 215
mditsworth@oneearthenergy.com

A characterization well, OEE #1, was drilled in 2022 to evaluate the geological formations at the One Earth CCS site and which provides site-specific data used within the permit submissions. The supporting documentation was prepared in accordance with the U.S. Environmental Protection Agency's (US EPA's) *UIC Control Program for Carbon Dioxide Geologic Sequestration Wells* (The Geological Sequestration [GS] Rule, codified in Title 40 of the Code of Federal Regulations [40 CFR 146.81 et seq.]).

OEE #1 was drilled as part of a US DOE-sponsored CarbonSAFE Phase III project, the Illinois Storage Corridor, managed by the Illinois State Geological Survey (ISGS) of the University of Illinois. The ISGS led the first US demonstration of CCS via the Illinois Basin – Decatur Project (IBDP) at the Archer Daniels Midland (ADM) facility in Decatur, IL. This project led to the first

Underground Injection Control (UIC) Class VI approvals for saline storage at the IBDP site and the subsequent commercial injection project, IL-ICCS, also at ADM in Decatur, IL. The same geological formations used at the Decatur sites for storage and containment are being proposed for the One Earth CCS site.

Pending subsequent approval, OEE #1 will be converted to an in-zone monitoring well for the storage project.

Neither an injection depth waiver nor an aquifer exemption expansion is being requested.

There are no federally recognized Native American tribal lands or territories within the proposed Area of Review (AoR).

GSDT Submission - Project Background and Contact Information
GSDT Module: Project Information Tracking ***Tab(s):*** General Information tab; Facility Information and Owner/Operator Information tab Please use the checkbox(es) to verify the following information was submitted to the GSDT: **x** Required project and facility details ***[40 CFR 146.82(a)(1)]***

Site Characterization

Regional Geology, Hydrogeology, and Local Structural Geology [40 CFR 146.82(a)(3)(vi)]

Injection and Confining Zones

Mt. Simon Sandstone Storage Complex

The term storage complex is used in this document to describe the geologic system comprising the storage reservoir and confining strata. The storage complex proposed for One Earth CCS is the Mt. Simon Storage Complex which includes the Cambrian Mt. Simon Sandstone as the primary storage reservoir and the Cambrian Eau Claire Formation as the primary confining strata. The stratigraphic relation of these formations is shown in Figure 1. These strata occur near the base of the intracratonic Illinois Basin, which is greater than 6,900 ft (2,100 m) deep in the region of the One Earth CCS site. The Eau Claire Formation appears to be an effective regional seal, and the site does not require secondary confinement. In addition to the Eau Claire, multiple strata within the Knox Group, Platteville Group, Trenton Limestone, and Maquoketa Group have low permeability and porosity that would serve as effective barriers to the vertical movement of fluids.

Injection Zone

The Illinois State Geological Survey (ISGS) subdivides the Mt. Simon Sandstone into lower, middle, and upper units. In all subdivisions, the lithology of the Mt. Simon Sandstone is dominantly quartz sandstone with components of siltstone, shale, and subarkose to arkose (Freiburg et al., 2014, 2015). The mineralogy is dominantly quartz with minor components of feldspar and clay minerals, mainly illite. Regionally, the lower and upper Mt. Simon units generally have porosity and permeability characteristics suitable for injection of fluids, whereas the middle has poorer reservoir quality.

A characterization well, OEE #1, was drilled 4 miles west of the One Earth Energy ethanol facility near Gibson City, IL, to characterize the Mt. Simon Sandstone reservoir and Eau Claire Formation seal capability in this area (Figure 1). OEE #1 was drilled to a total depth of 7,104 feet (2,165 m) measured depth (MD) and terminated in the Precambrian basement. The formation tops from OEE #1 are presented in Table 1.

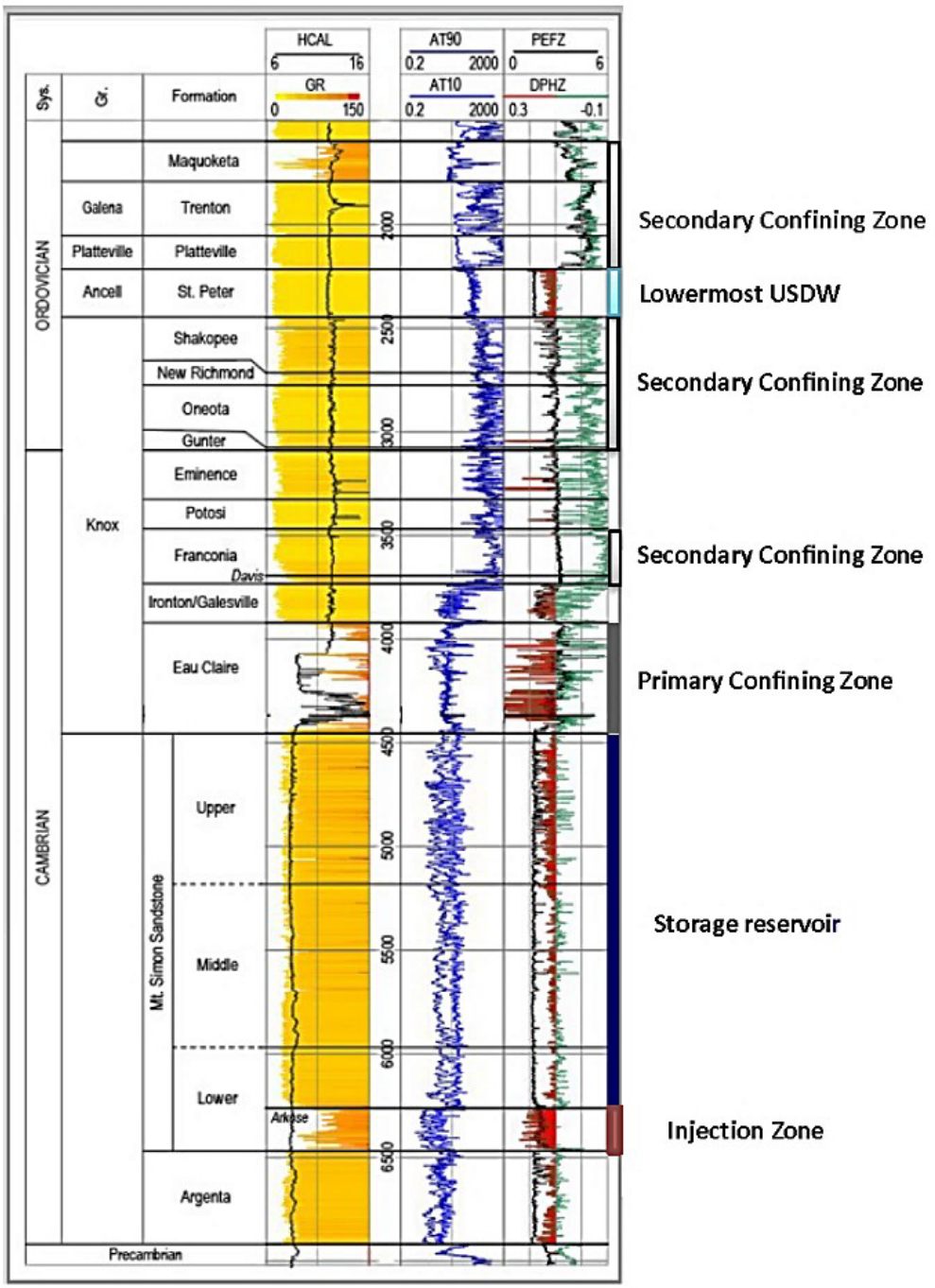

Figure 1. *Geophysical log traces from the One Earth #1 well displayed relative to the stratigraphic classification of the Cambrian and Ordovician Systems in Illinois. The Mt. Simon Storage Complex comprises the Mt. Simon Sandstone as the storage reservoir and the Eau Claire Formation as the primary confining zone. The injection zone is in the Arkose interval within the lower Mt. Simon Sandstone. Secondary confining strata are also indicated above the Eau Claire Formation. The lowermost USDW is the St. Peter Sandstone.*

Table 1. *Selected formation tops from the One Earth Energy #1 well, McLean County, Illinois. Formation thickness and measured depth are listed, along with average porosity, permeability, and total shale thickness values obtained from log analyses. The Eau Claire Formation is divided into three parts to aid OEE #1 well log and sample analyses discussed herein.*

Formation Name	Thickness (ft)	Top Depth (ft)	Elevation (ft SS)	Ave Porosity (%)	Ave Perm (mD)	Shale Thickness (ft)
New Albany Shale	150	753	88	15	0.011	149
Silurian	696	903	-62	10.8	1.01	48.5
Maquoketa Group	194	1,598	-757	9.2	0.002	177.5
Trenton Limestone	261	1,792	-951	3.6	0.009	1
Platteville Group	164	2,053	-1,212	2.1	0.00017	3
St. Peter Sandstone	232	2,217	-1,376	10.4	147.7	0
Shakopee Dolomite	266	2,449	-1,608	6.5	0.095	32.5
New Richmond Sandstone	43	2,715	-1,874	9.7	3.5	0.5
Oneota Dolomite	317	2758	-1,917	8.1	2.43	7.5
Gunter Sandstone	15	3,075	-2,234	11	86.7	0
Eminence Formation	236	3,090	-2,249	5.9	0.25	0
Potosi Dolomite	142	3,326	-2,485	5.2	0.23	1.5
Franconia Formation	206	3,468	-2,627	3.4	0.051	5
Davis	59	3,674	-2,833	4.2	0.004	22.5
Ironton Sandstone	120	3,733	-2,892	8.0	3.57	0
Galesville Sandstone	68	3,853	-3,012	10.3	43.57	0
Eau Claire Formation	534	3,921	-3,080	8.2*	0.006*	195*
(Eau Claire shale)	123	4,245	-3,404	8.0	0.017	123
(Elmhurst Sandstone member)	87	4,368	-3,527	8.7	0.37	38
Mt. Simon Sandstone (upper)	767	4,455	-3,614	11.2	26.7	94
Mt. Simon (middle)	747	5,222	-4,381	9.5	10.6	74
Mt. Simon (lower)	293	5,969	-5,128	8.9	6.2	33
Arkose interval	207	6,262	-5,421	14.4	87.2	-
Argenta (pre-Mt. Simon)	449	6,469	-5,628	8.5	2.2	79.5
Precambrian (undifferentiated)	22	6,918	-6,077	3.8	0.0003	-
Precambrian Rhyolite	38	6,940	-6,099			
Precambrian Granite		6,978	-6,137			

At OEE #1 the Mt. Simon occurs at 4,455 feet (1,358 m) MD and is 2,014 feet (614 m) thick. Within the lower Mt. Simon Sandstone are sandstones having an arkosic lithology that are the target injection zone for the One Earth CCS project. These beds are informally referred to as the Arkose (or "arkosic zone"). At OEE #1 the Arkose interval top is at 6,262 ft MD and is 207 ft thick. The salinity of Mt. Simon Sandstone formation water collected by two drill stem tests at 6,361 feet (1,939 m) MD in well OEE #1 were 166,000 mg/L and 165,500 mg/L. The properties of the storage and confining strata are described in the INJECTION AND CONFINING ZONE DETAILS section.

The Arkose interval can be traced extensively across the central Illinois Basin and this interval is used for CO_2 injection at the IL-ICCS project in Decatur, IL. Figure 2 presents a cross-section of the subdivisions within the Mt. Simon Sandstone from the Furrow #1, 27 miles northwest of OEE #1 to Hinton #7, 15 miles south of OEE #1. The cross-section also shows that similar characteristics are present in two deep wells approximately 40 to 55 miles southwest of OEE #1 at the VW #1 well in Decatur, IL, and McMillen #2 well in Christian County, IL, respectively.

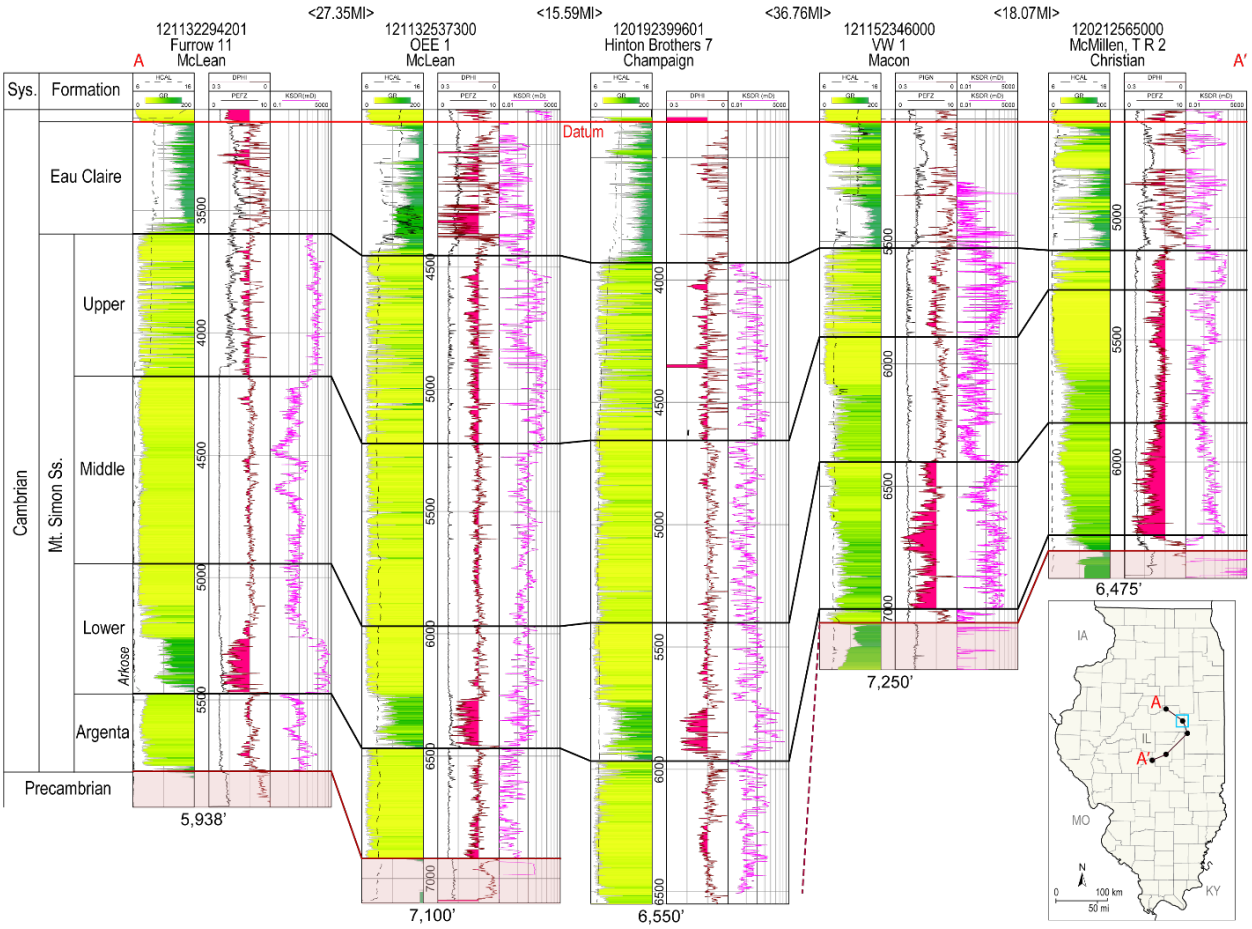

Figure 2. *North to south stratigraphic cross-section displaying the correlation of the Mt. Simon Sandstone in central Illinois. The blue box indicates the general area of the One Earth CCS project.*

The Mt. Simon is unconformably underlain by the basal Cambrian Argenta Formation (formerly called the pre-Mt. Simon), a sedimentary unit that is composed of shallow marine (Freiburg et al., 2015) and fluvial clastic deposits and unconformably overlies Precambrian felsic rocks of the Granite Rhyolite Province (Freiburg et al., 2016). The Argenta Formation underlies the Mt. Simon Sandstone in the central Illinois Basin and was considered part of the Mt. Simon until recently; the two units are typically mapped together by the ISGS at regional scale (Figures 2 & 3). At OEE #1, the top of the Argenta Formation is at 6,469 feet (1,972 m) MD, and the combined thickness of the Mt. Simon and the underlying Argenta is 2,463 feet (751 m), Figure 3.

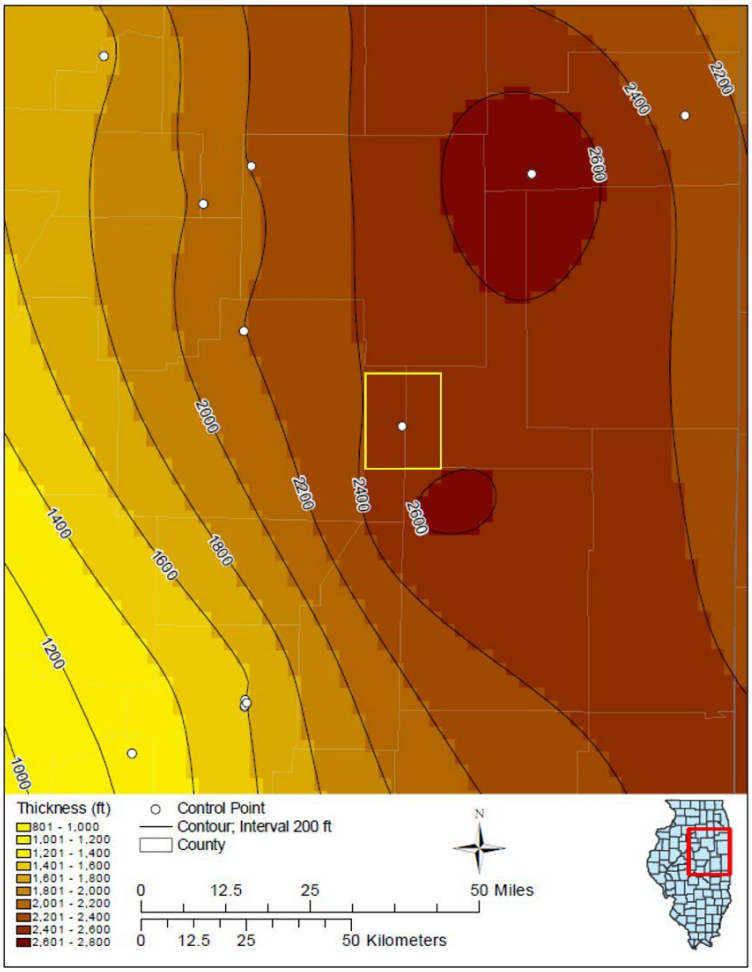

Figure 3. *Regional isopach map shows combined thickness of Mt. Simon Sandstone and Argenta sandstone. Yellow box outlines the general area of the One Earth CCS project.*

Primary Confining Zone

The Eau Claire Formation is the primary confining unit of the Mt. Simon Storage Complex. The Eau Claire Formation is a thick succession of fine-grained clastic rocks that underlies all of Illinois and has lithologies that include shale, siltstone and fine sandstone and carbonate (Buschbach, T. C., 1964).

At the OEE #1 well the Eau Claire Formation occurs at 3,921 feet (1,195 m) depth and is 534 feet (163 m) thick (Figure 4). The formation may be subdivided, and at OEE #1 there is a 123-foot (37 m) thick succession of shale from 4,245 to 4,368 feet (1,294 to 1,331 m) MD known regionally as the Eau Claire shale and which serve as impermeable beds preventing upward movement of fluids. The clay mineralogy of the Eau Claire shale is dominantly illite. The basal member of the Eau Claire Formation, known as the Elmhurst Sandstone, is gradational with the underlying Mt. Simon Sandstone. At One Earth CCS the Elmhurst occurs at 4,368 ft (1,331 m) MD and is 87 feet (27 m) thick and consists of a lower fine-grain sandstone that fines upward into siltstone interbedded with shale and mostly shale in the upper portion. The properties of the Eau Claire Formation are described in the INJECTION AND CONFINING ZONE section of this narrative.

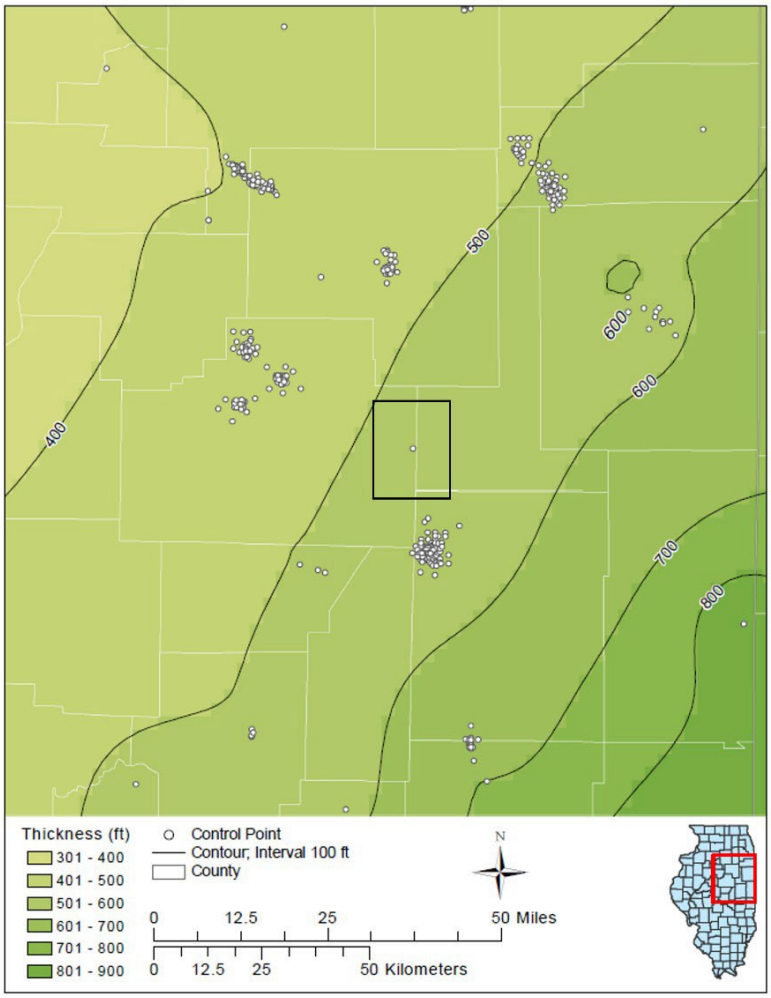

Figure 4. *Regional thickness of the Eau Claire Formation. Black box indicates the general area of the One Earth CCS Project encompassing the AoR.*

Secondary Confining Zones

Knox Group

The Knox Group is a regionally extensive and thick sequence of mainly carbonate rock that includes the Eau Claire Formation and overlying strata to the top of the Shakopee Formation. At OEE #1 the Knox Group is 1,920 feet (585 m) thick (Figure 5). Above the Eau Claire, thick dolomitic sequences within the Knox Group, including the Potosi Dolomite, Eminence Formation, and Oneota and Shakopee Dolomites, can serve as secondary confining zones (Figure 1). The confining zones are generally micro- to fine-crystalline dense dolomite having little to no porosity or permeability.

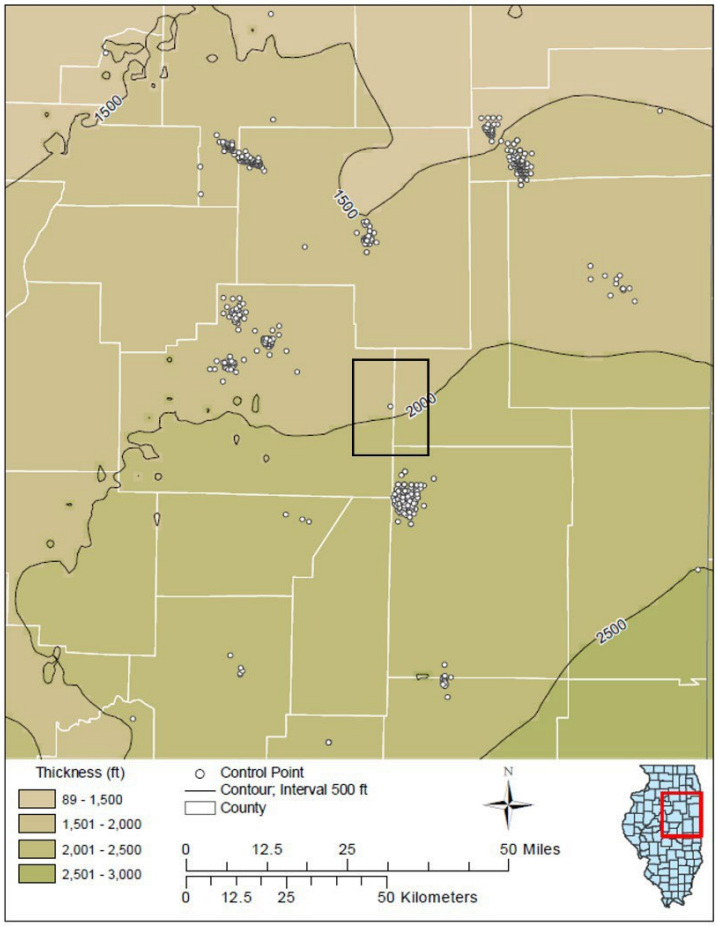

Figure 5. *Isopach (thickness) map of the Knox Group indicating its regional distribution. The general area of the One Earth CCS project encompassing the AoR is highlighted.*

Directly above the Knox Group is the St. Peter Sandstone that is the lowermost Underground Source of Drinking Water (USDW) at One Earth CCS (Figure 1). The St. Peter Sandstone is a pure quartz sand that occurs at 2,217 ft (MD) (676 m) and is 232 ft (71 m) thick at OEE #1. A DST in OEE #1 recovered formation water from the St. Peter Sandstone that has a total dissolved solids (TDS) concentration of 1779 mg/L. The St. Peter Sandstone is described in detail in the HYDROLOGIC AND HYDROGEOLOGIC INFORMATION section of this narrative.

Maquoketa Shale

The Ordovician Maquoketa Shale Group is a laterally continuous, impermeable confining zone present at the One Earth CCS site. At OEE #1 the top of the Maquoketa is at 1,598 feet (487 m) deep, and the formation is 194 feet (59 m) thick (Figure 1). The upper unit of the Maquoketa is dominated by dolomitic and calcitic shale and silty shale; the middle unit is dominated by limestone and muddy limestone; and the lower unit is dominated by dolomitic and calcitic shale and occasionally contains minor amounts of muddy limestone and silty shale.

New Albany Shale

The Devonian-Mississippian New Albany Shale Group is a thick, impermeable, and laterally continuous shale formation which acts as a seal regionally. The One Earth CCS project vicinity is

near the northern erosional limit of the New Albany Group. At OEE #1 the top of the New Albany is at 753 feet (230 m) MD and is 150 feet (45 m) thick.

General Geologic History

The One Earth CCS project is sited within the Illinois Basin, an intracratonic basin that formed during the early Paleozoic. The Illinois Basin (Figure 6) is bordered by a series of prominent structures (Kolata and Nelson, 1990), including the Kankakee Arch to the northeast, the Cincinnati Arch to the east, the Mississippi River Arch to the northwest, the Ozark Dome to the southwest, and the Nashville Dome to the southeast. The New Madrid Rift System, including the Rough Creek Graben and Reelfoot Rift, extends into the southernmost part of the Basin.

The arches and domes surrounding the Illinois Basin are structural features that contributed to the basin's evolution and extent. The Ozark Dome is a long-lived uplift cored by low-density granites and rhyolites (Nelson, 2010). The Kankakee Arch formed in Ordovician time (Nelson, 2010), and the Mississippi River Arch formed somewhat later after Early Pennsylvanian time (Nelson, 2010). The Cincinnati Arch is a long-lived high with uplift episodes in both the Devonian and the Carboniferous periods (E. O. E. B. (n.d.-a)). The Nashville dome is considered a southward geologic extension of the Cincinnati Arch (E. O. E. B. (n.d.-b)). The Pascola Arch is "partly responsible for closing off the southern end of the Illinois Basin." (Nelson, 2010). This arch probably developed in Late Pennsylvanian and Permian time (Nelson, 2010). These structural features have all helped to define the limits of the Illinois Basin.

Precambrian crystalline rocks form the basement of the Illinois Basin. The oldest sedimentary rocks in the Basin are the Middle Cambrian Mt. Simon Sandstone, which contains the injection zone for this project, and the Argenta sandstone, a stratigraphic unit that underlies the Mt. Simon in the central part of the basin (Freiburg et al., 2015). The Mt. Simon system was deposited over much of the current North American midcontinent in depositional environments including fluvial, eolian, and marginal marine (Freiburg et al., 2014; Reesink et al., 2020). Precambrian topography exerted substantial control over both the thickness and lithology of Mt. Simon deposits, including shedding the feldspars that helped create high porosity arkosic zones.

The Mt. Simon Sandstone is conformably overlain by the Eau Claire Formation which is the primary confining zone for the Mt. Simon Storage Complex. The Eau Claire is the basal unit of the Knox Group. The Knox Group is a thick succession of mostly marine, dominantly carbonate (limestone and dolomite) formations with secondary siltstone, shale, and sandstone components (Figure 1). The Knox Group was deposited across a large swath of the proto-North American continent during the Cambrian and Ordovician (Fritz et al., 2012). Thick, dense dolomites within the Knox (e.g., Oneota and Shakopee formations) are secondary confining zones that occur between the Mt. Simon Storage Complex and the St. Peter Sandstone which is the lowermost USDW (LUSDW).

Post-Knox deposits of the Ancell, Platteville, and Galena Groups (mostly carbonate formations, as well as the LUSDW) are overlain by the Maquoketa Group, a primarily shaly-silty sequence that contain impermeable strata serving as secondary confining zones to the storage site. After Maquoketa deposition, a thick succession of Silurian through Pennsylvanian rocks (dominantly carbonates and shales, with lesser amounts of sandstone) were deposited in the central Illinois area.

These units include the Devonian-Mississippian New Albany Shale Group (see INJECTION and CONFINING ZONES section) that is an additional secondary confining zone at the One Earth CCS storage site. The shallowest bedrock units in the One Earth CCS area are Pennsylvanian in age that are covered by a few hundred feet of much younger, unconsolidated sediments described in the HYDROLOGIC and HYDROGEOLOGY section.

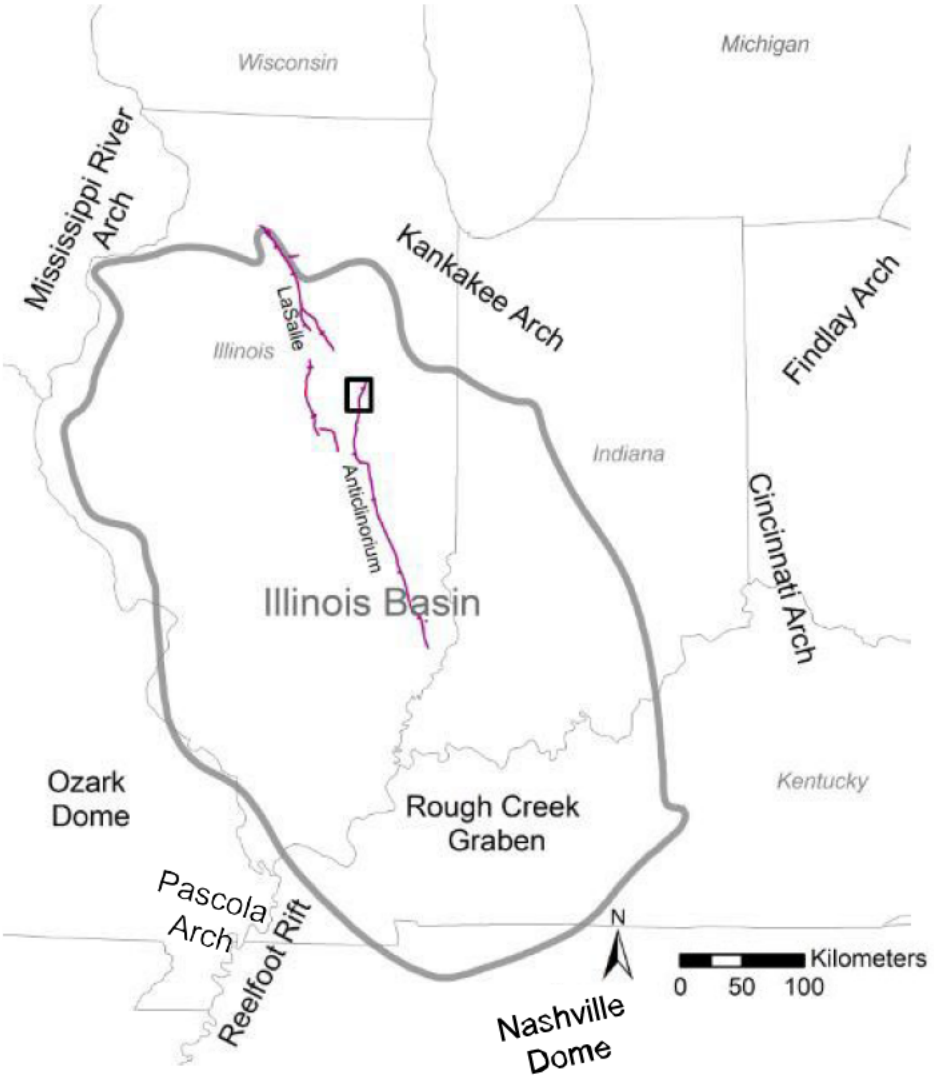

Figure 6. *Regional map of the central United States showing selected structural features within the Illinois Basin and the major structural features that surround it (Finley, 2005).*

Geologic Structures and Tectonic History

The Illinois Basin has been affected by three major tectonic episodes during the Phanerozoic Eon, including Rodinia-related rifting; widespread compressional (reverse) faulting during the assembly of the supercontinent Pangea in the late Paleozoic; and extensional (normal) faulting during the Mesozoic related to Pangea's breakup (Denny et al., 2020).

The most prominent structural feature in the Ford and McLean County area is the La Salle Anticlinorium (Nelson, 1995). The La Salle Anticlinorium is a large upward fold belt comprised of smaller domes, anticlines, monoclines (step-like folds), and intervening synclines; it trends N-S to NE-SW and is about 200 miles (320 km) long by 80 miles (130 km) wide. Major uplift of the La Salle Anticlinorium began during the Late Mississippian and lasted throughout most of Pennsylvanian time (Kolata and Nelson, 1990).

Two structural features associated with the anticlinorium, the Osman Monocline and Colfax Syncline, are near the area of the storage site (Figure 7). No deep faults are known within a 25-mile radius of the proposed site (Nelson, 1995). The nearest known major fault zone is the 85-mile-long (137 km) Sandwich Fault Zone, approximately 65 miles (105 km) north of One Earth CCS (Nelson, 1995).

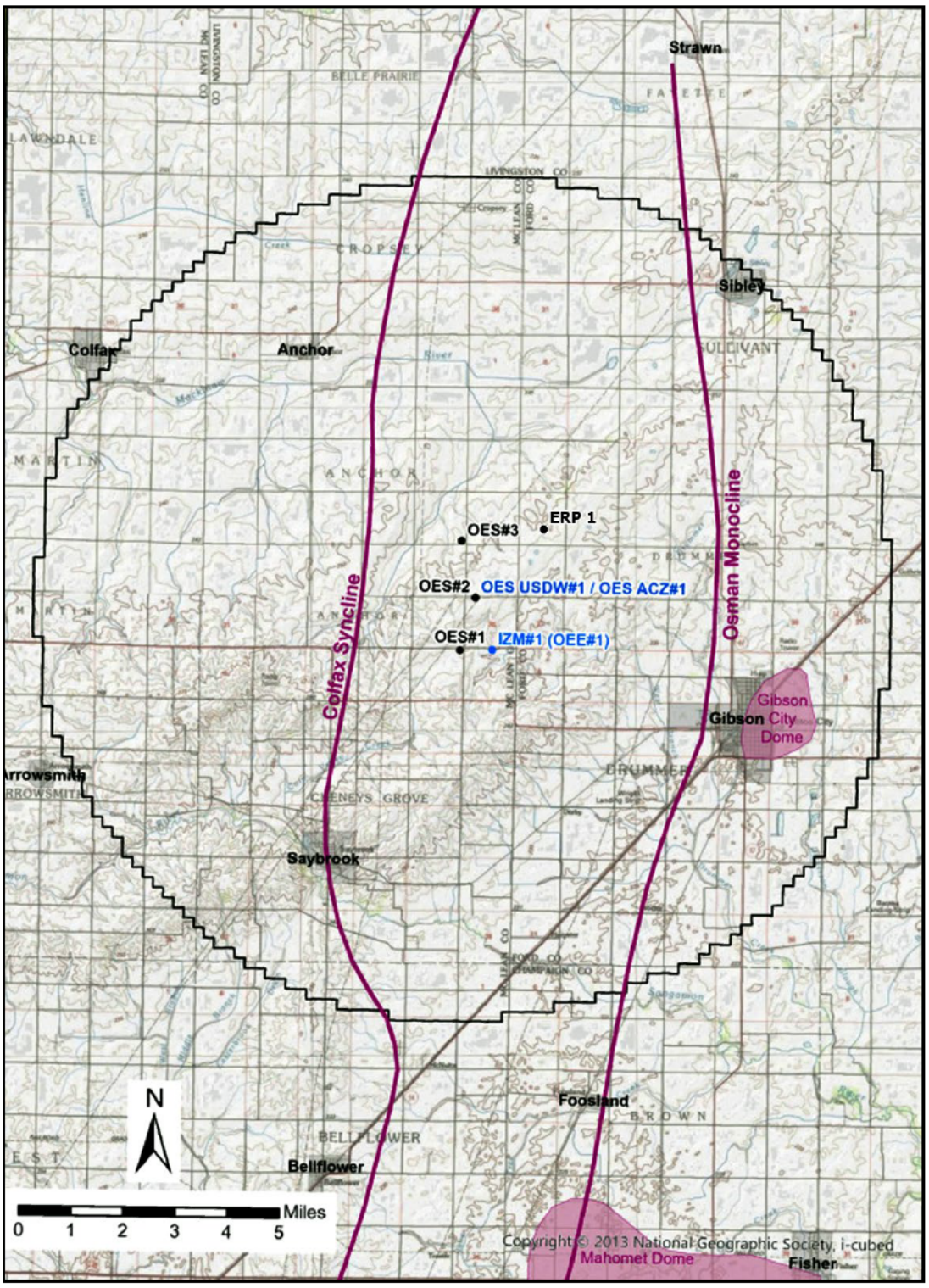

Figure 7. *Map showing projected locations of geological structural features (Nelson 1995) near Gibson City, in the vicinity of proposed well locations. The features shown (Colfax Syncline and Osman Monocline) are part of the La Salle Anticlinorium. Existing or planned project wells are located in the center of the map and labeled in larger bold print. The black circle is predicted area of review (AoR).*

Maps and Cross Sections of the AoR [40 CFR 146.82(a)(2), 146.82(a)(3)(i)]

Figure 8 shows the AoR for One Earth CCS based on differential pressure front after 20 years of injection, overlain on a topographic map of the immediate area around the project wells. This is the maximum extension of AoR in the project timeframe. The delineation of the AoR is described in the AoR and CORRECTIVE ACTION PLAN.

The injection zone and confining zone for the One Earth CCS project both extend laterally beyond the AoR limits. This is demonstrated by the regional thickness maps (Figures 3 and 4) and the cross-section shown in Figure 2 in the REGIONAL GEOLOGY section of this narrative. The strata are of generally consistent thickness with no evidence of stratigraphic pinch-out in the region. Additionally, there is no indication of structural trapping by faults or domes within the AoR.

2D seismic data indicates small offset faults may be present within the northeastern portion of the AoR. The faults transect the Mt. Simon Sandstone and the Eau Claire Formation and are associated with the Osman Monocline, and they are more than 3 miles east of the predicted maximum extent of the CO_2 plume. The small faults are predicted to be sealing based on the low throw of the faults, V_{shale} content, and ductile nature of the Eau Claire Formation and will not compromise containment. Other small faults identified within the AoR extend into the Argenta Sandstone or lowermost Mt. Simon Sandstone and do not reach the Eau Claire Formation so that containment is not impacted. No potential conduits for CO_2 to migrate out of the Mount Simon reservoir were identified in the AoR of the One Earth CCS storage site.

Information concerning the faults and fractures and their spatial relation to the injection wells is discussed in the FAULTS and FRACTURES section of this document.

The St. Peter Sandstone is the lowermost USDW present within the AoR and is 1,472 ft (449 m) above the top of the Eau Claire confining beds at OEE #1. There are no structural features or faults observed to intersect the St. Peter Sandstone in the AoR. As described in the REGIONAL GEOLOGY section there are several secondary confining zones within the Knox Group between the Eau Claire Formation and the St. Peter Sandstone in the AoR.

A total of 573 wells and borings are located within the AoR (Figure 8) as determined using the ISGS Wells and Borings Database supplemented by ISGS coal mine information. The resultant table detailing the identifying information, location, depth, and status of these wells and borings was uploaded to the GSDT tool.

Water wells are the main well type and account for 484 of the documented wells. Domestic, city, and industrial water wells average a depth of 120 feet (37 meters) with only 15 water wells exceeding 300 feet (91 meters) to a maximum depth of 400 feet (122 meters).

Additional wells and borings within the AoR include 34 oil and gas wells, along with 55 other penetrations including stratigraphic test wells, engineering borings, coal test holes, and one documented coal mine shaft located southeast of Anchor, IL, in McLean County. Of the total 89 non-water wells and borings identified within the AoR, two wells were completed to depths between 2,000 and 3,000 feet (610 and 914 meters). One well (API: 120530000100 and re-

drill/deepening API: 120530000102) has a TD within the Eau Claire Formation confining zone: the Erp #1 well, which was drilled for oil to a depth of 4,250 feet (1,295 meters) in the early 1940s, has a status of Dry and Abandoned.

The only well that fully penetrates the Eau Claire Formation caprock in the AoR is the OEE #1 stratigraphic test well drilled to characterize the One Earth CCS site.

Six additional wells are planned as part of injection and monitoring operations as described in the TESTING and MONITORING PLAN. Three injection wells, OES#1, OES #2, and OES #3 will reach the lower Mt. Simon Sandstone and fully penetrate the Eau Claire Formation. OES#2 will be drilled 1.05 miles north of OES#1, and OES#3 will be drilled 1.12 miles north of OES #2 (Figure 8). Two monitoring wells will be co-located near OES#2. Monitoring well OES USDW #1 is planned to be completed in the St. Peter Sandstone LUSDW and monitoring well OES ACZ #1 and OES ACZ #2 will be completed immediately above the Eau Claire Formation in the Ironton-Galesville Sandstone. OEE #1 is planned to be converted to an in-zone monitoring well. A second in-zone injection well will be drilled within the AoR after injection commences.

Other historical coal test holes potentially not captured in the queried data sources are unlikely, but, if present, they would be less than 600 feet (183 meters) deep based on the regional trend of coals mapped through the area. Regional maps were checked for the presence of surface or underground extraction sites for sand & gravel or industrial minerals (Miao, 2016) and none were found to be located within the AoR.

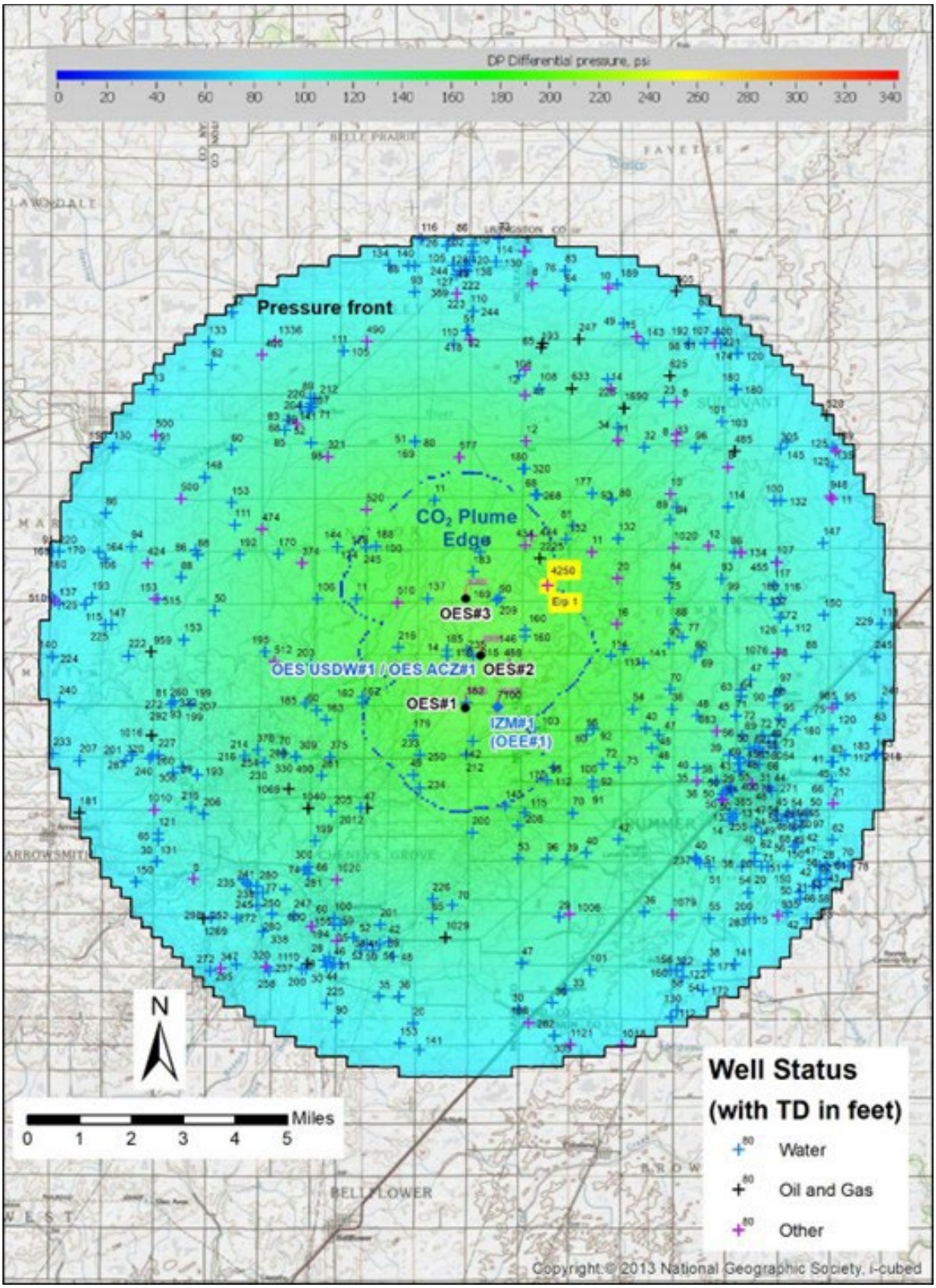

Figure 8. *Water, Oil/Gas, and Other wells & borings located within the Area of Review (AoR). Well data are from Illinois State Geological Survey databases. USGS topographic map base shows land surface features, water bodies, and infrastructure through the area. Existing or planned project wells are located in the center of the map and labeled in larger bold print.*

Data from the U.S. EPA's Cleanups In My Community (CIMC) database and the Illinois EPA's Site Remediation Program (SRP) database were reviewed and all sites within the proposed One Earth Sequestration (OES) Area of Review (AoR) were plotted (Figure 9). Only one registered site from either database falls within the AoR: the Illinois Bell site in Gibson City, Illinois (U.S. EPA ID ILD980823744). This industrial/commercial property lies within the Gibson City municipal boundary, and a No Further Remediation (NFR) letter was issued on June 26, 2006.

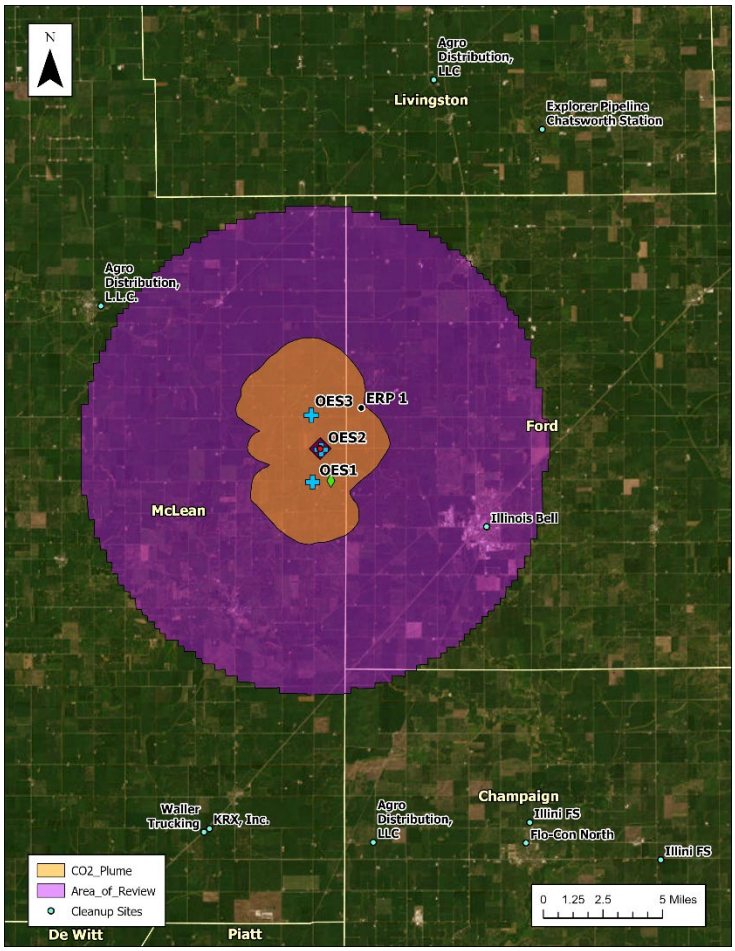

Figure 9. *Location of Illinois Bell cleanup site in Gibson City, IL, also showing the OES AoR (purple), CO_2 plume (orange), proposed injection wells (blue crosses). Data was sourced from the U.S. EPA (https://map22.epa.gov/cimc/) and IL EPA (https://epa.illinois.gov/topics/cleanup-programs/bol-database/srp.html).*

Faults and Fractures [40 CFR 146.82(a)(3)(ii)]

Evidence for Faults and Fractures

Within the Area of Review (AoR) four 2D seismic lines were available to evaluate the structure and stratigraphy of the One Earth CCS area (Figure 10). Stratigraphic tops and sonic and density logs from the OEE #1 well were used to construct a synthetic seismogram to correlate well data to the 2D seismic data. Figure 10 shows the well tie of OEE #1 to east-west Line 7 and seismic reflectors labeled corresponding to the well stratigraphy. One small offset fault is identified on this

line that terminates within the lower Argenta just above the Precambrian unconformity. No other faults are observed on this line.

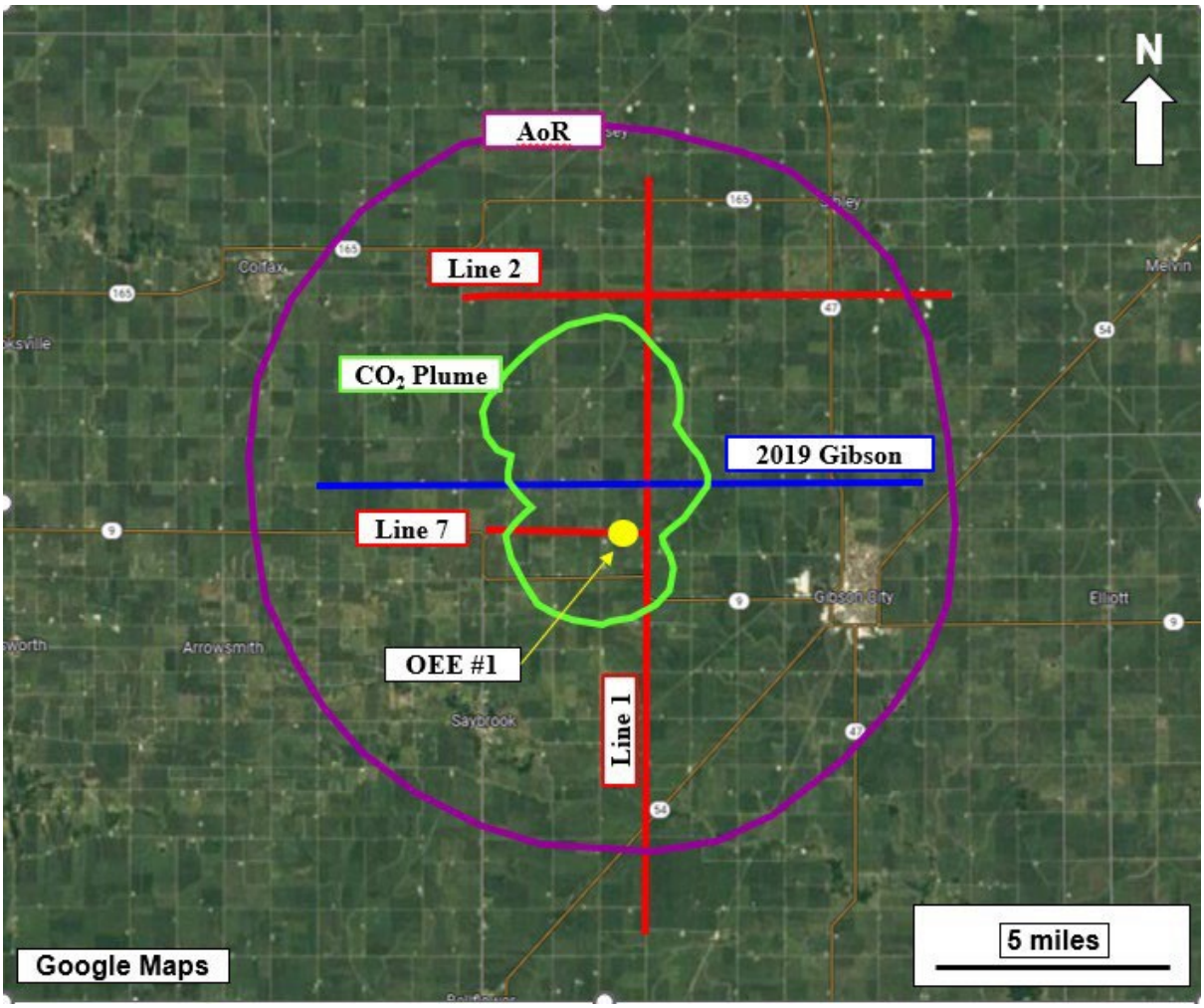

Figure 10. *Base map of the One Earth CCS area showing the location of the four seismic lines (in red and blue), OEE #1 well (yellow), AoR (purple), and predicted CO_2 plume maximum extent (green). Note the AoR and CO_2 plume outlines have been generalized.*

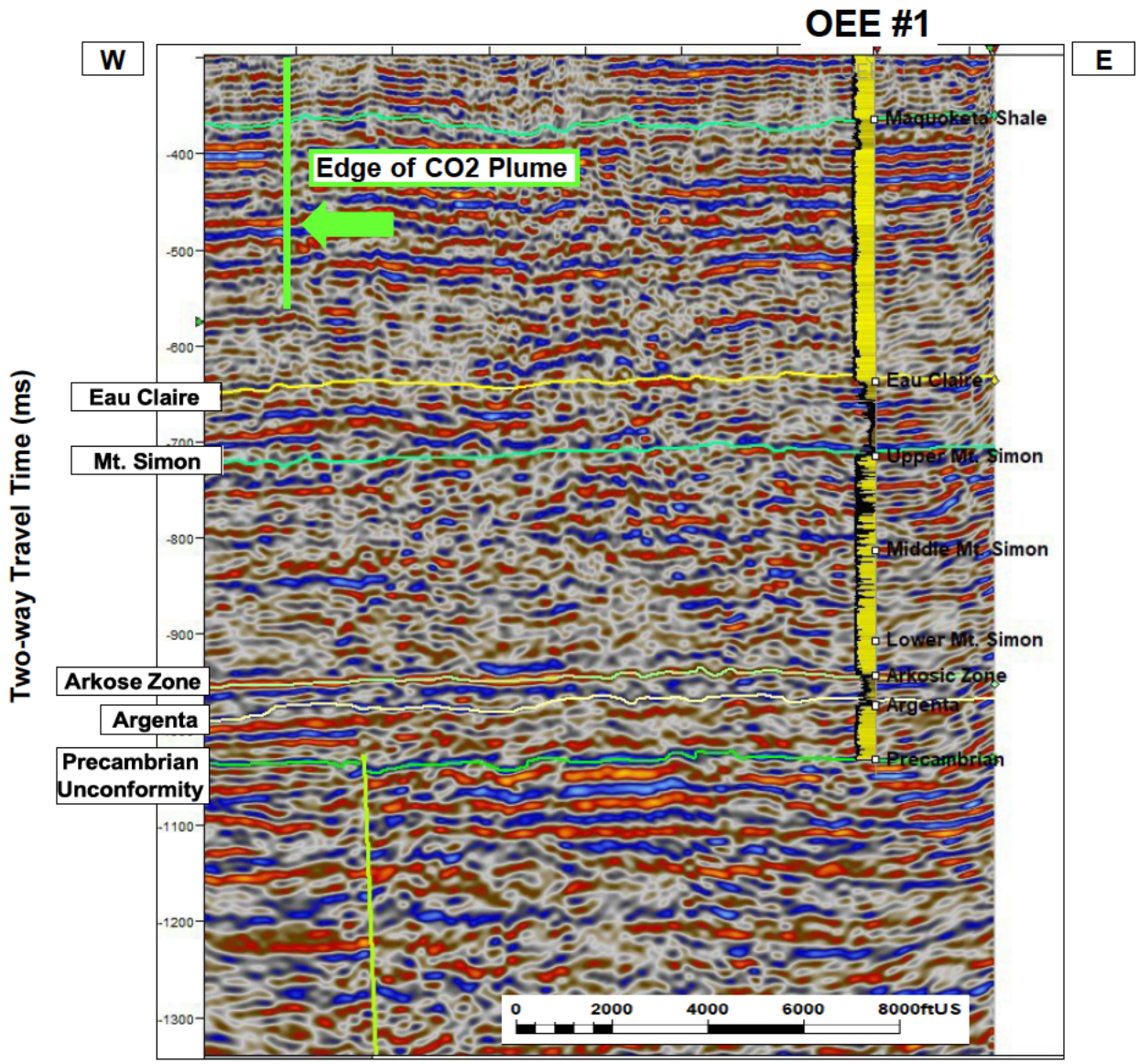

Figure 11. *Seismic Line 7 shows the OEE #1 well with stratigraphic tops correlated to specific seismic reflectors. The single mapped fault does not reach the Mt. Simon Sandstone.*

Figure 12 displays the interpreted east-west 2019 Gibson seismic line. Five high angle faults with interpreted offsets of 50-150 feet (15-46 m) are observed on the east side of the line. The fault identified in dark blue terminates in the Argenta Sandstone, whereas the green fault terminates in the lower Mt. Simon Sandstone. The other faults identified by light blue, orange, and magenta are within the Precambrian basement.

Figure 13 shows north-south Line 1, which displays five high angle faults having similar offsets and terminations as observed in the 2019 Gibson line. In Line 1 there are no faults observed transecting the Mt. Simon storage reservoir, nor any resolvable faults present in the Eau Claire primary confining zone.

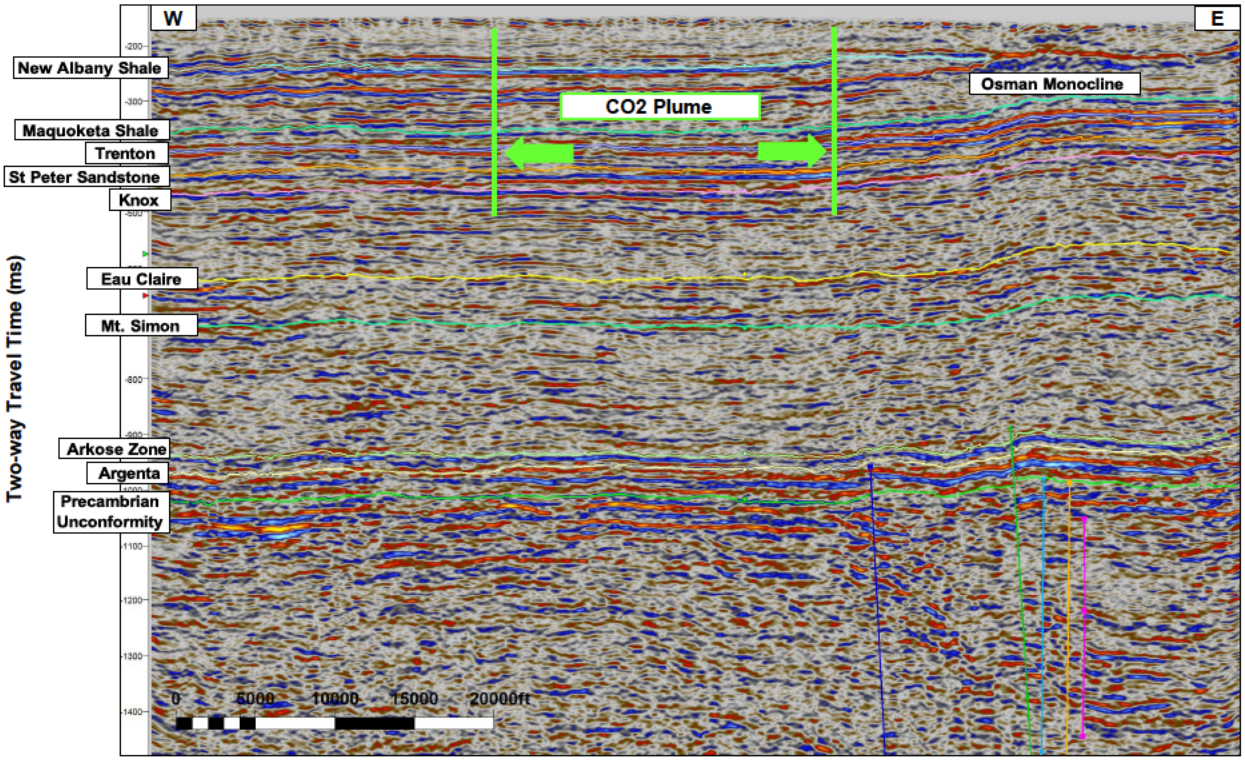

Figure 12. *Seismic line Gibson 2019 showing faulting in the Precambrian, Argenta, Arkose interval, and lower Mt. Simon. The interpreted faults do not reach the primary seal Eau Claire formation.*

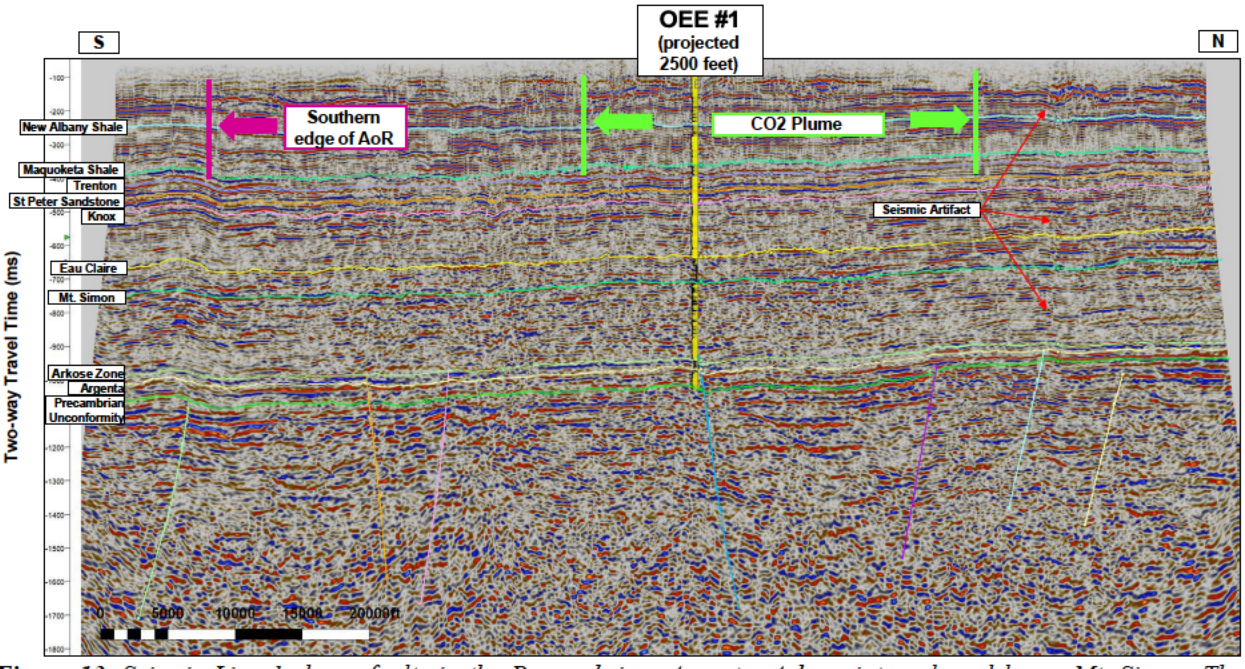

Figure 13. *Seismic Line 1 shows faults in the Precambrian, Argenta, Arkose interval, and lower Mt. Simon. The interpreted faults do not reach the primary seal Eau Claire formation. Vertical lineation visible from near surface down to lower Mt. Simon is interpreted as a seismic artifact resulting from a shallow anomaly.*

The remainder of the seismic Line 1 to the south traverses through another glacial valley but likely sees much more gradual changes in glacial sediment thickness, and therefore the seismic

processing was able to correctly image the subsurface, unlike the narrower valley at the northern end of the line that had much more abrupt thickness changes.

Another item to note is that the zone of disturbed seismic reflectors, while overall vertical, shows some “waviness”. In other words, it is not planar. Faults do not behave in this manner—faults can have broad curvature, but they do not have the kind of high frequency waviness/sinuosity that is visible on the artifact. This is another point of evidence that indicates it is not a fault
Figure 13 shows east-west Line 2. At the eastern side of the seismic profile, the Osman Monocline is observed. Within the core of the Osman Monocline small offset faults are interpreted in the Mt. Simon and Eau Claire Formation.

Near the top of the seismic reflection profile, from a time of zero to about 190 milliseconds (ms), there is a zone of high amplitude, low-frequency disturbed seismic reflectors. Directly beneath this, starting at about 450 ms and going to about 850ms, is a wavy, near-vertical line of disturbed seismic reflectors. These two components make up the seismic artifact.

The source of this seismic artifact is the shallow geology, which consists of varying thickness of glacial sediments. Figure 1 shows a portion of an ISGS map of the glacial drift thickness over the entire state of Illinois (ISGS, 2015). Before the glacial episodes in the Quaternary, this part of Illinois contained a system of large rivers and smaller subsidiary rivers and streams that eroded valleys into the bedrock. During several glacial episodes, these bedrock valleys were filled with glacial sediments, resulting in the flat topography that is present today. The seismic artifact appears to have been caused by the presence of a narrow bedrock valley filled with unconsolidated glacial sediments.

On Figure 14, at the location of the northern end of seismic line 1, note that there is a northwest-trending zone of thick glacial sediments shown by the pink color, which represents thicknesses between 300 and 400 feet. This is a narrow bedrock valley that was filled in with glacial sediments. The presence of this narrow valley alters the paths of the seismic waves during acquisition, which is visible as they are of high amplitude, low frequency reflectors from zero to 190 milliseconds. The seismic processing was not able to completely correct for this, resulting in the zone of wavy disrupted seismic reflectors directly below this valley with localized thick glacial sediments.

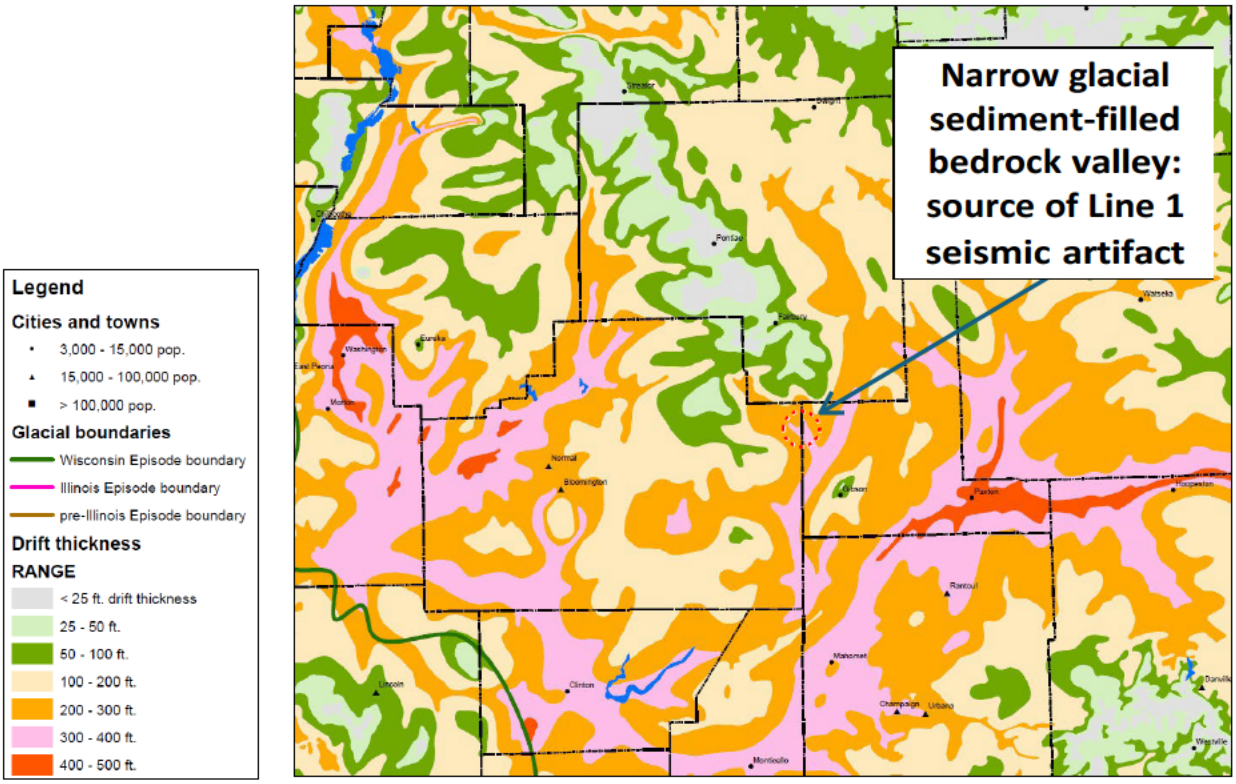

***Figure 14**. ISGS glacial drift thickness map. Source: [Drift Thickness Map | Resources | UIUC]*

As shown in Figure 15 these small faults are located within the AoR but outside of the CO_2 plume. The Osman Monocline and associated faults are interpreted to be oriented north-south (Figure 15).

As part of the detailed subsurface characterization of the area around the OEE #1 characterization well, a 3D seismic survey was acquired in 2022. The survey was intended to characterize the subsurface where a portion of the CO_2 plume will be present during injection.

Similar to the process with the 2D seismic data, a synthetic seismogram was constructed from the log data of the OEE #1 well and tied to the 3D survey at inline 105. The well-tie results give the same tie as the tie to the 2D seismic, confirming that the 2D and 3D interpretations are consistent.

Like the 2D seismic interpretation, the horizons interpreted on the 3D survey include the top of New Albany Shale, top Maquoketa Shale, base Maquoketa Shale/top Trenton, top St. Peter Sandstone, top Shakopee (Knox), top Eau Claire, top Mt. Simon, top Arkose Zone, top Argenta, and top Precambrian.

Mapping of the Arkose Zone, the injection interval, on the 3D survey supports the presence of high porosity within this zone. Across the entire survey, the top of the Arkose Zone is a moderate-to-strong-amplitude, low-impedance, continuous reflector, indicative of its high porosity relative to the overlying Lower Mt. Simon.

The 3D survey revealed generally southwest-dipping stratigraphy with small faults and gentle folds. Figure 11 is the time structure map of the top of the Arkose Zone. Relief on this surface is

caused by both faults and folds. The north/northeast part of the 3D area is a structural high that is related to the Blue Fault (see Figure 12, 13, 14, and 15 in the updated Narrative document). To the southwest is a plunging saddle with lows to the south and west. The deepest reflectors of the 3D seismic is formed in part by a small high-angle reverse fault, which is the east-west trending green fault shown on the west side of the map in Figure 13.

Figure 17 shows the faults mapped on the 3D survey. Most of the mapped faults originate in the Precambrian and tip out in either the Argenta, Arkose Zone, or the Lower Mt. Simon.
Figure 18 shows a north-south crossline through the central part of the east-west trending blue fault, which is the largest fault interpreted on the 3D. This normal fault is about 4,000 feet in length with a maximum throw of approximately 150-200 feet at the Precambrian unconformity.

Figure 19 shows a NW-SE traverse through several faults, highlighting the varied orientations and styles of faults seen on the 3D. The yellow and red faults are high-angle reverse faults, dipping in opposite directions, only 400-1,000 feet apart. A possible explanation for their proximity is that the faults originally formed at separate times in the Precambrian and were then reactivated later in the Paleozoic. Both the red and yellow faults are about 3,000 feet in length, with maximum fault throw of approximately 100 feet. The light and dark blue faults are small high-angle normal faults, and are about 1,800 and 400 feet in length, respectively. The light blue fault has a maximum fault throw of approximately 80 feet, and the dark blue fault, being smaller, has a maximum throw of about 50 feet.

Figure 19 shows another view of the red fault, as well as the larger green fault on the western edge of the 3D survey. Both are high-angle reverse faults. The total length of the green fault is unknown as it continues off the western edge of the survey. Maximum offset of the fault visible on the 3D survey appears to be approximately 100 feet.

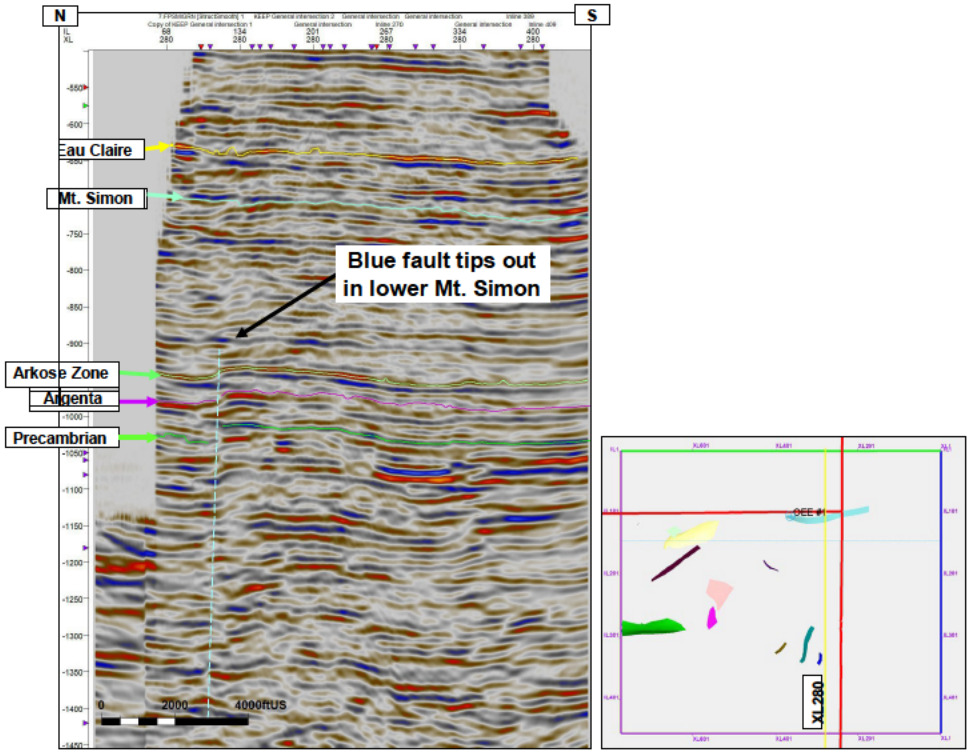

Figure 15 *Crossline 280: 1,700 ft east of OEE #1, showing additional view of Blue Fault as well as the seismic character of the Paleozoic and Precambrian sections.*

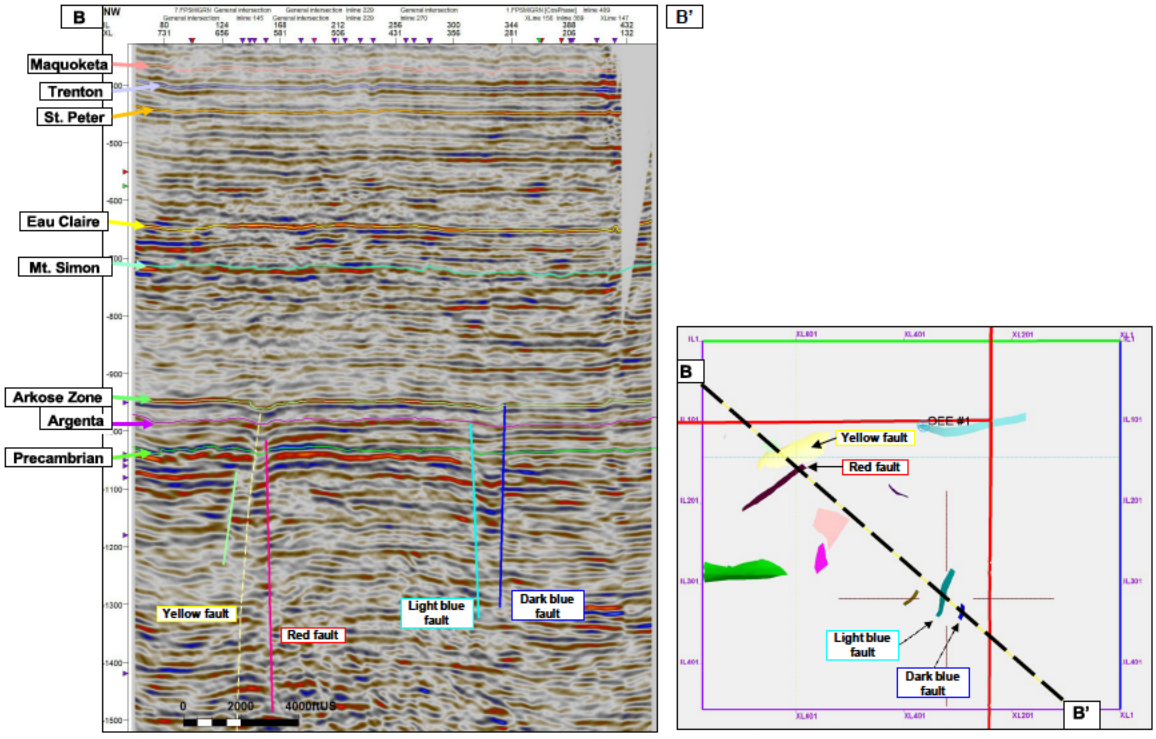

Figure 16*. NW-SE B-B' Traverse, showing several faults with different orientations, throws, and lengths. The yellow and red faults are high angle reverse faults. The light blue and dark blue faults are high angle normal faults.*

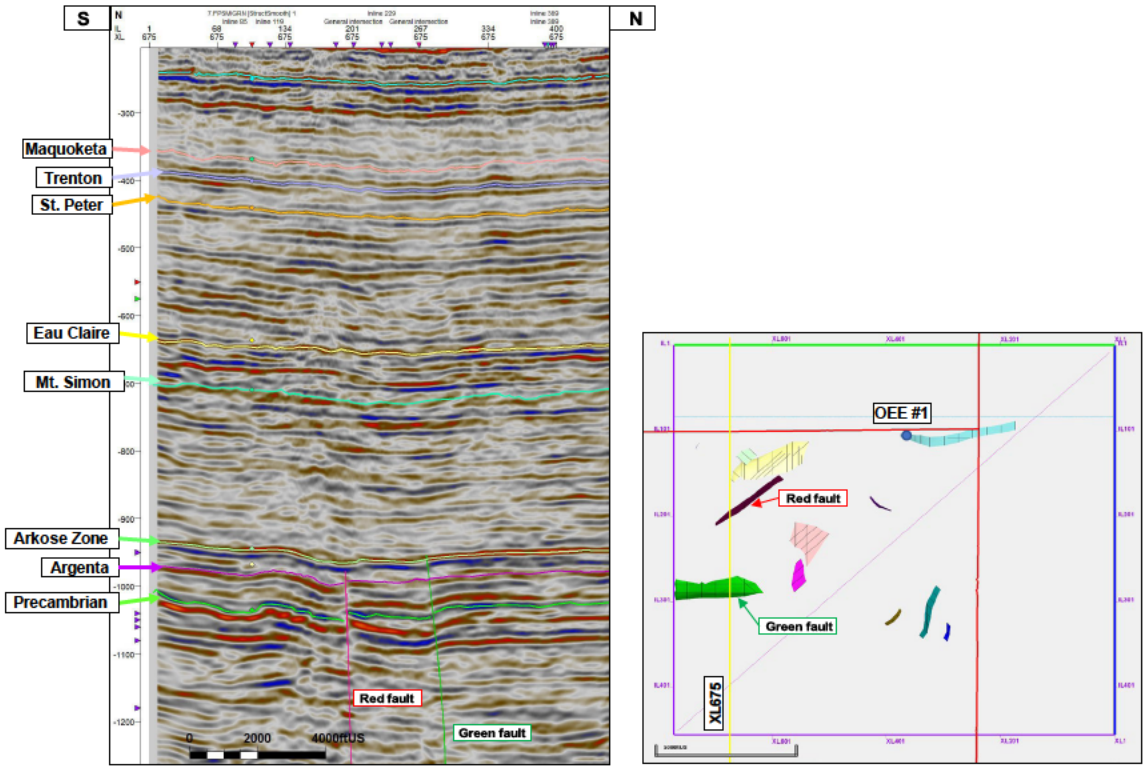

Figure 17 *Crossline 675, showing green and red reverse faults. Both are reverse faults with minor offset, and both tip out in or just below the Arkose Zone.*

Within the 3D survey, there are no faults that completely transect the Mt Simon Sandstone; all mapped faults die out in the Argenta, Arkose Zone, or lower Mt Simon. No faults were identified that transect the Eau Claire Formation confining zone. The 3D survey shows no impact to containment in the area of the survey.

The 3D survey did not reveal any observable facies changes or significant thickness changes in any of the stratigraphy.

Because of the short lengths of all faults mapped on the 3D survey, these faults are not expected to have any significant impact on the injection of CO_2.

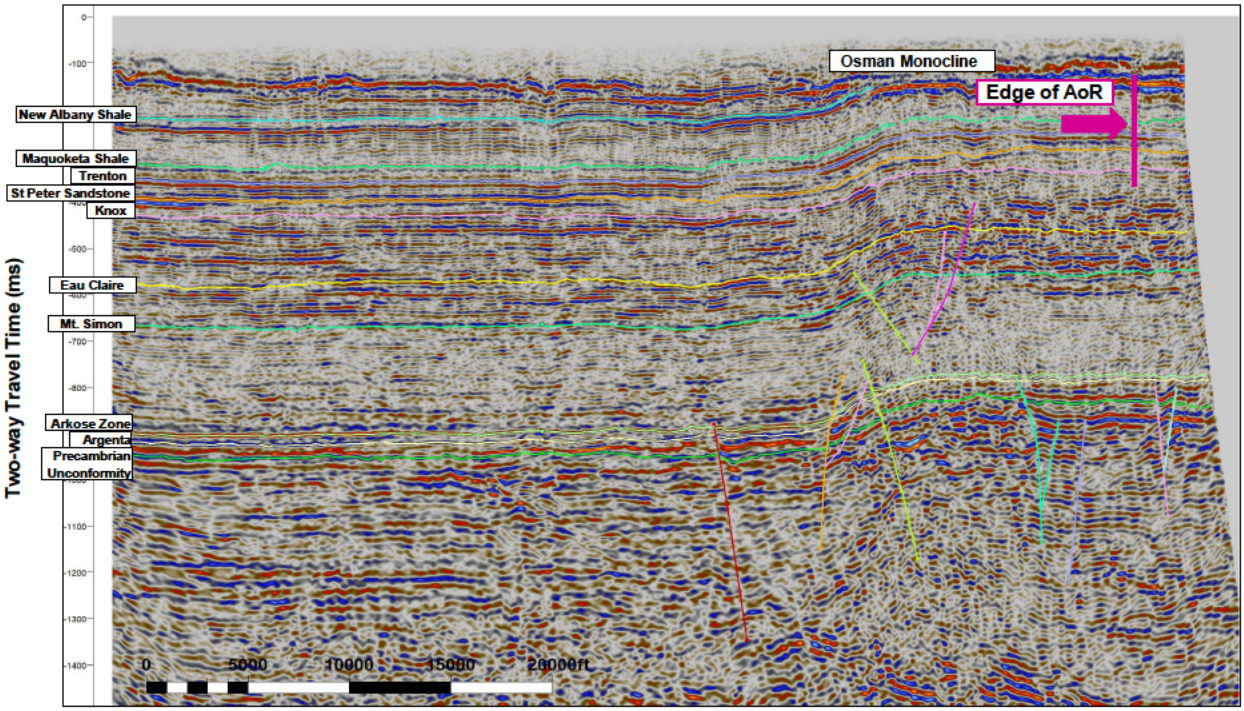

Figure 18. *Seismic Line 2 showing 1) minor extensional "keystone" faults in the core of the monoclinal fold that nucleate in the Mt. Simon and transect through the Eau Claire, and 2) minor faulting in the Precambrian basement and faults terminating in the Argenta, Arkose interval, and Lower Mt. Simon.*

Offset along the small normal faults in the core of the Osman Monocline show decreasing throw from the base of the Eau Claire and upwards. Two of these faults die out with the Eau Claire, and one dies out in the section just above the Eau Claire within the Galesville-Ironton formation. The maximum throw, therefore, of these faults within the Eau Claire is at the base of the Eau Claire. Here, the throw across all three of these small faults is between 4-6 milliseconds two-way travel time. The average seismic p-wave velocity within the Eau Claire based on the sonic log of the One Earth Energy #1 well is about 13,700 feet/second. Using this velocity and the two-way travel time, the offset in depth can be calculated, using the equation {twtt/2} x velocity. Based on this data, the offset of these small normal faults are approximately 27 to 41 feet at the base of the Eau Claire and decreasing upwards.

Uncertainty regarding basement faults includes their orientation and the amount of offset or throw. A primary method to determine fault orientation on 2D seismic data is to recognize the same fault on two different seismic lines; however, the length of the basement faults is not enough to extend to different seismic lines. The fault throw along basement faults is difficult to ascertain because of discontinuous amplitudes of seismic reflectors within the Precambrian. The presence of basement faults is not considered to impact storage or containment.

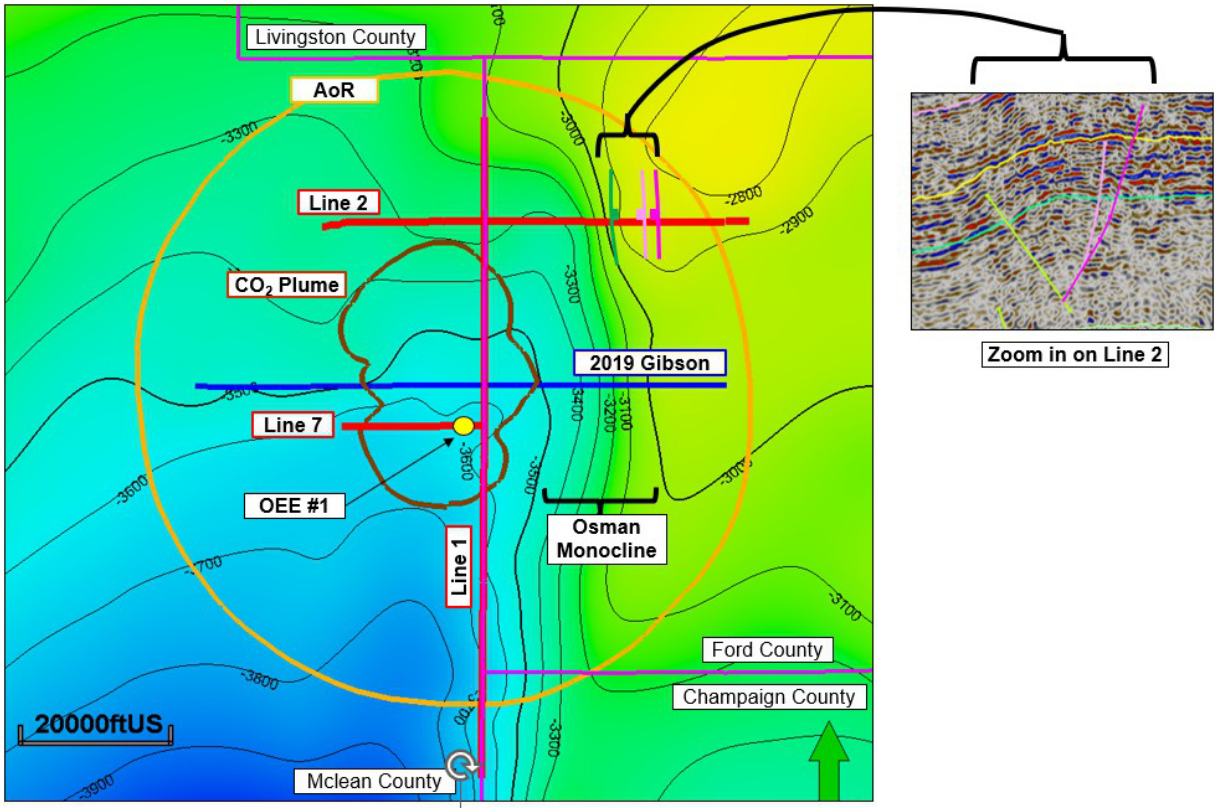

Figure 19. *Depth structure map of the top of the Mt. Simon sandstone, showing the north-south trend of the monoclinal structure and interpreted north-south orientation of small-offset normal faults visible on Line 2. Note the AoR (in orange) and CO_2 plume (brown) outlines have been generalized.*

Impact on Containment

On Line 1, Line 7 and 2019 Gibson 2D seismic lines no faults are identified in the AoR that transect the Mt. Simon Sandstone and Eau Claire Formation. On seismic Line 2 small offset normal faults are interpreted that nucleate within the Mt. Simon and continue into the Eau Claire Formation. One fault (magenta, shown in inset of Figure 19) transects the Eau Claire and terminates in overlying Knox strata. These small faults are within the AoR but outside of the prognosed CO_2 plume by about 3.4 miles (5.5 km) (Figure 19).

The small faults interpreted on Line 2 that transect the Eau Claire are evaluated to be sealing and non-transmissive to fluids. This is based on the small offset of the faults relative to the Eau Claire thickness and clay content, and on high Shale Gouge Ratios (Yielding, 2002) determined for the Eau Claire Formation. X-Ray Diffraction (XRD) analyses of Eau Claire core from 3948.91 feet (1204 m) MD and 3989.88 feet (1216 m) MD indicate clay content of 22% and 54%, respectively, consisting mostly of the phyllosilicate minerals illite and smectite with lesser amounts of kaolinite and chlorite. Yielding (2002) states that fault rocks with >40% phyllosilicates will form clay/shale smears, and much of the Eau Claire meets this phyllosilicate threshold. From 4,060-4,368 feet MD, 1,237-1,331 m MD) clay content exceeds 40% with Vshale averaging 0.70. Considering the high Vshale of the Eau Claire and the low fault throw relative to the overall thickness, SGR is expected to be essentially 100%. These analyses indicate that the portion of the fault within the Eau Claire will be sealing, and containment will not be impacted by presence of

the faults. Additional information on Eau Claire sealing capacity is presented in the GEOMECHANICAL and PETROPHYSICAL INFORMATION section.

A Formation Micro Imager log (FMI) was obtained in the OEE #1 well from 4,057 feet (1,237 m) MD (131 feet [40 m] below the top of the Eau Claire) to 7,103 feet (2,165 m) depth in the Precambrian basement. The FMI data indicate that the lower 398 feet (121 m) of the Eau Claire logged by the FMI tool is almost unfractured, except for a few widely spaced, isolated fractures, all less than one foot in height. Given the isolated nature of these small fractures, there is no indication of fracture interconnectedness within the Eau Claire primary seal.

Tectonic Stability

Faults originating in the Precambrian basement that are not associated with the monoclinal structure have not been active since Cambrian time. There are some subtle thickness changes in the Cambrian-aged Argenta, Arkose interval, and Lower Mt. Simon formations related to interpreted syn-depositional fault movement along the basement-involved faults, but no changes in thickness of strata overlying the Mt. Simon can be attributed to these faults, suggesting there has been little active faulting since Cambrian time.

Faults associated with the formation of the Osman monoclinal structure were possibly active into late Mississippian and Pennsylvanian time (Nelson 2010). These faults are part of the LaSalle Anticlinorium, which formed in response to the Ancestral Rocky Mountains orogeny (McBride 1998, McBride and Nelson 1999).

Overall, the combination of 2D seismic, 3D seismic, FMI data, stratigraphic continuity, small fault offset, and high sealing capacity of the Eau Claire Formation demonstrates that the structural setting does not pose a risk to CO_2 containment.

In East Central Illinois, the area of the One Earth CCS project, earthquakes above M 2.5 are rare. See SEISMIC HISTORY section.

Injection and Confining Zone Details [40 CFR 146.82(a)(3)(iii)]

Depth, areal extent, and thickness of the injection and confining zones

Characteristics of the injection and confining zones are also described in the REGIONAL GEOLOGY section of this document. The Mt. Simon Sandstone is the storage reservoir for One Earth CCS and is 2,014 feet (614 m) thick and occurs at 4,455 feet (1,358 m) depth in well OEE #1 (Figure 1). The Mt. Simon Sandstone can be subdivided into upper, middle, and lower units and their depths and thicknesses at OEE #1 are provided in Table 2. The One Earth CCS injection zone is in the lower Mt. Simon Sandstone within an interval referred to as the Arkose. At OEE #1 the Arkose interval is 207 ft (63 m) thick and occurs at a depth of 6,262 ft (1,909 m). The dip angle and azimuth for Arkose, based on the model area used for reservoir simulation, is approximately 0 to 4.9 degrees predominantly to the south.

Table 2. *Selected formation tops from OEE #1 well, McLean County, Illinois. The Eau Claire Formation is divided into three parts to aid OEE #1 well log and sample analyses discussed herein.*

Formation Name	Thickness (ft)	Top Depth (ft)	Elevation (ft SS)	Shale Thickness (ft)
Eau Claire Formation	534	3,921	-3,080	195*
(Eau Claire shale)	123	4,245	-3,404	123
(Elmhurst Sandstone member)	87	4,368	-3,527	38
Mt. Simon Sandstone (upper)	767	4,455	-3,614	
Mt. Simon (middle)	747	5,222	-4,381	
Mt. Simon (lower)	293	5,969	-5,128	
Arkose interval	207	6,262	-5,421	
Argenta (pre-Mt. Simon)	449	6,469	-5,628	
Precambrian (undifferentiated)	22	6,918	-6,077	

*Values are for the Eau Claire Formation exclusive of the Eau Claire shale and Elmhurst Sandstone member.

Petrophysical analyses of geophysical logs and rock cores obtained at the OEE #1 are the primary method of determining injection and confining zone properties. A detailed suite of geophysical logs collected in this well allow a continuous evaluation of mineralogical, lithological, and petrophysical characteristics across the injection formation and confining zones. Core samples and rock cuttings are also available for the Eau Claire Formation and the Mt. Simon Sandstone.

A full suite of geophysical logs including standard triple combo (Gamma ray [GR], resistivity, neutron-density porosity [NPHI]), spectral Gamma ray (SGR), photoelectric (Pe), Nuclear Magnetic Resonance (NMR), and Elemental Capture Spectroscopy (ECS), bulk Density (RHOZ), density porosity (CPHI), and formation image (FMI) logs were acquired at the OEE #1 well used for petrophysical interpretations of the Mt. Simon Sandstone and the Eau Claire Formation.

Lithologic and mineralogy properties of the Mt. Simon and Eau Claire Formation were assessed using petrophysical cross plots of Pe against bulk Density (RHOZ). The average of NPHI and density porosity (DPHI) were determined to calculate the total porosity of the intervals. Cross plots of thorium-potassium derived from the SGR log were used to identify clay mineral type and to distinguish shale and clay-rich intervals from the pure sandstone, limestone, and dolomite. The NMR logs were used to assess the presence of the clay mineral and fine grain sediments and determine the bound water and free water in the pore spaces quantitively.

Injection Zone

The sediments of the lower and middle Mt. Simon Sandstone were deposited mainly in mixed fluvial and aeolian environments that became progressively more distal from the sediment source and with delta, channel sands and lagoonal facies being present in the upper Mt. Simon Sandstone. Regionally, the lower and upper units generally have good to excellent reservoir characteristics, and the middle has less favorable reservoir quality. In addition to continuous geophysical log measurements, 85 rotary sidewall core (RSWC) and 70 full diameter core (FDC) samples were obtained from strata in OEE #1 for routine core analysis. Log analyses and routine core analyses were conducted to estimate the porosity, permeability, and bulk density of the injection and confining zones. The results of log analyses and permeability and porosity measurements from RSWC and FDC are shown in Table 3.

The upper Mt. Simon is composed of fine- to coarse-grained quartz sandstones, interbedded with massive to finely planar laminated feldspar sandstones and is 767 feet (233 m) thick in OEE #1.

The range of log- and core-based porosity and permeability values for the upper Mt. Simon are presented in Table 3.

The middle Mt. Simon consists of massive planar parallel and low-angle to trough cross-stratified, medium- to coarse-grained pure quartz sandstone, interbedded with thin intervals of feldspar sandstone and is 747 feet (228 m) thick at OEE #1. The range of log- and core-based porosity and permeability values for the middle Mt. Simon are presented in Table 3. The middle Mt. Simon strata will serve to retard vertical movement of CO_2 injected into the lower Mt. Simon (Arkose interval).

The lower Mt. Simon consists of fine- to coarse-grained quartz sandstones with variable feldspar and minor clay content. The lower Mt. Simon Sandstone also includes the Arkose interval that is presented separately. The lower Mt. Simon, not including the Arkose interval, is 293 feet (89 m) thick. The range of log- and core-based porosity and permeability values for the lower Mt. Simon are presented in Table 3.

The Arkose interval is a massively bedded fine to medium- grained feldspar sandstone with intervals of large-scale cross-stratification. At OEE #1, and elsewhere in the Illinois Basin, the "arkosic zone" can have enhanced porosity and permeability developed from diagenetic (post-depositional) alteration of the rocks through dissolution of feldspar grains and by clay coatings preventing porosity occluding cementation. Photomicrographs of Arkose interval samples from the OEE #1 well (Figure 20) indicate that factors influencing the porosity and permeability include 1) the dissolution of feldspar grains, and 2) presence of clay minerals preventing silica overgrowth around quartz grains. These diagenetic processes have enhanced the injectivity and storage potential within portions of the injection zone. The salinity of Mt. Simon Sandstone formation water within the Arkose interval is 166,000 mg/L and 165,500 mg/L as determined from two drill stem tests at 6,361 feet (1,939 m) MD in OEE #1. The range of log- and core-based porosity and permeability values for the Arkose interval are presented in Table 3.

The spatial distribution of porosity and permeability vertically and laterally within the Mt. Simon Sandstone storage reservoir in the AoR of the One Earth CCS site is described by the development of static models for the site and presented in the AOR and CORRECTIVE ACTION PLAN. Computational simulations based on these models, also presented in the AOR and CORRECTIVE ACTION PLAN, indicate the storage capacity in the Mt. Simon Sandstone at One Earth CCS exceeds 90 Mt CO_2 based on the injection of 4.5 Mta CO_2 for 20 years.

Table 3. *Ranges of porosity and permeability in the Mt. Simon Sandstone storage reservoir and in the Arkose interval injection zone. Log based porosity was derived from neutron-density logs; log-based permeability used porosity relationships and nuclear magnetic resonance logs; core porosity and permeability used data from rotary side wall core (RSWC) and full diameter core (FD). Porosity is shown as percent, permeability as millidarcy (md).*

Log Porosity (N-D)				
Zones	**Median**	**Arithmetic Mean**	**Min**	**Max**
Upper	0.133	0.134	0.07	0.199
Middle	0.11	0.11	0.06	0.17
Lower	0.1	0.1	0.06	0.15
Arkose	0.187	0.184	0.07	0.26

Permeability (NMR)_mD				
Zones	**Median**	**Arithmetic Mean**	**Min**	**Max**
Upper	26	58	0.009	1065
Middle	10	19	0.1	140
Lower	6	10	0.07	67
Arkose	83	201	0.000008	1717

Core Permeability (RSWC & FD)_mD				
Zones	**Median**	**Arithmetic Mean**	**Min**	**Max**
Upper	59	229	1.05	830
Middle	29.6	28.5	0.036	89.3
Lower	12.5	54.5	1.27	236
Arkose	35	351.3	0.002	2000.9

Core Porosity (RSWC & FD)				
Zones	**Median**	**Arithmetic Mean**	**Min**	**Max**
Upper	0.12	0.119	0.08	0.15
Middle	0.1	0.1	0.06	0.13
Lower	0.108	0.101	0.05	0.126
Arkose	0.157	0.147	0.01	0.23

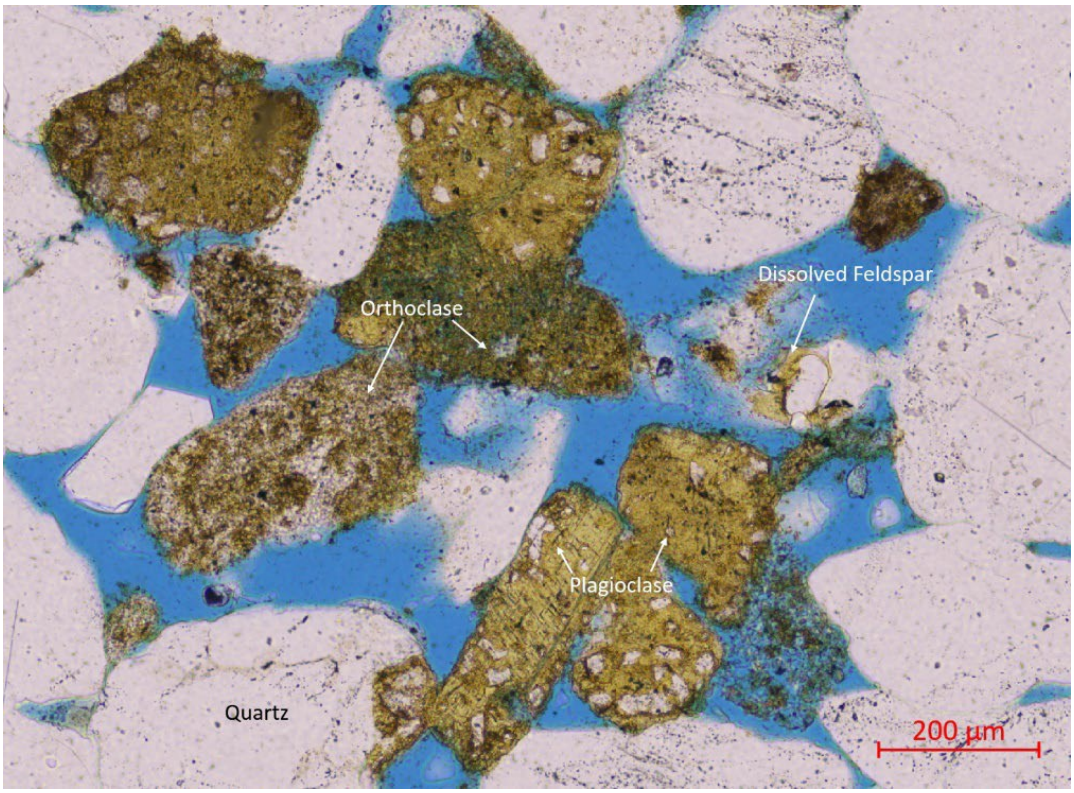

***Figure 20**. Photomicrograph of whole core Arkose interval sample from the OEE #1 well at 6,360.15 feet depth, magnified 10x, under plain-polarized light, showing porosity stained in blue.*

Confining Zone

The Eau Claire Formation is the primary confining zone and is 534 feet (163 m) thick and occurs at 3,921 feet (1,195 m) depth at OEE #1 (Figure 21). The Eau Claire Formation may be subdivided into three units (Table 2), and at OEE #1 there is a 123-foot (37 m) thick succession of shale from 4,245 to 4,368 feet (1,294 to 1,331 m), known regionally as the Eau Claire shale, that comprises impermeable strata that would prevent upward movement of fluids. Total shale intervals within the Eau Claire comprise sealing strata of 356 feet (108 m) thickness. Other units include the basal Elmhurst Sandstone member from 4,368 to 4,455 feet (1,331 to 1,358 m), and the uppermost Eau Claire Formation from 3,921 to 4,245 feet (1,195 to 1,294 m). The dip angle and azimuth for Eau Claire Formation, based on the model area used for reservoir simulation, is approximately 0 to 5.1 degrees predominantly to the south. The geophysical log signature of the Eau Claire Formation is shown in Figure 20. Core analyses are shown in Tables 4 and 5.

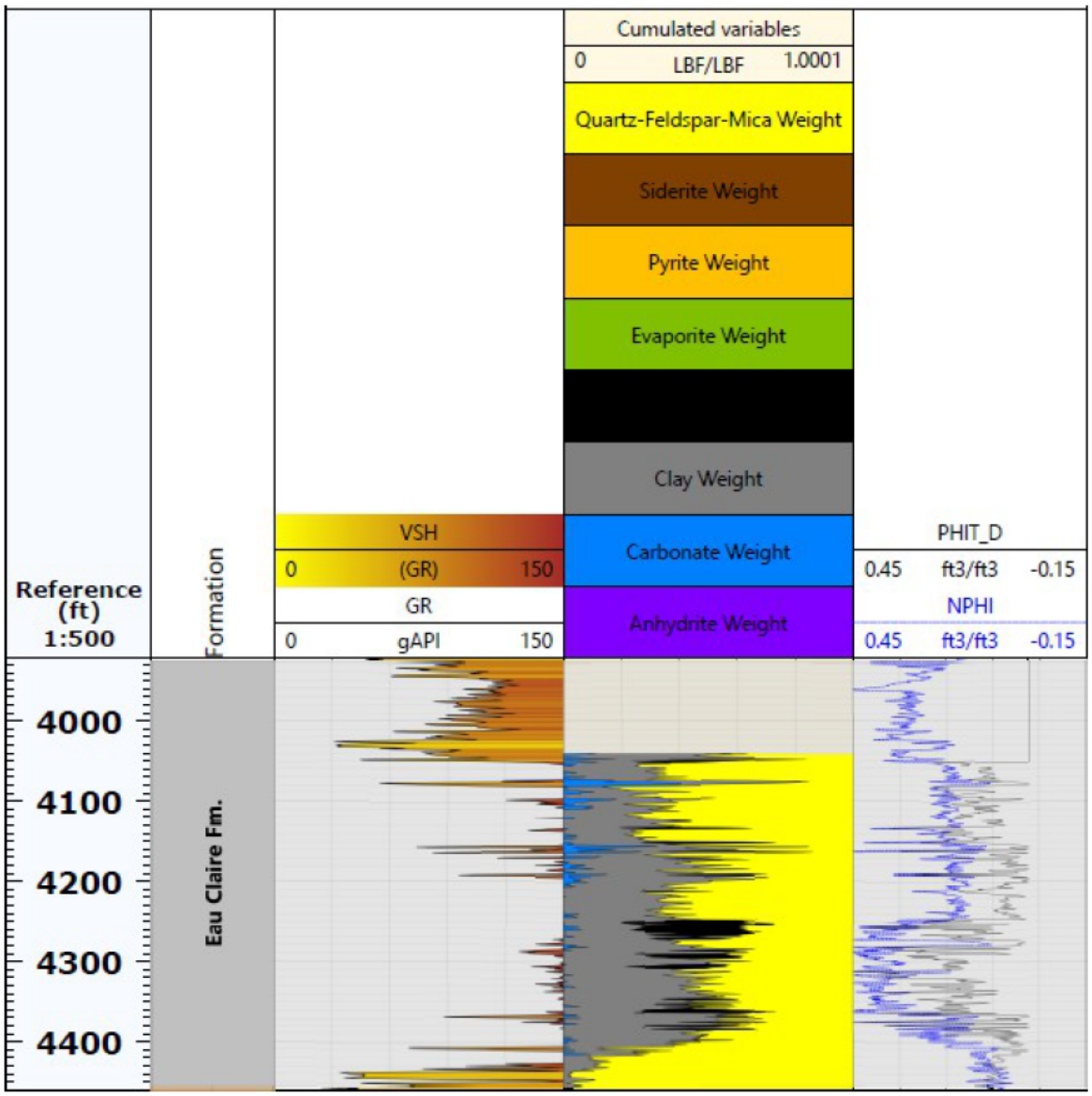

Figure 21. *Geophysical logs vs depth for the Eau Claire Formation from the OEE #1 well.*

Table 4. *OEE #1 rotary sidewall core porosity and permeability statistics.*

Formation	Count	Porosity (%)			Permeability (mD)		
		Average	Minimum	Maximum	Average	Minimum	Maximum
Eau Claire Fm	2	4.2	4.1	4.3	0.002	0.002	0.002
Eau Claire Fm *(Elmhurst member)*	3	6.5	2.5	9.5	32	0.007	31.9

Table 5. *OEE #1 full diameter core porosity and permeability statistics.*

Formation	Count	Ave. Bulk Density (g/cm^3)	Porosity (%)			Permeability (mD)		
			Average	Minimum	Maximum	Average	Minimum	Maximum
Eau Claire Fm	1	2.77	7.2	7.2	7.2	0.063	0.063	0.063

Sealing Capacity of the Eau Claire Formation

Mercury injection capillary pressure analyses (MICP) were performed on samples of the Eau Claire Formation to evaluate its confining characteristics. For samples from OEE #1 a range of $scCO_2$ column heights were calculated using contact angles of 20°, 40°, 60° to bracket wettability uncertainty. In addition, based upon the sample MICP entry pressure (Hg/air), the threshold pressure of the CO_2/brine system was modified by 20% (either low or high) to capture variability in pore volume and permeability related to variable seal mineralogy. Table 6 summarizes the Eau Claire seal capacity relative to different contact angles to account for variations in wettability and mineralogy.

Table 6*. Eau Claire Formation – Seal Capacity determined from MICP analysis. The results are presented as a range of +/- 20% from the sample analyses.*

CO_2 Column Height ft. (m) @ CA 20°	CO_2 Column Height ft. (m) @ CA 40°	CO_2 Column Height ft. (m) @ CA 60°
min – sample - max	**min – sample - max**	**min – sample - max**
680 (207) – **851** (259) – **1021** (311)	**555** (169) – **694** (211) – **833** (254)	**362** (110) – **453** (138) – **544** (166)

For the Eau Claire depth range (3,921 to 4,455 feet – 1,195 to 1,358 m) and average formation pressure (1,832 psi, using a gradient of 0.453 psi/ft) contact angles ranging from 20 – 40° were used to calculate wettability. This results in seal capacity estimates ranging from 555 – 1,021 feet (169 – 311 m) of CO_2 column being held by the Eau Claire Formation. As indicated above a minimum and maximum range based upon a 20% deviation from sample measurements accounts for mineralogy and bedding variability inherent within the shale-rich formation. These analyses indicate that the Eau Claire is a highly effective confining zone for the storage of CO_2. The confining characteristics of the Eau Claire are further discussed in the GEOMECHANICAL and PETROPHYSICAL INFORMATION section.

Porosity and permeability estimates from the MICP analyses additionally indicate the Eau Claire to be an effective confining zone. Sample ID 1 (Eau Claire Formation) in Table 7 indicates that 100% of the pore volume in this sample consists of nanopores that are indicative of very effective confining characteristics.

Table 7. *Summary of MICP pore throat sizes, entry pressures, and permeability estimates for selected samples from the OEE #1 well.*

Sample ID	Depth	Hg Inj Porosity	Median Pore Throat Size	Nanopores (1nm < Dia < 1µm)	Micropores (1µm < Dia < 62.5µm)	Mesopores (62.5µm < Dia < 4mm)	Mercury/Air Entry Pressure	Air/Brine Entry Pressure	Swanson Permeability
	(ft)	(fraction)	µm	(%PV)	(%PV)	(%PV)	(psi)	(psi)	mD
43	2,275.00	0.129	19.378	9.94	90.06	0.00	5.15	1.00	187.446
40	3,270.00	0.003	0.133	96.83	3.17	0.00	191.55	37.12	1.5E-4*
37	3,615.01	0.012	2.909	36.00	64.00	0.00	16.60	3.22	0.416
33	3,673.90	0.002	0.021	100.00	0.00	0.00	1573.56	304.94	3.4E-6*
30	3,695.31	0.022	0.056	100.00	0.00	0.00	344.15	66.69	9.1E-4*
29	3,711.90	0.005	0.069	100.00	0.00	0.00	386.73	74.94	5.6E-5*
26	3,749.99	0.004	0.123	100.00	0.00	0.00	274.65	53.22	9.2E-5*
25	3,759.90	0.007	0.688	59.49	40.51	0.00	46.72	9.05	8.0E-3*
21	3,781.92	0.141	26.984	4.47	95.53	0.00	3.63	0.70	386.556
17	3,822.03	0.040	0.055	100.00	0.00	0.00	549.41	106.47	1.3E-3*
15	3,837.00	0.047	0.033	100.00	0.00	0.00	1108.84	214.88	6.5E-4*
12	3,850.07	0.024	0.015	100.00	0.00	0.00	1766.60	342.35	5.6E-5*
11	3,861.01	0.012	0.031	100.00	0.00	0.00	780.26	151.21	7.9E-5*
9	3,875.92	0.183	41.352	0.24	86.68	13.08	1.62	0.31	1539.902
7	3,889.93	0.182	20.305	0.38	99.62	0.00	3.64	0.71	395.144
5	3,914.87	0.024	0.117	94.56	5.44	0.00	151.25	29.31	4.4E-3*
1	3,989.88	0.020	0.008	100.00	0.00	0.00	4497.19	871.52	1.3E-5*

*Permeability below the accepted limit (<0.01 mD, Swanson, B.F.1981)

Experimental results and modeling by Roy et al. (2014) using samples of Eau Claire Formation from the Illinois Basin collected at Decatur, IL, have shown that advective flow and ionic diffusion of CO_2 from the Mt. Simon Sandstone into the Eau Claire is expected to be insignificant.

A summary of Mercury Injection Capillary Pressure (MICP) data analyses on all core samples collected in the Mt. Simon Sandstone (injection zone) from OEE1 at the OES site are presented below. Detailed results of each MICP analysis are available to the Director upon request.

In addition, core samples will be collected from the Arkose zone during drilling operations for installation of the injection well and MICP will be performed on them. These results will be incorporated into the iterative geologic and reservoir models for the OES site.

Table 8. *Summary of MICP pore throat sizes, entry pressures, and permeability estimates for selected samples from the OEE #1 well.*

Mercury Injection Capillary Pressure Result Summary									
Sample ID	**Depth**	**Hg Inj Porosity**	**Median Pore Throat Size**	**Nanopores (1nm < Dia < 1µm)**	**Micropores (1µm < Dia < 62.5µm)**	**Mesopores (62.5µm < Dia < 4mm)**	**Mercury/Air Entry Pressure**	**Air/Brine Entry Pressure**	**Swanson Permeability**
	(ft)	**(fraction)**	**µm**	**(%PV)**	**(%PV)**	**(%PV)**	**(psi)**	**(psi)**	**mD**
2-58	4,368.99	0.084	0.138	100.00	0.00	0.00	490.32	95.02	0.019
2-54	4,407.98	0.147	27.760	1.21	94.80	3.99	2.55	0.49	421.467
2-53	4,442.05	0.058	17.127	16.49	83.51	0.00	4.59	0.89	36.780
2-50-1	4,580.05	0.120	7.760	30.64	69.36	0.00	16.60	3.22	29.737
2-48	4,665.03	0.111	12.813	9.18	90.82	0.00	11.66	2.26	69.044
2-47	4,790.02	0.163	33.216	2.25	96.46	1.28	3.23	0.63	809.042
2-38	5,073.99	0.105	9.908	10.94	89.06	0.00	9.24	1.79	39.892
2-24	5,800.04	0.068	26.063	9.56	90.44	0.00	3.63	0.70	89.318
2-26	5,870.26	0.089	15.408	12.38	87.62	0.00	7.31	1.42	58.364
2-22	5,998.04	0.090	2.013	29.24	70.76	0.00	13.11	2.54	5.010
2-18	6,150.01	0.075	3.687	23.81	76.19	0.00	9.24	1.79	24.334
2-9	6,595.02	0.143	0.713	63.68	36.32	0.00	52.53	10.18	0.730
2-4	6,775.08	0.049	2.209	32.54	67.46	0.00	14.74	2.86	2.059
2-1	6,903.04	0.148	9.095	19.22	80.78	0.00	6.51	1.26	65.893

Variability in thickness of the injection and confining zones within the AoR

Both the storage reservoir (including the injection zone) and the confining zone extend well beyond the AoR at One Earth CCS and exhibit generally consistent thicknesses throughout the AoR. The cross-section shown in Figure 22 indicates the lateral extent and consistent thickness of the injection and confining zones at One Earth CCS. Regional maps and cross sections additionally indicate lateral continuity of the injection and confining strata across 10's to 100's of miles, which is well beyond the area under consideration for the proposed storage site (see REGIONAL GEOLOGY section, Figures 2, 3, and 4). The extent and consistency in thickness of the injection and confining zones is also indicated by the 2D seismic profiles collected to characterize this site and presented in the FAULTS and FRACTURES section.

Thickness variations the confining zone or injection zone will have no impact on storage and containment efficacy at One Earth CCS.

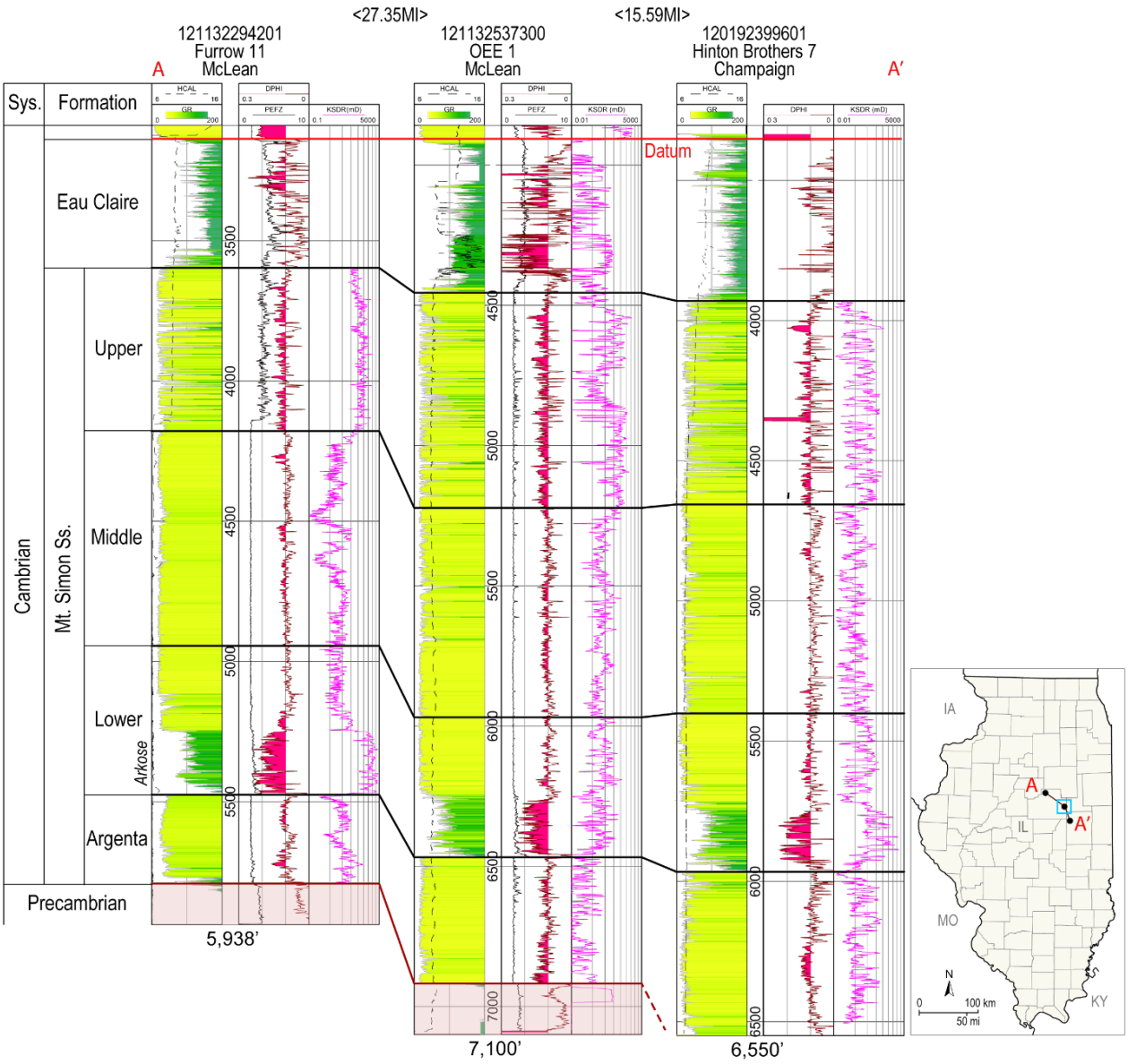

Figure 22. *Cross-section of the injection zone (Arkose interval), storage reservoir (Mt. Simon Sandstone) and confining zone (Eau Claire Formation) across the AoR indicating lateral extent and consistent thickness.*

Mineralogy of the injection and confining zones

The mineralogy of the storage reservoir, injection zone and confining zone is known through log analyses, core analyses, and thin section petrography as well as regional knowledge. The mineralogy of these units is dominated almost exclusively by silicate minerals. The Mt. Simon Sandstone is dominantly quartz with variable amounts of feldspar and minor components of illite and mixed layer clays and minor kaolinite. The Eau Clair Formation similarly is mainly quartz and phyllosilicates, mainly illite with minor mica, smectite and kaolinite, with carbonates present in the upper portion of the formation (see Figure 21). The silicate minerals are generally unreactive

with CO_2 and CO_2 saturated brine. Additional aspects of mineralogy and reactivity are discussed in the GEOCHEMISTRY section.

Overlying Strata and Secondary Confining Zones

Galesville Sandstone consists predominantly of fine-grained, moderately sorted sandstone with thin interbeds of gray to blue-gray shale. In the One Earth Energy #1 the Galesville is 68 feet (21 m) thick. Based upon MICP analysis shown in Table 5, Samples 11 and 12 (taken within the Galesville) indicate that the pore volume consists of 100% of nanopores with a permeability estimate within the nanodarcy range. These intervals should be considered as vertical fluid movement baffles.

Ironton Sandstone consists of medium-grained, well sorted, sandstone with traces of glauconite with thin to medium-scale intervals of shale, shaly siltstone and shaly limestone. The Ironton is 120 feet (37 m) in the One Earth Energy #1. MICP analysis indicates (Table 5) that Samples 17 and 15 indicate a pore volume comprised 100% with micro to nanopores and a permeability estimate within the micro to nanodarcy range. This interval should also be considered as a baffle to vertical migration of fluid movement.

Overall, 21 RSWC samples were taken from the Ironton and Galesville formations showing a high range of porosity and permeability at the upper part of Galesville and throughout the entire interval of the Ironton. The bulk density of the Davis, Franconia, and Potosi (described below) are between 2.77 to 2.83 g/cc indicating the formations are predominately composed of dolomite; the core analyses for these formations show an average porosity of less than 5% and permeability of 0.02 mD. These formations with low range of porosity and permeability can act as a secondary seal for the vertical movement of the CO_2 flow.

Davis (basal Member of the Franconia Formation) is light brown, and consists of thin shale intervals with very fine-grained, well sorted, slightly calcareous shaly sandstone. The Davis is 59 feet (18 m) in the One Earth Energy #1. MICP analyses also indicates a pore volume consistent with a makeup of 100% nanopores in Samples 33, 30, 29 (Table 5). A permeability estimate within the nanodarcy range is possible. This interval should also be considered as a baffle to vertical migration of fluid movement.

Franconia Formation light brown, very fine-grained, well sorted dolomitic sandstone with traces of green glauconite and very rare pink grains and some intervals of dolomite/limestone**.** The Franconia is 206 feet (63 m) in the One Earth Energy #1.

Potosi Dolomite consists of white-cream, very fine to fine crystalline, hard, dolomite rare clear quarts overgrowths that is very slightly glauconitic at the top and glauconitic and sandy at the base. The Potosi is 142 feet (43 m) in the One Earth Energy #1.

Eminence Formation consists of fine-to medium-grained dolomite with light blue gray to gray chert and scattered fine-medium clear quartz grains. The Eminence is 236 feet (72 m) in the One Earth Energy #1.

Gunter Sandstone consists of clear, fine to medium-grained sandstone with trace fine clasts with calcareous cement. The Gunter is 15 feet (4.6 m) in the One Earth Energy #1.

The **Oneota Dolomite** is a yellow to buff, fine-grained dolomite with fine quartz grains. The Oneota is 317 feet (97 m) in the One Earth Energy #1.

New Richmond Sandstone is a light gray-brown siltstone with traces of very fine sand. The New Richmond is 43 feet (13 m) in the One Earth Energy #1.

The **Shakopee Dolomite** is light gray to cream, mostly packstone with silt-sized rounded grains, frequently sparry dolomite. The Shakopee Dolomite is 266 feet (81 m) in the One Earth Energy #1.

St. Peter Sandstone is a clean, fine-grained, rounded to well-rounded, quartz rich sandstone measuring approximately 232 feet (71 m) thick. Only one RSWC was taken and analyzed from the St. Peter Sandstone having a porosity of 14.8 % and a permeability of 80 mD.

Platteville Group consists of tan with white, hard, sparry limestone with some crystalline calcite and trace of wackestone with fine-medium angular clasts. The Platteville Group is 164 feet (50 m) thick in the One Earth Energy #1.

Trenton Limestone (Galena Group) consists of tan with white, hard, sparry limestone with some crystalline calcite and trace of wackestone with fine-medium angular clasts. The Platteville Group is 261 feet (80 m) thick in the One Earth Energy #1.

The Ordovician **Maquoketa Group** is a laterally continuous impermeable confining layer which functions as a secondary seal in the Cambro-Ordovician storage complex in the Illinois Basin. Medina et al. (2019) evaluated the regional seal capacity of the Maquoketa using a lithofacies model to define three main units (upper, middle, and lower) and quantify five distinct lithologies. The top of the Maquoketa in the One Earth Energy #1 well is 1,598 feet (487 m) deep, and the formation is approximately 194 feet (59 m) thick at the proposed drill site.

The Devonian-Mississippian **New Albany Shale Group** is a thick, impermeable, and laterally continuous shale formation which acts as a potential tertiary seal in the Illinois Basin storage complex. The New Albany Shale was identified at 753 feet (230 m) measured depth (MD) with a thickness of 150 feet (46 m) in the One Earth Energy #1 well.

Geomechanical and Petrophysical Information [40 CFR 146.82(a)(3)(iv)]

Determination of the geomechanical characteristics of the confining zone

The confining zone (i.e., Eau Claire Formation) was logged with the Schlumberger Sonic Scanner Di-Pole sonic tool in OEE #1. Laboratory triaxial compression tests on core samples from this zone were also conducted from a measured depth of 4,313.5 feet (1,315 m). Triaxial compression tests with ultrasonic velocity measurements were conducted on three samples from this depth to determine static elastic properties and Mohr-Coulomb yield and ultimate strength. Figure
23 shows a plot of the log-derived (solid lines) and laboratory-derived (dots) elastic and unconfined compressive strength properties for the Eau Claire shale section of the OEE #1 well. The figure shows three log-derived Young's moduli. The two labeled "static V" and "static H" are the vertical (in black) and horizontal (in red) Young's moduli that were computed using a modified form of the Morales static-to-dynamic correlation formula by Schlumberger log analysts (Morales, R.H. and Marcinew, R.P.1993).
This static-to-dynamic correction has the form

$$EE_{sssssssssss} = 10^{AA+0.77\ \log(\rho\rho EE_{dddddd})}$$

The A and B parameters differ depending on the porosity of the rock, with three groups being used: 10-15% (A=0.02), 15-25% (A=-0.11), and greater than 25% (A=-0.72). The correlation was not developed for rock with porosities less than 10%. In Figure 23 the Young's modulus labeled "iso dynamic" is an isotropic Young's modulus calculated direction from the sonic log P- and S-wave velocities and density with no static-to-dynamic correction applied. As shown in the figure the log-derived static Young's modulus values are lower than the laboratory values at the depth that was sampled for laboratory testing. However, the log-derived dynamic modulus agrees very well with the laboratory measured value, suggesting that this log-derived estimate is more reliable for the Eau Claire shale at the site. The core sample used to measure the horizontal Young's modulus (red dot in Figure 23) was also performed with a larger confining pressure (5000 psi) compared to the two samples used to measure the vertical Young's modulus (500 and 1500 psi, black dot in Figure 23). Since the Young's modulus generally increases with confining pressure this likely overestimates the degree of elastic anisotropy. The differing confining pressures were used to map out the friction angle. As Figure 23 shows, the isotropic dynamic Young's modulus closely matches the vertical Young's modulus measured in the laboratory, while the static moduli computed using the modified Morales correlation are much lower than the values measured in the laboratory. This is likely because this correlation primarily is applicable to rocks with relatively high porosity (>10%), while the Eau Claire shale at this location had a measured porosity of 9.5% in a sample from measured depth 4369 feet (1332 m).

Figure 23 also shows the log-derived vertical and horizontal Poisson's ratios along with the laboratory measured values, which are in good agreement. The strength properties are estimated from log-derived correlations by Schlumberger analysts using a proprietary correlation. The two parameters used to express the Mohr-Coulomb (MC) failure criterion are the unconfined compressive strength (UCS) and the cohesion. Three core samples from the Eau Claire shale were tested to failure using confining pressures of 500, 1,500, and 5,000 psi. Figure 24 shows an example of the stress and strain data collected during the test with 1,500 psi confining pressure. The vertical axis on this plot is the deviatoric stress, which in this case is the difference between the axial load applied to the sample and the confining pressure applied to the radius of the cylindrical sample. The solid black line is the axial strain, the two dashed lines are the two radial strains, and the blue curve is the volumetric strain of the sample. The red regions are the regions used to determine the elastic properties. When most rocks begin to yield the volume strain begins to decrease, which indicates an expansion since the sign convention is positive in compression. This is caused by microcracks beginning to form as the sample begins to fail in shear. For this sample the change in direction of the volumetric strain occurs at a deviatoric stress of 16,635 psi. The sample continues to support an increased load after the onset of yield, ultimately failing at 19,067 psi with 0.8% strain at failure.

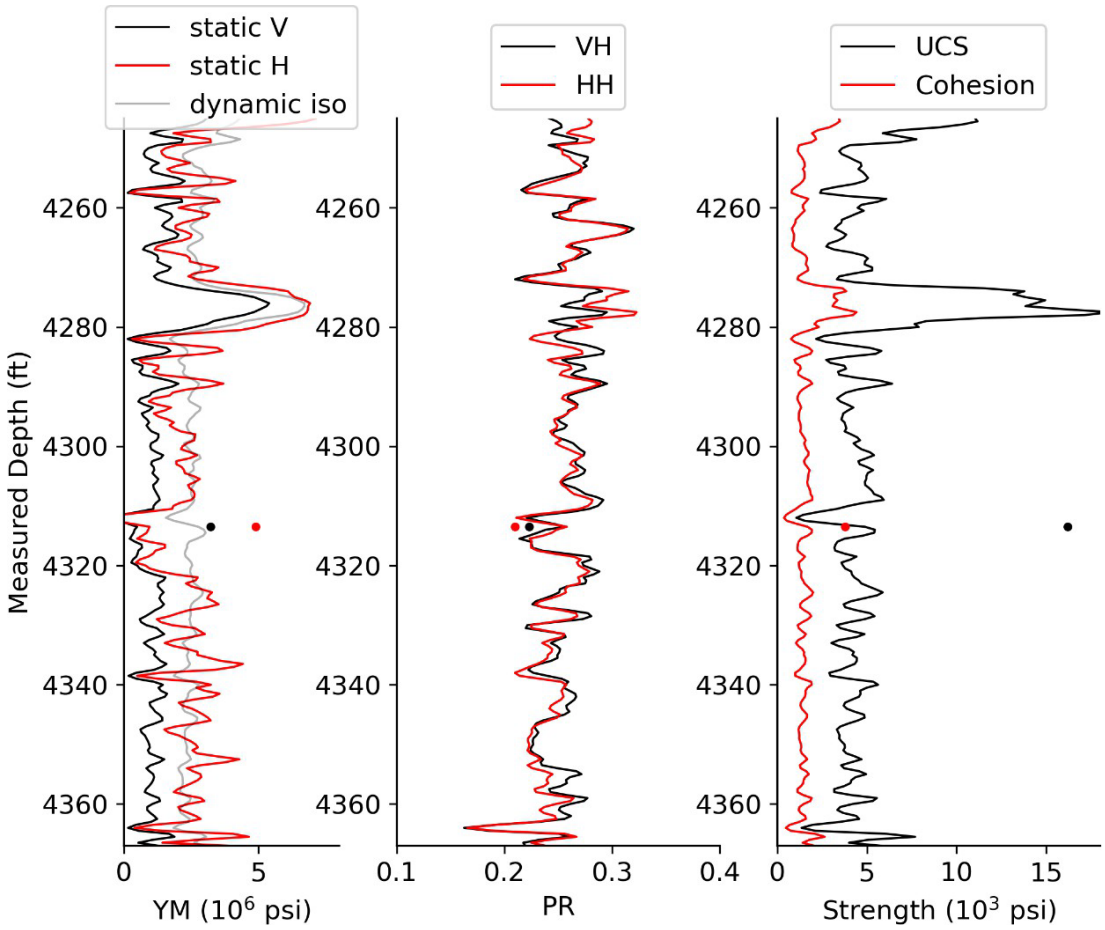

Figure 23. *Plot of the sonic log-derived (solid lines) anisotropic Young's modulus (YM), Poisson's ratio (PR), and strength together with laboratory measurements (solid circles) for the Eau Claire shale primary confining zone in the OEE #1 well. Log-derived static Young's moduli (static V & static H) are the quasi-static modulus computed using the modified Morales static-to-dynamic correction. The "dynamic iso" Young's modulus is the dynamic isotropic modulus calculated direction from the P- and S-wave sonic velocities and density. Strength is quantified in terms of Mohr-Coulomb unconfined compressive strength (UCS) and cohesion parameters. Laboratory UCS and cohesion values were estimated from three confined compressive strength tests with confining pressures of 500, 1,500, and 5,000 psi.*

Figure 23 shows the results from the three confined compressive strength tests in a Mohr diagram, both in terms of yield and ultimate strength. The difference between yield strength and ultimate strength is a common measure of ductility since it reflects how much plastic deformation a rock can withstand before it begins to lose strength. In the three tests in the Eau Claire shale the difference between yield and ultimate strength was greater than 2,000 psi.

Since these tests provide a measurement of the MC properties at the point where the samples were taken, correlations were used between sonic velocities and MC properties to extrapolate results throughout a formation. The plot on the right side of Figure 23shows log-derived MC strength properties using a proprietary Schlumberger correlation. The log-derived values are lower than the laboratory measured values for both the UCS and cohesion, but the log-derived values are

considered indicative of the degree of variability of the strength within the Eau Claire shale confining zone.

For reference in the midcontinent of the US, despite a high degree of uncertainty in the maximum horizontal stress, differences between horizontal principal stresses at the depths considered in this permit application are seldom greater than a few thousand psi since the principal stress differences are limited by frictional strength of faults, which are much weaker than the shear strength of intact rock. The changes in stress caused by injection are roughly proportional to the injection pressure. In contrast, the core testing shows that compressive yield strength varies from just over 16,000 psi under 500-1,500 psi confining pressure, to more than 27,000 psi with 5,000 psi confining pressure. For reference the lower bound estimate for the effective confining stress (average of three principal stresses minus the pore pressure) is approximately 2,500 psi. Therefore, even with the largest stress differences and changes in stress caused by injection, the Eau Claire shale will be well below its bulk yield strength of under in situ conditions. Even after failure this rock continues to support an increasing load while accommodating large strains of nearly 1%, which is quite a ductile response.

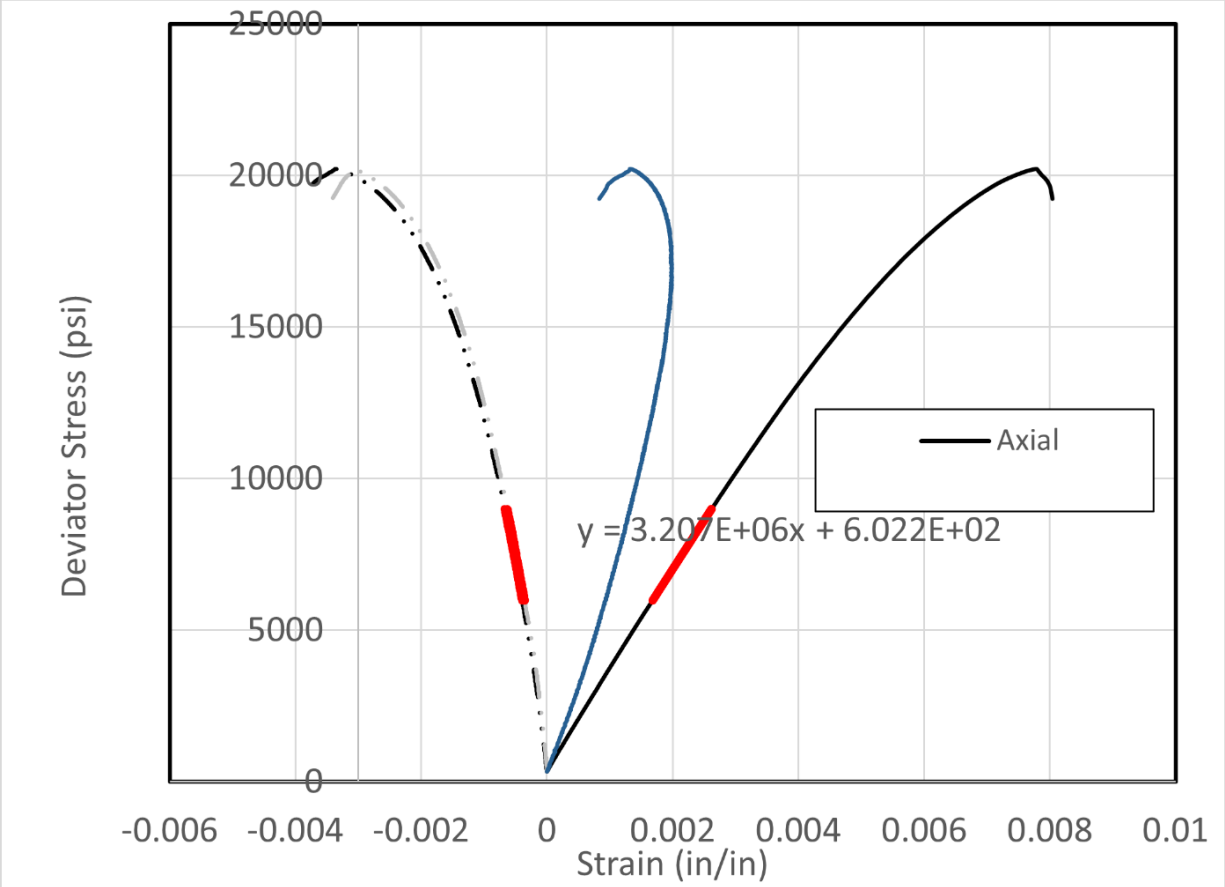

Figure 24. *A plot of the deviatoric stress versus strain for an Eau Claire shale triaxial compression test at 1500 psi confining pressure. The solid black curve is the axial strain (positive in compression), the dashed lines are the radial strains, and the blue curve is the volumetric strain.*

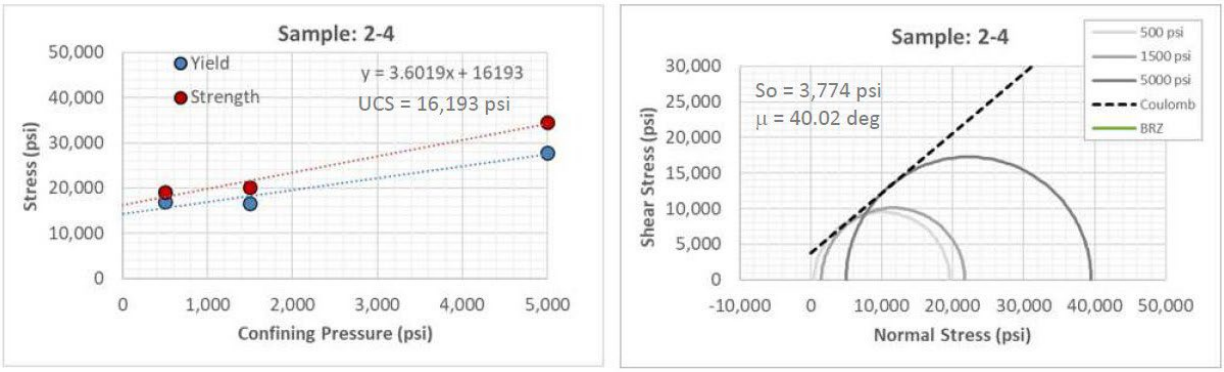

Figure 25. *Results of the conventional triaxial compression tests at the minor principal stress at 500, 1,500, and 5,000 psi.*

In addition, X-Ray CT scanning was conducted before and after the test to detect pre-existing fractures (Figure 26 and Figure 27). Pronounced weak planes or fractures are not visible at pre-test X-Ray CT scans for either sample. The failure plane for the sample tested with 1500 psi confining pressure (Figure 24) fails on the plane of maximum shear stress caused by the external loading, and so does not indicate a significant strength anisotropy that influenced the test. However, based on the failure plane observed in the test conducted at 5,000 psi confining pressure (Figure 25), it seems apparent that the failure plane is not aligned perfectly with the direction of maximum shear stress and therefore likely indicates a plane of weakness inside the rock that was not evident on the pre-test CT image. Since this sample was oriented with its axis in the horizontal direction in situ, it is likely that this is a bedding plane.

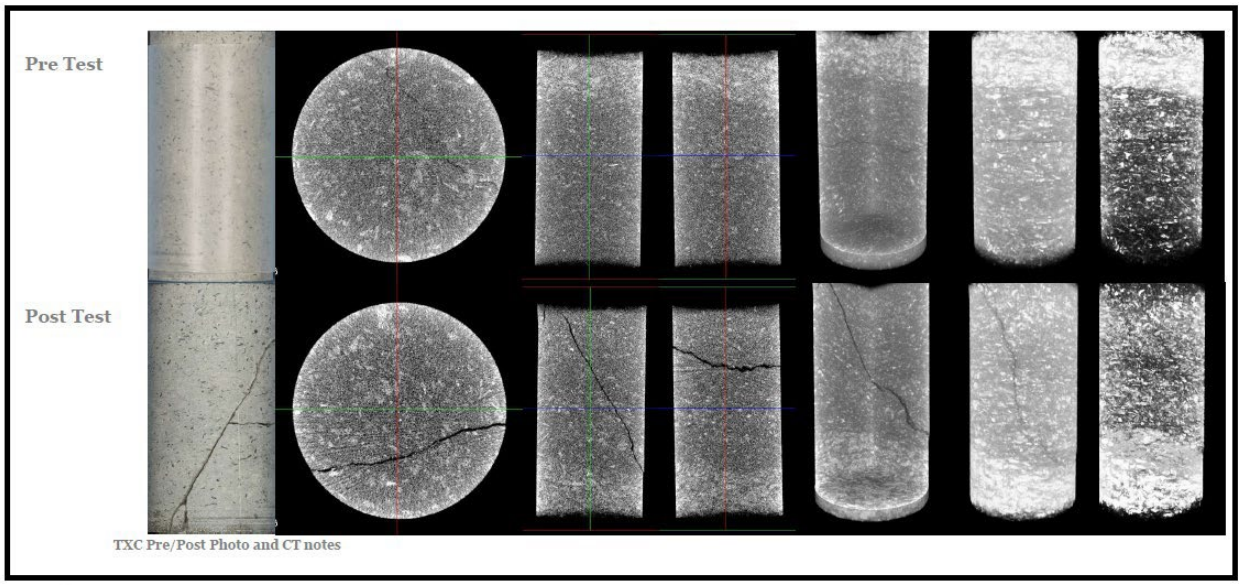

Figure 26. *Photographs and results of X-Ray CT scanning of the Eau Claire Shale specimen for the conventional triaxial compression test at the minor principal stress of 1500 psi with the axis of the sample aligned with the vertical direction in situ. The failure plane follows the plane of maximum shear stress due to the applied loads and so does not indicate a significant preferred weak plane.*

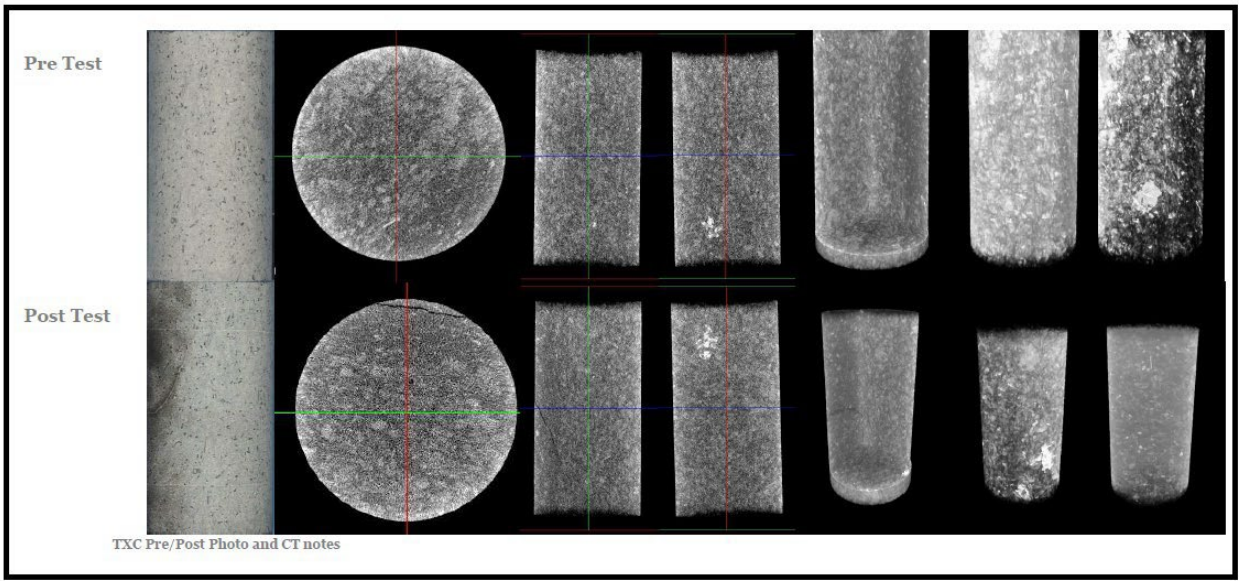

Figure 27. *Photographs and results of X-Ray CT scanning of the Eau Claire Shale specimen for the conventional triaxial compression test at the minor principal stress of 5000 psi with the axis of the sample aligned with the horizontal direction in situ. The observed failure plane is likely to be associated with the pre-existing weak bedding plane.*

Identification of fractures & faults

Four 2D seismic lines were acquired within the area of interest for injection to aid in the identification of fractures within the confining zone. 2D seismic data have the power to resolve regional faults and fractures with significant offset within the study area. There are no resolvable faults or fractures present with the Eau Claire primary sealing interval on three of the four seismic lines acquired (Line 1, Line 7, Gibson City 2019). There are however several small faults observed on seismic Line 2 that extend into the base of the Eau Claire formation and then terminate. The faults are interpreted to be small offset "keystone" extensional normal faults within the core of a monocline. While these faults are located within the Area of Review, they are located outside of the modeled CO_2 plume extent greater than three miles (SEE FAULTS AND FRACTURES section).

A full well bore Formation Micro Imager (FMI) log was also acquired to aid in the identification of fractures within the confining zone (Figure 28). FMI logs have the power to delineate high resolution stratigraphic and structural features including fractures within the well bore. The FMI logs at the OEE #1 well indicate a minimal number of fractures within the confining interval. The P32 measure of fracture intensity (fracture area per volume of wellbore) remains low throughout the entirety of the confining interval and never exceeds ~2-3/feet (.61-.91 m). Additionally, most of the planar discontinuities identified with the FMI log are characterized as bedding planes, slumping, or other depositional features. The only evidence for fracturing within the confining interval was a single fracture identified at a measured depth of ~4390 feet (1338 m). This single fracture extends ~2 feet (.61 m) vertically within the volume of the wellbore and appears to be an isolated feature. There is no evidence of displacement and is not expected to have any impact on CO_2 containment.

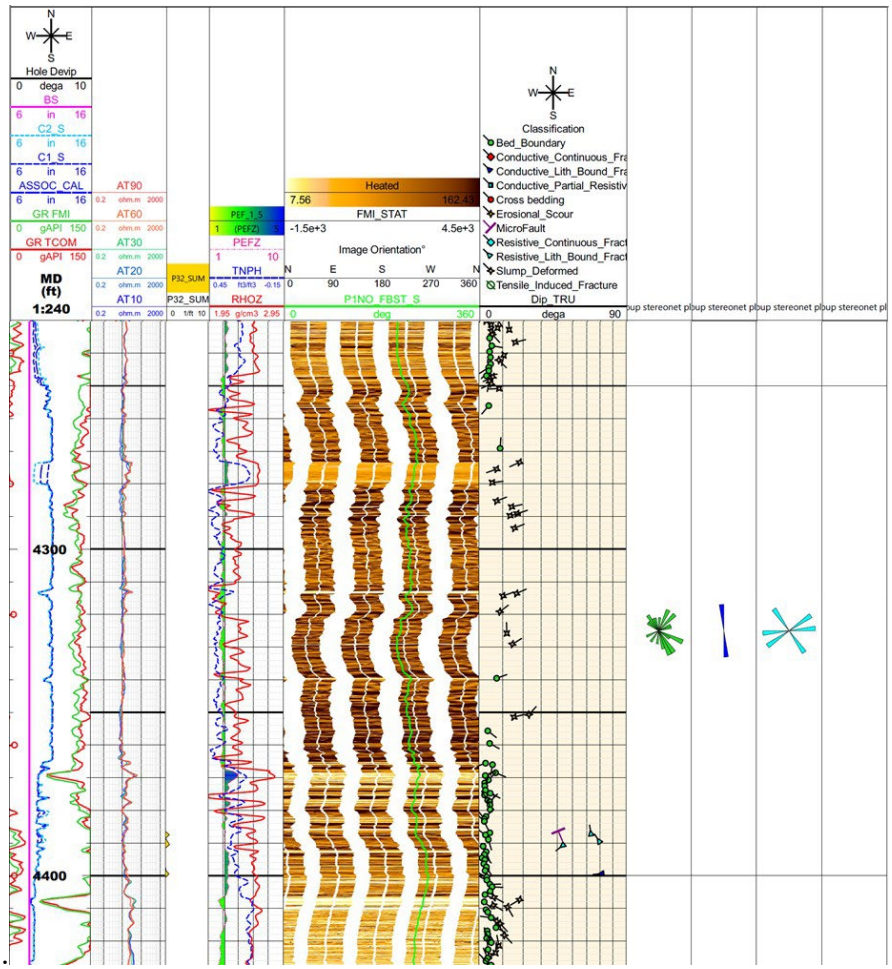

***Figure 28**. Formation micro imager (FMI) log of the confining interval. The yellow curve labeled P32_SUM measures the fracture density within the volume of the wellbore and shows that there are little to no fractures present within the measured section.*

Anomalies or uncertainties in the data

Geomechanical characterization of the Eau Claire Shale formation was conducted on a limited set of specimens (total of three), so a rigorous statistical analysis is not possible. However, the log results, including those shown in Figure 29 are very likely indicative of the degree of heterogeneity within the Eau Claire Formation. As discussed above, the strength and ductility evident in these tests is much greater than both the native stress conditions and the modest changes in stress anticipated to occur because of injection. Therefore, shear failure of the bulk rock is very unlikely given the test results and degree of heterogeneity observed within the section of the Eau Claire Formation sampled at this site. The primary geomechanical risks are therefore not bulk shear failure of the confining formation, but tensile fracture if the injection pressure were to exceed the in-situ stress in the confining zone or shearing along any planes of weakness (FAULTS and FRACTURES).

Lithostatic Stress Magnitude

The lithostatic stress is the weight of all overlying rock units at given depth and is best estimated with borehole density logs from the ground surface to the depth of interest. For practical reasons

it is seldom possible to run density logs for the shallowest portion of most wells. For the OEE #1 well density logs were run for all depths below the surface casing, but because of washouts in the section above approximately 386 feet (118 m), the density logs were not reliable in this section. In this section and in a few short deeper sections where poor hole conditions resulted in anomalous density values, missing values were replaced with a density of 2.5 g/cm^3, which is close to the average of the density values in the rest of the well. The middle plot in Figure 29 shows the corrected density log along with a plot of a running average of the overlying density for each depth. The plot on the right-hand side of this figure shows the lithostatic stress gradient computed from the integration of corrected density log to each depth. Also shown in the dashed line on the right-hand plot is the average lithostatic gradient of 1.12 psi/ft along the well trajectory computed by averaging the integrated density log.

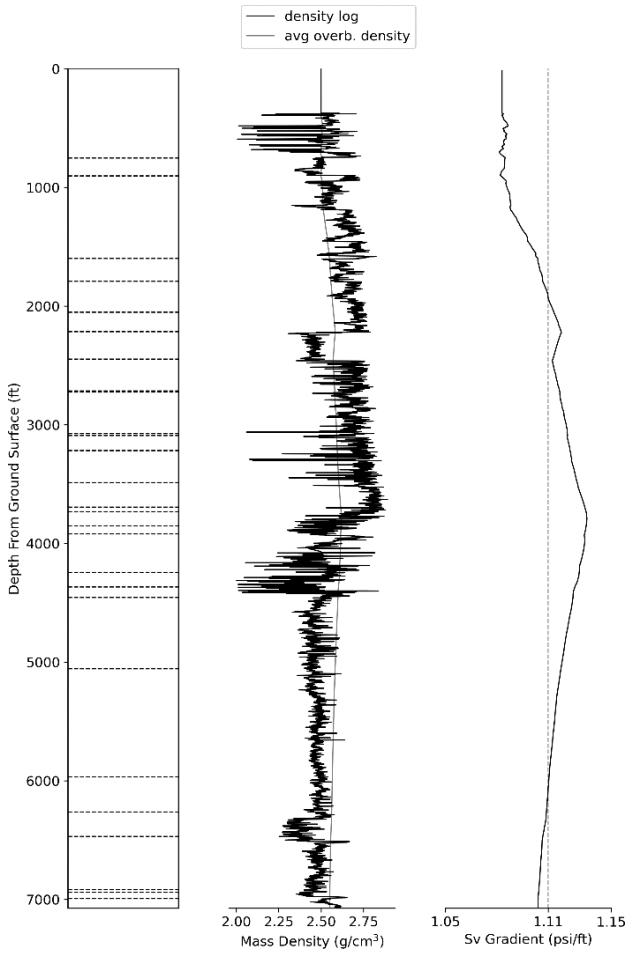

Figure 29. *Left: Plot of the density log (with anomalous values removed) along with a running average of the overlying density for each depth; Right: integrated density log along with trend line of 1.11 psi/ft*

Average pore pressure of the confining zone

Pore pressure changes associated with subsurface operations perturb in situ stress conditions and can cause faults or fractures to slip because of reduced normal effective stress and increased shear stress. Pore pressure was measured in the St. Peter's sandstone and in the Mt. Simon sandstone formations using drill-stem testing (DST). The DST consisted of two flowing periods followed by two shut-in periods, which are used to determine the static pore pressure. Figure 30 shows a plot

of the data from the second (longer) shut-in period for the Mt. Simon test. The pressure gauge plotted was located at a depth of 6,353.5 feet (1,937 m) TVD measured from the ground surface (5,527.5 feet [1,685 m] TVD subsea elevation). Though the pressure had nearly equilibrated at the end of the shut in, the bottom plot in the figure is a Horner plot, which is used to extrapolate the pressure build data to effectively infinite time. The Horner plot extrapolation shows that the static formation pressure in the Mt. Simon at this depth is 2,772 psi (0.436 psi/ft), which is consistent with a static water column to the ground surface (normal pressure gradient).

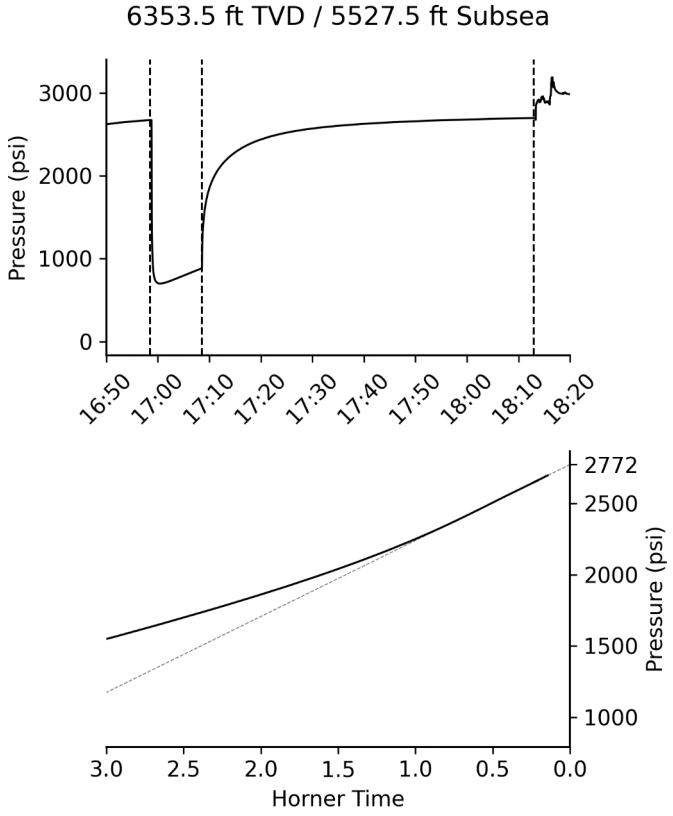

Figure 30. *Top: plot of the second flow/shut-in cycle of the drill-stem test (DST) in the Mt. Simon; Bottom: Horner plot of the shut-in data with linear fit extrapolating the pressure to infinite time showing a pore pressure of 2772 psi, which equates to a pore pressure gradient of 0.436 psi/ft TVD*

Principal Stress Directions

Regional observations and site-specific data obtained in the OEE #1 well provide meaningful indicators of the regional state-of-stress. Beginning with the largest scale trends in stress field, (Lund Snee and Zoback) recently developed a continuous quantitative model of the faulting regime throughout North America, using an updated catalog of stress orientations, well-constrained earthquake focal mechanisms, and sense of fault slip at numerous locations across the continent. The derived map (Figure 31) shows a continent-scale transition from compressional faulting regimes (i.e., strike-slip and/or reverse faulting regime) in eastern North America to strike-slip faulting in the mid-continent to predominantly extension in western intraplate North America. This continent-scale analysis leads to the expectation that the proposed injection site is located in a

transition zone, dominated by strike-slip faulting regime with the maximum horizontal stress direction in a NE-SW orientation.

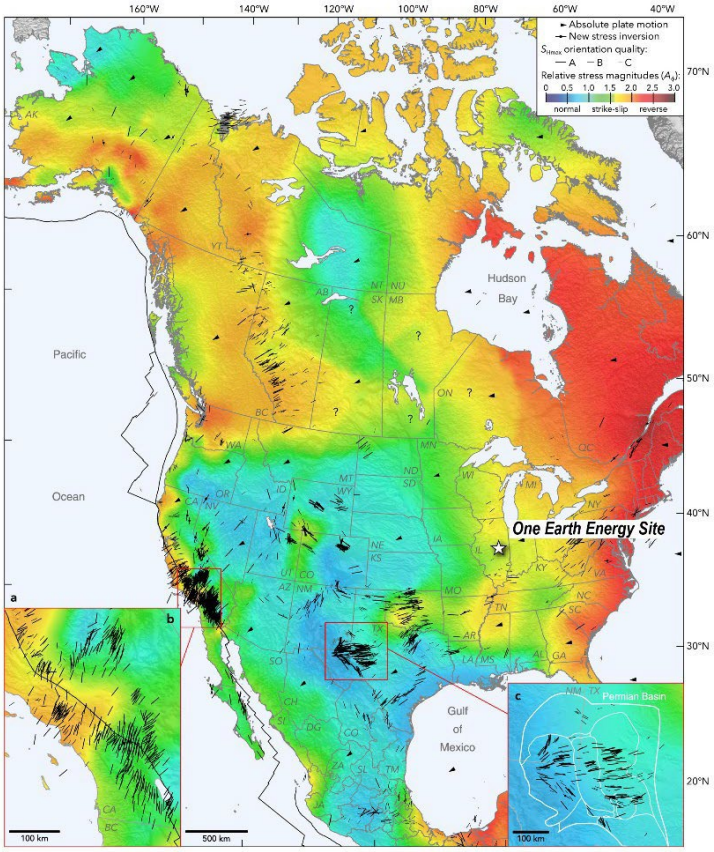

Figure 31. *Map of relative stress magnitude in North America (Lund Snee and Zoback 2020) with location of the One Earth Energy proposed injection site*

There are two independent indicators of the azimuth of the maximum horizontal stress in the OEE #1 well: drilling-induced tensile fractures (DITF) observed on the formation microimager (FMI) logs, and shear wave polarization observed on the di-pole sonic logs. DITF form when the difference between the horizontal principal stresses and cooling caused by the drilling mud result in a stress concentration at the borehole wall such that the tensile strength of the rock is exceeded. DITF are expected to form in the azimuthal direction of the maximum horizontal stress. DITF were primarily found in the Middle Mt. Simon Sandstone from 5,299 feet to 5,760 feet (1,615 to 1,756 m) MD. Figure 32 shows three examples of DITF sets observed in this section. They all have a relatively consistent orientation of 60-70 degrees, with a matching set 180 degrees offset. Some of these, as shown on the right-hand side of the figure, form in en-echelon sets of fractures. This typically occurs when the principal stress directions or planes of material anisotropy are not aligned with the well direction. This could indicate that the principal stress directions deviate from strictly vertical/horizontal over some sections of the well.

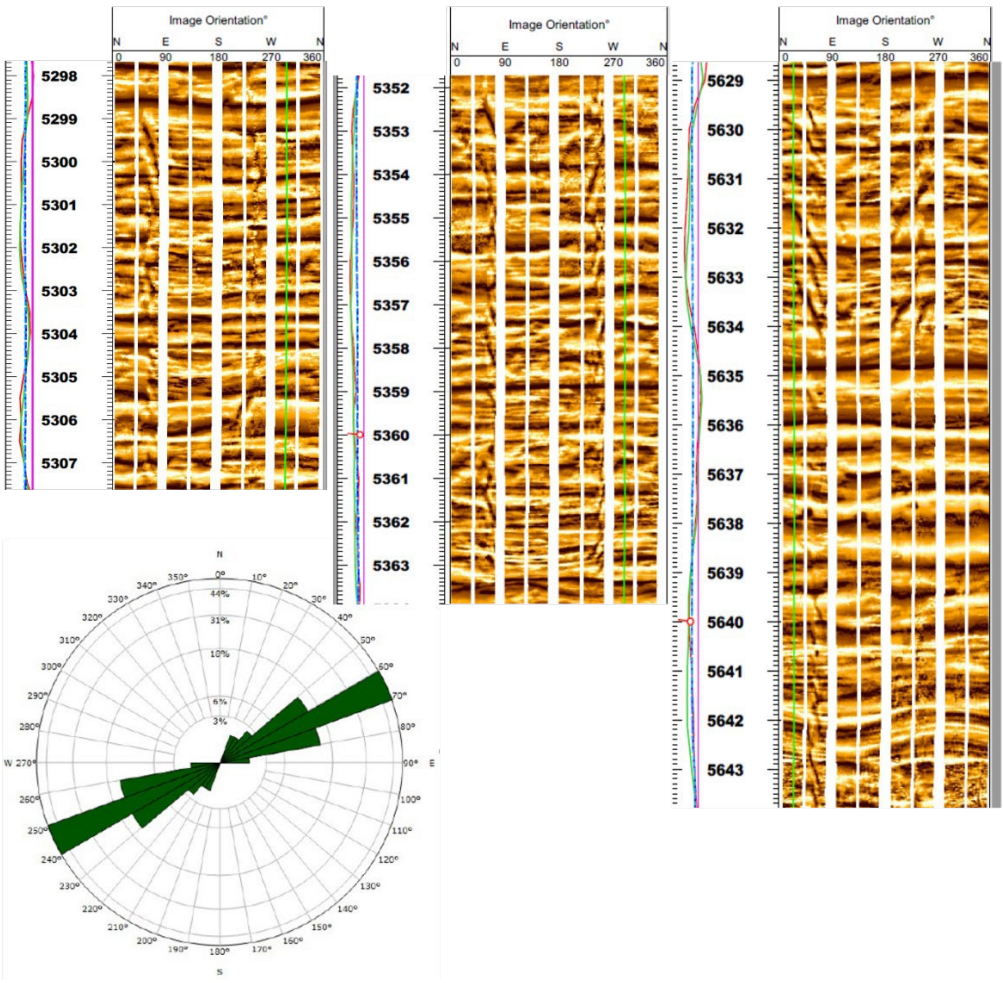

Figure 32. *Examples of drilling-induced tensile fractures (DITF) identified in the OEE #1 well, along with a rose plot showing the azimuthal distribution of all identified DITF. DITF occur primarily over the depth range from 5,299 feet MD through 5,760 feet (1,615 through 1,756 m) MD show a relative consistent azimuth of 60-70 degrees. The example on the right shows en-echelon fractures, a possible indication that the principal stress directions could be rotated from vertical/horizontal at this depth.*

Further strengthening this estimate of the horizontal stress directions for the site is the observation of a very consistent azimuth of fast shear waves in the Schlumberger SonicScanner di-pole sonic log shown in Figure 33. This figure shows a rose plot of the azimuth of fast shear waves where significant shear wave splitting was observed and attributable to the state of stress. This was determined by a change in azimuth of fast and slow shear waves with frequency, which is a reliable indicator that the polarization of shear waves is caused by stress rather than intrinsic anisotropy of the formation (Sun and Prioul, 2010).

Both site-specific indicators of the principal stress directions show a high degree of consistency with each other and with the regional trend of stress direction. For the region, there are 7 averaged measurements within 47 to 90 miles surrounding this site - DITF (68º – [Bauer, R.A., M. Carney, and R.J. Finley, 2016]) and minifrac (68º – [Frommelt 2010]) at Decatur, hydraulic fracs at FutureGen (51º Paleozoic & 68º Precambrian – [Cornet, F.H., 2010]) and 2 earthquake focal solutions 63º & 73º – 6-28-2004 & 6-17-2021).

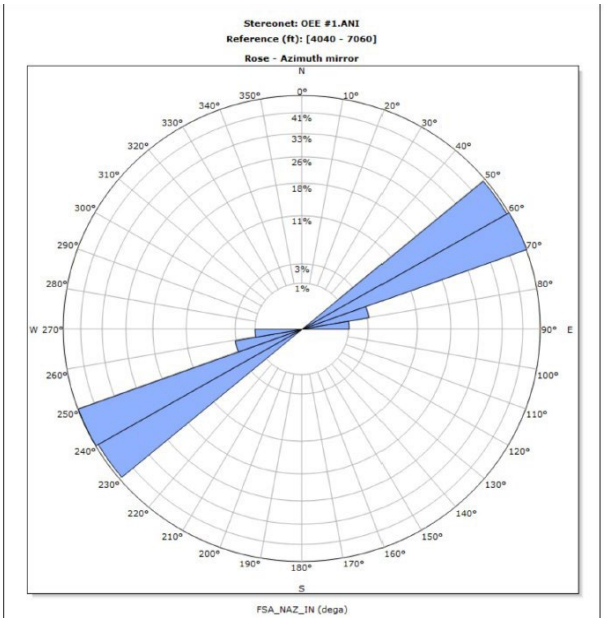

***Figure 33**. Tensile induced fracture orientation on a stereonet projection of the azimuth of fast shear waves where significant stress-induced anisotropy was observed on the Schlumberger SonicScanner di-pole sonic log*

Magnitude of Minimum Horizontal Stress

The stress magnitudes that are of primary interest are the minimum horizontal stresses in the Eau Claire confining zone and in the Mt. Simon sandstone injection reservoir, as these are the stresses that control the risk of unintentional hydraulic fracturing. The differences between the minimum and maximum principal stresses are important for the risk of fault slippage and induced seismicity.

Even with quality hydraulic fracture-based stress measurements, some uncertainty can remain in the principal stress magnitudes, particularly for the maximum horizontal stress. Because of this the State of Stress Assessment Tool (SOSAT) was developed under the DOE National Risk Assessment Partnership (NRAP) to apply a Bayesian uncertainty quantification approach to integrating many sources of information to estimate the situ stress. The output of this tool is a joint probability distribution for the principal stresses at a point in the subsurface., which can also be used to evaluate the probability of geomechanical risks such as unintentional hydraulic fracturing or fault activation. This tool can be applied with very little information, in which case it results in a relatively broad probability distribution for the stresses. With more information the uncertainties generally diminish and the probability distributions for the stresses become more constrained. In the remainder of this section the SOSAT tool is used to construct a probability distribution for the stresses along the depth profile of the OEE #1 well beginning with the more broadly applicable constraints on the state of stress and then moving toward more detailed site-specific information.

The most broadly applicable constraint on the state of stress in the subsurface is based on the argument that the frictional strength of faults and fractures, with are assumed to be pervasive at some scale, limits the magnitude of the shear stresses (Zoback, M.D. 2003). Using this principle, a critically oriented normal fault places a limit on the difference between the minimum horizontal stress and the lithostatic stress. Similarly, a critically oriented strike-slip fault places a limit on the difference between the two horizontal principal stresses and a critically oriented thrust fault limits

the difference between the maximum horizontal principal stress and the lithostatic stress. Exactly what the magnitude of these limits are depends on the friction coefficient and pore pressure on a given fault or fracture. It is common to just assume a reasonable value for the friction coefficient, mostly commonly 0.6. The SOSAT tool instead specified a probability distribution for the friction coefficient, reflecting the uncertainty in this parameter. Bayes' law is then used to propagate this uncertainty through into probabilistic bounds for the principal stress magnitudes.

Beyond this most basic constraint provided by frictional strength of faults and fractures, as discussed above and illustrated in Figure 34, the relative magnitudes and directions of the principal stresses tends to vary in systematic ways over geographic regions, reflecting the tectonic processes driving the state of stress. Because such information is generally qualitative and therefore contains some ambiguity and uncertainty, the SOSAT tool incorporates this information by allowing the user to specify probabilities for each of the three Andersonian faulting regimes.

As will be discussed in more detail below, the vast stress measurements at the formations and depths of interest for the proposed injection site indicate that the minimum horizontal stress is less than the lithostatic stress. Measurements at much shallower depths indicate minimum horizontal stress values greater than the lithostatic stress, however such trends from shallow settings generally do not correlate with the ratios of horizontal to vertical stress at depth (Brown, E. and E. Hoek 1978), so we will only focus on measurements in the vicinity of the proposed site that are at similar depths. While estimates for the magnitude of the maximum horizontal stress have been made at these sites, they carry a high degree of uncertainty. Therefore, before integrating site-specific data we apply a prior probability with equal probability assigned to normal and strike-slip faulting, and a 5% to thrust faulting. There are indications that the faulting regime likely varies from formation-to-formation and this constraint on the stress does not preclude this from happening, it merely expresses that normal and strike-slip faulting are the dominant a priori expectation. Using only the constraints imposed by frictional strength of faults and fractures, and the regional trends at depth, results in a stress profile that is nearly linear with depth, only deviating from linearity due to the variations in lithostatic stress resulting from integrating the density log.

The closest know stress measurements to the OEE #1 well are from well CCS#1 of the Illinois Basin- Decatur Project (IBDP) in Macon County, Illinois, and from the FutureGen 2.0 #1 well in Morgan County, Illinois. The IBDP used a wireline-deployed straddle packer tool to conduct mini-frac tests in the Eau Claire and Mt. Simon Sandstone formations. The tests in the Eau Claire formation were at 5,435 feet (1,657 m) measured depth and showed that the fracture propagation pressure was between 5,078 and 5,323 psi, with the fracture opening observed at 4,656 psi during the last injection phase when the fracture was at its largest extent. The fracture closure pressure was determined to be 4,603 psi. The resulting fracture propagation pressure gradient is 0.93-0.98 psi/ft, and the minimum horizontal stress gradient is 0.85 psi/ft. As explained in more detail below, the fracture propagation pressure includes the pressure required to overcome rock toughness as well as viscous losses within the fracture, and thus depends on injection rate, fracture geometry, and fluid rheology and is an upper bound to the minimum principal stress. The fracture closure pressure is a much more meaningful measure as it is independent of these factors and a more accurate measure of the magnitude of the stress as well as a more conservative quantity to use for choosing safe injection pressure. The minifrac test in CCS#1 in the Mt. Simon formation was not

able to generate a hydraulic fracture at an injection pressure of approximately 5,990 psi, which places an upper bound on the fracture initiation pressure of 0.95 psi/ft.

The FutureGen2.0 #1 well used the same wireline-deployed straddle packer tool to conduct minifrac measurements in the Mt. Simon and the Precambrian basement. Three tests in the Mt. Simon were able to determine the fracture closure pressure: 2,174 psi at 4,122 feet (0.53 psi/ft), 3240 psi at 4156 feet (0.78 psi/ft), and 2,800 psi at 4,236 feet (0.66 psi/ft). Subsequent image logging showed that the induced fractures were mostly vertical with strikes of approximately 51˚ degrees in the Mt. Simon tests and 54-77˚in the Precambrian basement.

Analysis of the in-situ minimal horizontal stress in the Eau Claire based on DFIT

A diagnostic fracture injection test (DFIT) was conducted in an interval of the Eau Claire Shale in the OEE #1 well. An inflatable packer was set with its center at 4,290 feet (1,308 m) MD (4,275 feet (1,303 m) TVD) while the bottom of the well at the time was 4,310 feet (1,314 m) MD (4,295 feet (1,309 m) TVD). The drilling mud was displaced with 63 barrels of 2% KCL and then a ball was dropped to inflate the packer. Pressure was measured at the surface with pressure gauge on the rig standpipe, and on two downhole pressure gauges. Figure 34 shows a plot of the raw pressure data reported for the surface and downhole pressure gauges along with the pump rate (a 31 second time offset has been applied to account for a difference in the clocks used to record the surface and downhole pressure data).

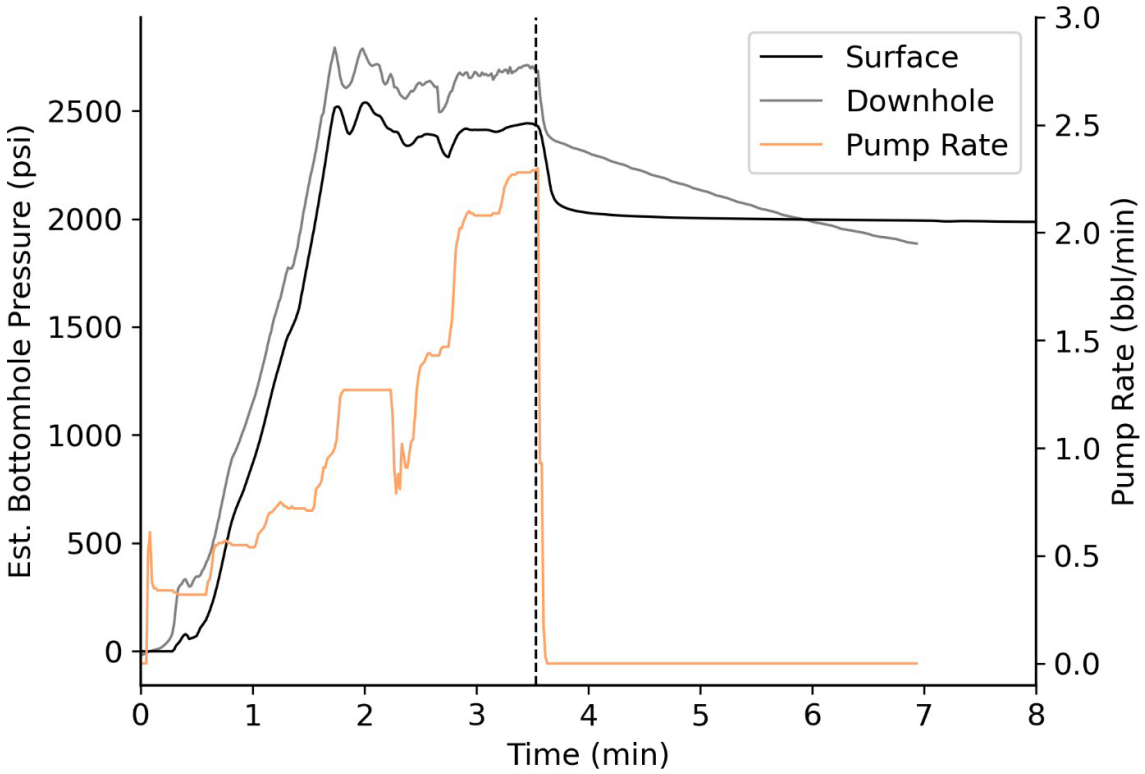

Figure 34. *Plot of surface and downhole pressure readings and pump rate for the DTIF conducted in the Eau Claire shale*

The injection rate was increased in approximately 0.25 bbl/min steps with the fracture initiating while the rate was being increased from 0.75 to 1.0 bbl/min. The pressure was steadily and rapidly increasing in all these rate steps before fracturing. It is almost certain that if the first- or second-rate steps (0.25-0.5 bbl/min) had been maintained the formation would have fractured at those rates. Therefore, a conventional method of plotting injection rates versus injection pressures to infer the fracturing pressure cannot be used in this case since there are no rates where the pressure stabilizes below the fracturing pressure in this test.

The analysis focused on the surface gauge pressure, as the downhole pressure gauge shows an unusual response. Figure 35 is a plot of the bottom hole pressure estimated from the surface pressure by adding a 4,290 feet head of 8.43 lb/gal (density of 2% KCL). This figure zoomed in on the very end of the pumping period. As the plot shows, a rapid pressure drop of approximately 300 psi is observed when the pumping is stopped (from approximately 4,300 psi to approximately 4,000 psi estimated bottom hole pressure). The pressure after this sudden pressure drop, called the instantaneous shut-in pressure (ISIP), is a good approximation for the fracture propagation pressure. In this case, the ISIP is approximately 4,000 psi. The corresponding fracture propagation pressure gradient is 0.94 psi/ft which is identical to the lower bound in the Eau Claire mini-frac test in IBDP's CCS#1 well.

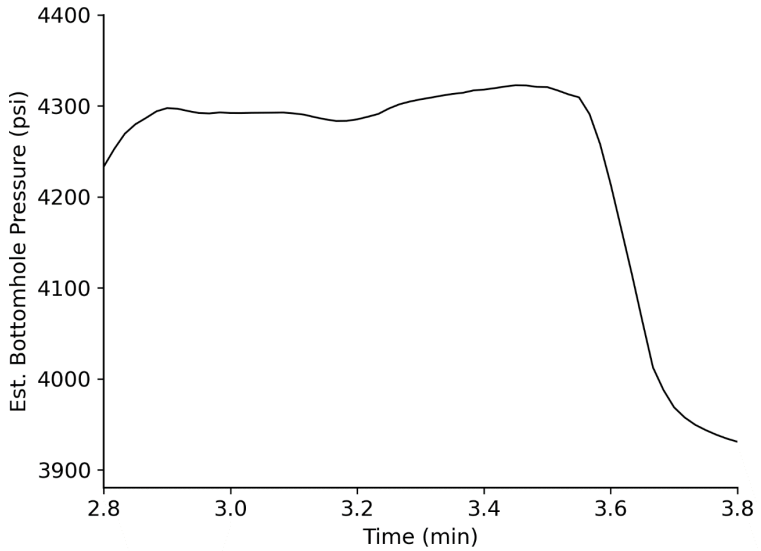

Figure 35. *Plot of the bottom hole pressure estimated from the surface pressure by adding a 4,290 feet (1,308 m) head of 8.43 lb/gal (density of 2% KCL)*

The difference between the fracture propagation pressure and the minimum principal stress, $\sigma\sigma_3$, called the net pressure, is responsible for fracture growth. From numerical simulations and experiments in the lab and field it is known that the net pressure increases with the pumping rate, fluid viscosity, and fluid temperature (Economides, M. and K. Nolte 2000). Fluid chemistry also plays a role, with low pH fluids generally resulting in lower net pressures in silicious and carbonate-rich rocks (Atkinson, B.K., 1984). Since the objective is to inject supercritical CO_2, a fluid with a lower viscosity, lower pH and likely a lower temperature than the brine pumped in this DFIT test, the only way to ensure that no fractures propagate in the sealing formation is to

ensure that no positive net pressure develops, which requires evaluating the minimum principal stress rather than the fracture propagation pressure.

The minimum principal stress can often be estimated accurately using the shut-in period of a DFIT test. The most well validated method for inferring $\sigma\sigma_3$ involves plotting the pressure after shut-in versus a nonlinear function of time called the G-function or G-time (Economides, M. and K. Nolte 2000, McClure, M., et al. 2019). When the fracture closes, the pressure is expected to begin declining more quickly for a time before slowing down again. An example of this from the literature (McClure, M., et al. 2019) is shown in Figure 36.

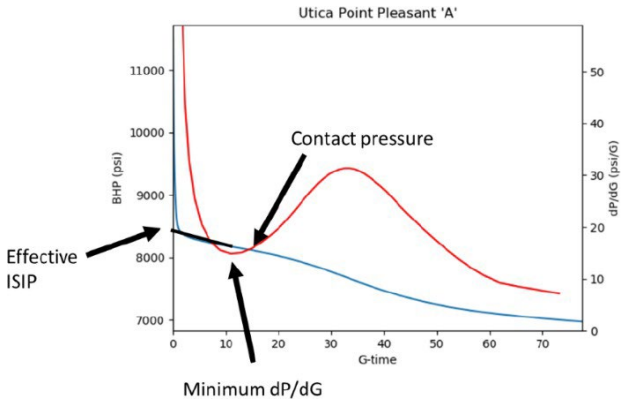

***Figure 36**. Example of the expected response of the bottom-hole pressure versus G-function for a DFIT test in the Utica shale. The blue curve is the pressure, and the red curve is the slope of the pressure versus G-function. The minimum principal stress estimated from this data is 8025 psi (McClure et al, 2019), the point labeled "Contact pressure" at approximately G-time=17*

To estimate the minimum principal stress, the surface pressure versus G-time function was interpreted and is shown in Figure 37. As the curve shows, after ISIP (3,900-4,000 psi), the pressure versus G-time curve is decreasing with a slowly decreasing slope from G=0.5 to the end of the test at G=2.5. During this time the pressure decreases by only approximately 40 psi. Based on the literature and the observations in the mini-frac test in CCS#1, the net pressure is likely in the 300-600 psi range, so the fracture would not be expected to close until the pressure declined by much more. Since the shut-in was terminated after approximately 3.5 minutes (approximately equal to the injection time), only an upper bound on $\sigma\sigma_3$, equal to the ISIP (≈4,000 psi), is possible from this data. It is reasonable to expect that $\sigma\sigma_3$ is in the range of 4,000 to 3,000 psi (net pressure of 0-1,000 psi) in the Eau Claire shale at 4,275 feet (1,303 m) TVD (0.70-0.94 psi/ft). This is within the range expected by the extended Eaton stress model (Thiercelin and Plumb, 1994) constructed by Schlumberger from the di-pole sonic logs (0.77-0.86 psi/ft) at this depth.

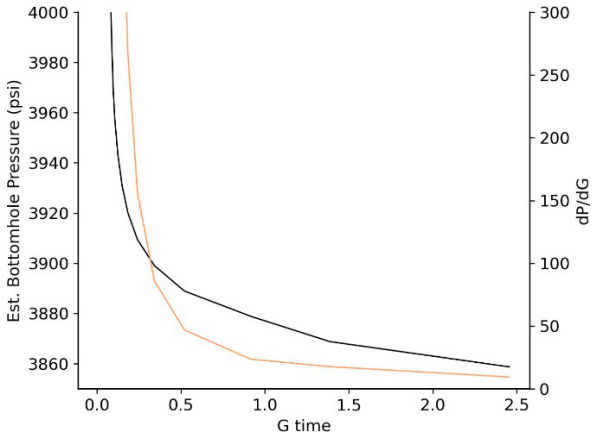

Figure 37*. Estimated bottom-hole pressure versus G time for the Eau Claire Shale DFIT test*

Combining the measurements from CCS#1 and the DFIT in the OEE #1 well, a probability distribution for the minimum horizontal stress in the Eau Claire Shale was constructed using a truncated normal distribution. The mean of the distribution was selected to be 0.85 psi/ft, which was the closure pressure identified in the CCS#1 mini-frac test. A standard deviation of 320 psi, (equal to half of the difference between the closure pressure and the propagation pressure in the CCS#1 and OEE #1 DFIT). The distribution was truncated at 3 standard deviations. The resulting stress probability distribution for the Eau Claire Shale at the depth of the DFIT measurement is illustrated in Figure 38. The plot on the left shows the probability density function for the minimal principal stress, and on the right, joint probability for the minimum and maximum horizontal stresses. This also illustrates high degree of uncertainty for the maximum horizontal stress, with possible values ranging from about 5,000 to 10,000 psi, which is expected for strike-slip faulting regime.

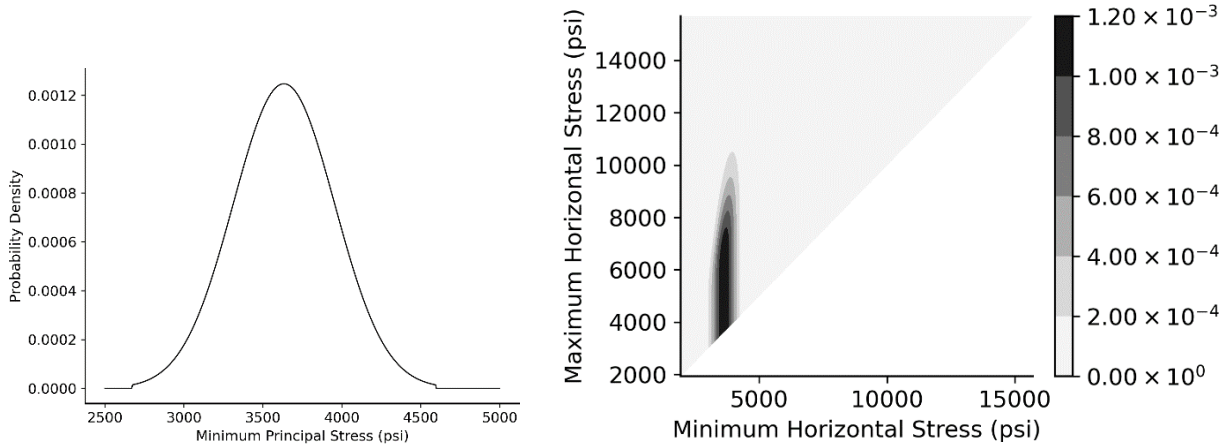

Figure 38. *Estimation of horizontal stresses using SoSAT at the Eau Claire shale at 4,275 feet (1,303 m) TVD. On the left, probability density for the minimal principal stress, and on the right, joint probability for the minimum and maximum horizontal stresses.*

A similar probability density function was developed for the Mt. Simon and Precambrian basement using data from IBDP's CCS#1 and the FutureGen 2.0 #1 data. For the Mt. Simon a mean of 0.75 psi/ft was used, and the standard deviation was selected to 652 psi, which is half of the difference

between the smallest measured value in the FutureGen 2.0 data set (0.53 psi/ft) and the mean. For the Precambrian basement a mean value of 0.85 psi/ft was used and a standard deviation of 348 psi was used, which again was half of the difference between the mean and the lowest measured value in the FutureGen 2.0 tests (0.82 psi/ft). Both of these distributions were also truncated at 3 standard deviations on both sides of the mean.

The magnitude of the minimum horizontal stress generally depends on the mechanical properties of each formation, and often varied nonlinearly within each formation due to local heterogeneities. Several models have been developed, primarily by the petroleum industry, to predict stress magnitudes from wireline logs and core measurements by making assumptions about the relationship between measured mechanical properties and the state of stress. Among these the most common is the extended Eaton stress model, which assumes that present day stresses arise primarily from the elastic compression of each geologic formation by a combination of the lithostatic stress and horizontal tectonic strains. The isotropic form of this model has the form,

$$SS_{hmmssmm} = \frac{vv}{1 - vv}\left(SS_{vv} - \alpha\alpha PP_{pp}\right) + \frac{EE}{1 - vv^2}\epsilon\epsilon_{hmmssmm} + \frac{EEvv}{1 - vv^2}\epsilon\epsilon_{hmmssmm} + \alpha\alpha PP_{pp}$$

$$SS_{hmmssmm} = \frac{}{1 - vv}\left(SS_{vv} - \alpha\alpha PP_{pp}\right) + \frac{}{1 - vv^2}\epsilon\epsilon_{hmmssmm} + \frac{}{1 - vv^2}\epsilon\epsilon_{hmmssmm} + \alpha\alpha PP_{pp}$$

where SS_{vv} is the lithostatic total stress, EE is the Young's modulus, vv is the Poisson's ratio, $\alpha\alpha$ is Biot's poroelastic coefficient, and $\epsilon\epsilon_{hmmssmm}$ and $\epsilon\epsilon_{hmmssmm}$ are the model's fitting parameters, which are often referred to as the tectonic strains since they are meant to quantify the effect of regional tectonic forces (Thiercelin, M.J. and R.A. Plumb 1994). A transversely isotropic form of this model is also commonly used. This model is generally used to provide a continuous estimate of the horizontal principal stresses based on a continuous estimate of the lithostatic stress derived from a density log, and the Young's modulus, Poisson's, and Biot coefficient derived from sonic logs. As discussed in the section above, there is often a significant difference in the magnitude of the Young's modulus when it is measured with sonic logs versus quasi-static laboratory compression tests. It is generally believed that quasi-static laboratory compression tests better represent the compressive stresses applied by the overburden and tectonic forces, so preference is given to laboratory-measured values. Because of this, various correlations have been developed to estimate the static Young's modulus (as the laboratory-derived value is called) from the dynamic Young's modulus (as the sonic-derived value is called). As shown in Figure 23, these correlations often show considerable error (~50% for the Eau Claire shale), especially for low porosity rocks.

When the elastic properties are well calibrated by laboratory tests and the tectonic strain parameters are calibrated based on high-quality stress measurements, the extended Eaton model often works very well at providing reasonable estimates for horizontal stresses in a region with similar geologic formations and tectonic environment. In some cases, however, some rock types exhibit significant inelastic responses such as creep and plastic yielding that are neglected by the elastic response assumed in the extended Eaton model (Sone, H. and M.D. Zoback 2014). This is most common in shales, particularly organic-rich shales, evaporites, and weak poorly consolidated sandstones. Pressure solution in carbonates has been suggested as another inelastic mechanism responsible for changes in stress in some cases (Magnenet, V., F.H. Cornet, and C. Fond 2017). Both creep and plastic yielding tend to result in an increase of the minimum principal stress, making it closer to the lithostatic stress and/or the maximum horizontal stress. The most extreme example of this type

of process is in salt formations where, because of the tendency of salt to creep, the state of stress is nearly isotropic and equal to the lithostatic stress in most salt formations. In less extreme forms the minimum principal stress does not fully reach the maximum principal stress (lithostatic or maximum horizontal stress) because the creep or yielding process diminishes with the difference between the principal stresses and eventually reaches an equilibrium.

To our knowledge the nonlinearities in the rheology of the formations of interest have not been well characterized such that it is difficult to know if a model for the in-situ stress can be constructed via a purely elastic-tectonic model or if a creep or yield-based model is needed for some formations. In any case for the purposes of establishing safe injection pressures it is best to rely on direct measurements of the minimum principal stress via hydraulic fracturing measurements (Haimson, B.C. and F.H. Cornet 2003, ASTM 2008) since even a well-calibrated stress model can yield errors of several hundred psi. For many oilfield applications, such as selecting drilling mud weights for wellbore stability or fracture height growth, errors of several hundred psi are often not significant. However, in a CO_2 injection application where the safe injection pressure limit is set up to 90% of the estimate for the minimum principal stress, the errors in stress models can approach and even exceed the 10% safety factor. Therefore, accurate and conservative measurement of the minimum principal stress instead of relying solely on a log-derived stress model is critical. Nonetheless, log-derived stress models can be useful and provide a reference estimate for the stresses and their likely variability for non-critical applications and will be included in the analysis below.

Figure 39 shows the depth profile of the principal stresses developed using the SOSAT tool with these formation-specific probability distributions together with the frictional faulting and regional faulting regime constraints. The light grey region indicates the 70% confidence interval and the dark grey indicates a 95% confidence interval. The depth ranges where these bounds are widest are the zones where no formation-specific probability distribution was used and reflect only the frictional faulting and regional faulting regime constraints. The black dashed line is the vertical stress profile developed by integrating the density logs, as discussed above. The dashed blue line indicates the estimated pore pressure profile of 0.43 psi/ft based on the DST tests described above. The green and red curves are the sonic-log derived stress model developed by Schlumberger using an extended Eaton model.

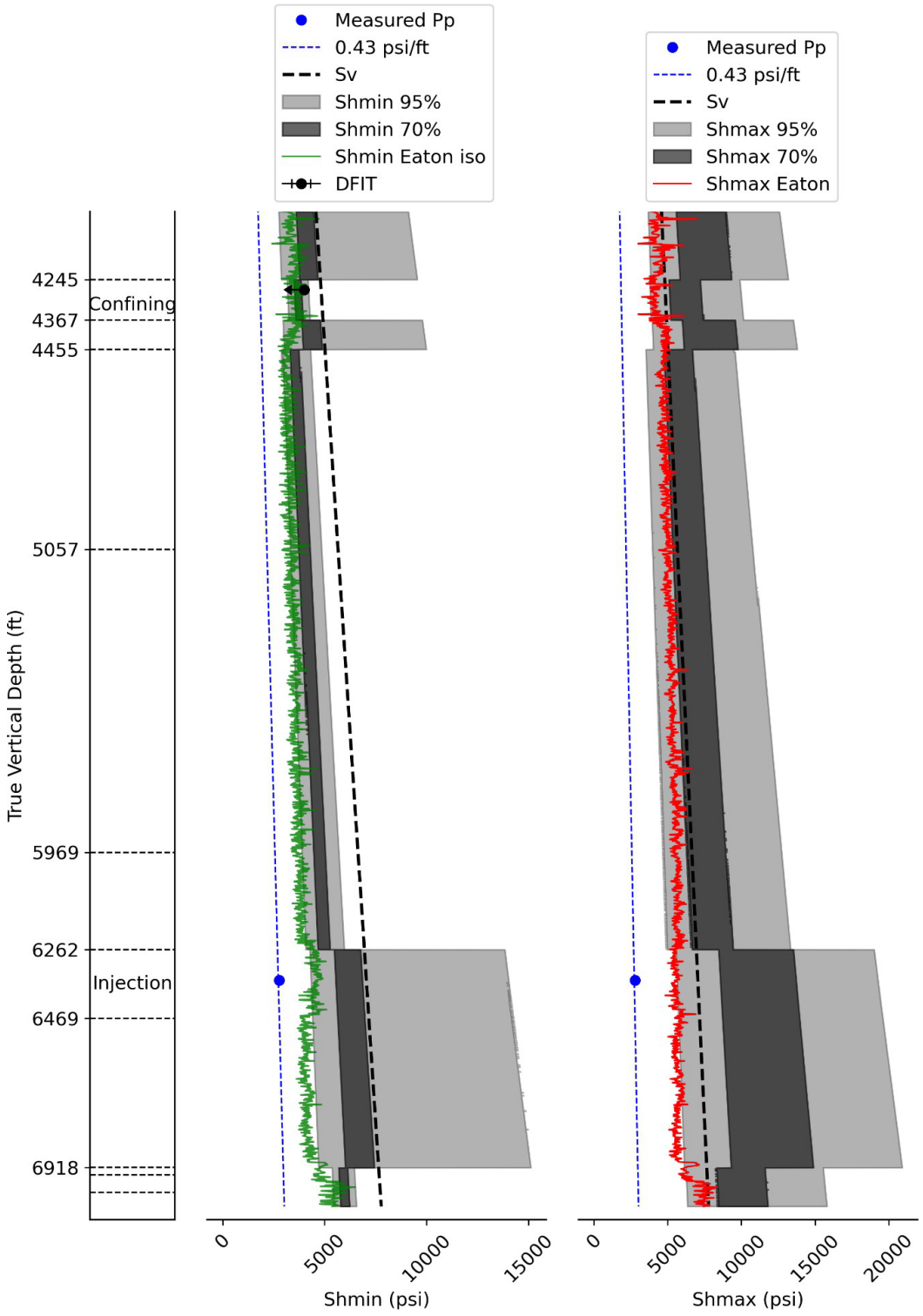

Figure 39. *State of stress distribution along a depth profile. Color bands indicate from broadest to narrowest (light gray to black) the 95% and 70% confidence interval for Shmin (right) and Shmax (left). Pp is represented with a dashed blue line and Sv with a dashed black line. The green and red curves are Eaton stress models derived from the sonic logs using isotropic elastic properties.*

Seismic History [40 CFR 146.82(a)(3)(v)]

In east-central Illinois, the region of the One Earth CCS project, earthquakes above magnitude 2.5 are rare. Figure 40 shows the map of earthquakes in Illinois from 1795 to 2019. Table 9. documents three seismic events having magnitudes of 3.2 to 4.2 are documented during the past 20 years within a radius of 100 miles of OEE #1 using the USGS Earthquake Catalog https://earthquake.usgs.gov/earthquakes/search/ and none are located within the project AoR.

Seismic frequency and intensity are most prominent in southern Illinois (Figure 40) where multiple seismic zones are located: the New Madrid Seismic Zone (NMSZ), the Wabash Valley Seismic Zone (WVSZ), the Saint Genevieve Seismic Zone (SGSZ), and the Rough Creek Graben (RCG).

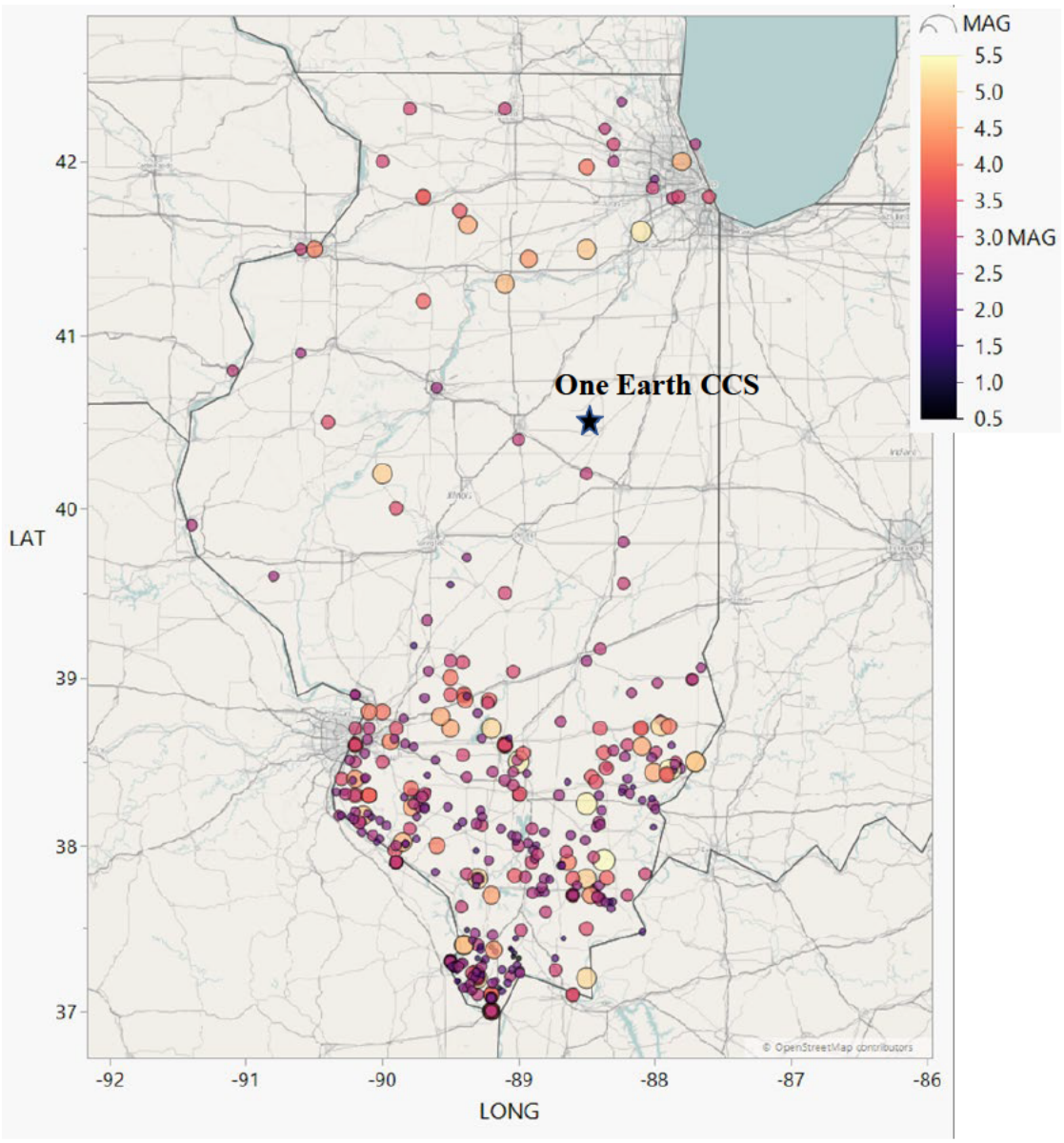

***Figure 40**. Map of Illinois Earthquakes (Full catalog N = 419 (earthquakes from 1795 – 2019).*

Table 9. *20 Year record of Earthquake Activity within a 100-mile radius of the One Earth Energy facility*

Distance (Miles)	Date	Latitude	Longitude	Magnitude	Location	Depth (Miles)
74	2021-06-17	39.8305	-87.2866667	3.82	Illinois-Indiana border region	3.89
95	2013-11-04	41.7999	-87.8247	3.2	0.62 miles SSW of Lyons, Illinois	0.62
72	2004-06-28	41.46	-88.9	4.2	7.46 miles NW of Dayton, Illinois	6.21

The USGS National seismic hazard map (Figure 41) depicts seismic risk based on peak ground accelerations having a 2 percent probability of being exceeded in 50 years. This is based on the most recent USGS models using seismicity (event frequency and magnitude) and fault-slip rates (https://www.usgs.gov/media/images/2018-long-term-national-seismic-hazard-map). The Seismic Hazard Map separates Illinois into multiple risk zones where the highest potential occurrence of larger magnitude events is in southernmost Illinois. The relative seismic risk at the One Earth Sequestration site is considered minimal.

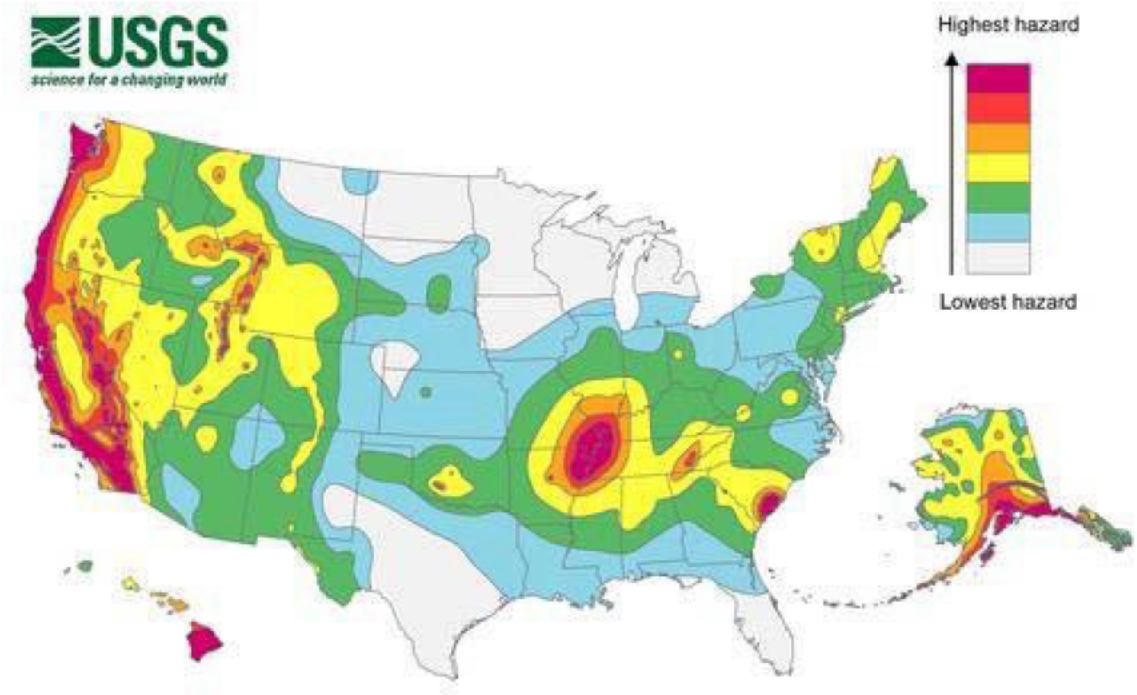

Figure 41. *2018 Long-term National Seismic Hazard Map (USGS)*

The USGS seismic hazard maps indicate the area including the One Earth Sequestration facility and proposed Area of Review (AoR) to have peak ground acceleration of approximately 6 percent of gravity (%g), based on the USGS Earthquake Hazard and Probability Map tool (https://earthquake.usgs.gov/hazards/interactive/). There is a 2 percent probability that the peak ground acceleration would approach approximately 7 percent g within 50 years for generic rock site conditions (Vs30 ≈ 760 m/s), based on the USGS National Seismic Hazard Model.

Hydrologic and Hydrogeologic Information [40 CFR 146.82(a)(3)(vi), 146.82(a)(5)]

The Illinois State Geological Survey (ISGS) is an official repository for records of wells drilled in the state of Illinois with records archived for over 700,000 wells dating back to the late 1800s. Many older well locations were documented from historical data records, a driller's log, or a well construction report, leaving out some level of locational accuracy. Although drillers have been providing latitude and longitude coordinates increasing since 2006 and ISGS staff have corrected well point coordinates in some areas, location description information on source documents have not been reviewed by ISGS staff and could be subject to future correction.

Water production wells, shallow monitor wells, and dry water well attempts were queried and plotted (Figure 42) within the One Earth Sequestration project Area of Review (AoR). The results of the water records query were 484 locations ranging in depth from 11 feet to 400 feet (3.4 to 122 m).

The AoR extends across eastern McLean County, western Ford County, and into northwestern Champaign County. Within the AoR land use is generally rural with scattered residences and agricultural activity. Gibson City is the largest population center within the AoR, with an estimated 2020 population of 3,340. The communities of Saybrook, IL (2020 population of 721), Anchor, IL (2020 population of 241), and Cropsey, IL also are within the AoR.

The USDWs within the AoR are the saturated sands and gravels within Wedron and Mason Groups (shallow and surficial aquifers), the Upper and Lower Glasford Formations, and Banner Formation, which will be discussed in the following sections. Several wells within the Gibson City municipal boundary in the southeastern AoR, and a well south of Gibson City, penetrate up to 400 feet (122 m) deep and produce from the carbonates of the Silurian and Devonian. The bedrock potential of the region will be discussed in more detail in the following sections. The lowermost USDW within the AoR is the Ordovician age St. Peter Sandstone at a depth of approximately 2,200 feet (670 m).

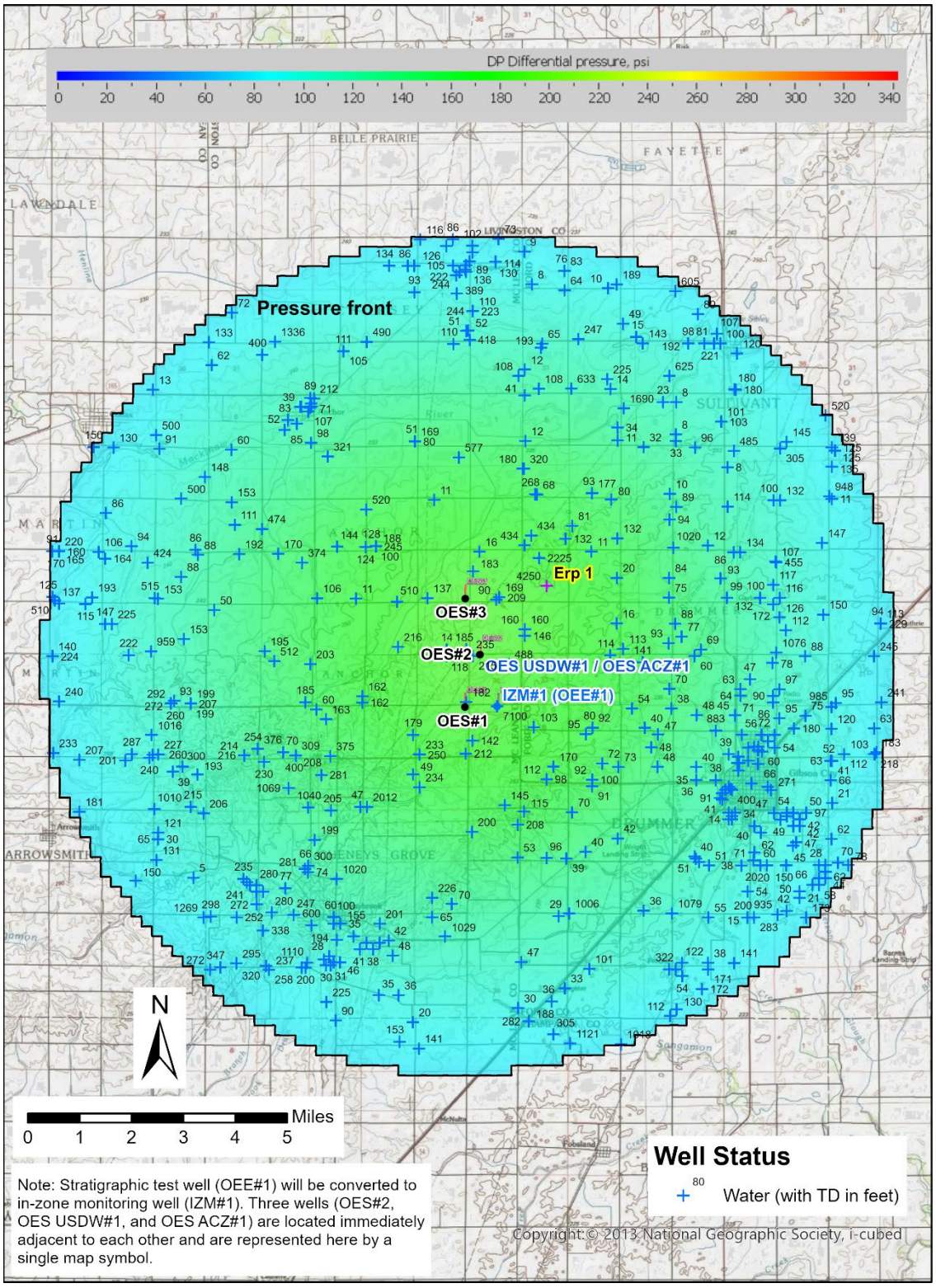

Figure 42*. Water production wells, shallow monitor wells, and dry water well attempts were identified within the One Earth Sequestration project AoR. The blue crosses are the water well locations with the total depth in feet.*

Groundwater resources are separated into 1) unconsolidated aquifers and 2) bedrock deposits: shallow bedrock sources are commonly used in the northern one-third of the state while the deep bedrock sources are most widely used in northeastern Illinois (IDNR 1999b). Most of the groundwater resources in the Ford and McLean County area are in the unconsolidated aquifers.

Unconsolidated Aquifers

The unconsolidated aquifers are sources of water to communities, industries, and rural residents of east-central Illinois (Stumpf et al., 2012). Using water wells and other data sources, these aquifer units have been extensively mapped in the approximately 400 feet (122 m) thick (Figure 43) glacial and non-glacial sediments that overlie the bedrock surface. Within the AoR, the unconsolidated sand and gravel aquifers are used as drinking water sources for many households, and the individual formations which contribute to water use throughout the area are discussed below. These formations are generally considered to be within the Mahomet Aquifer System (Figure 39).

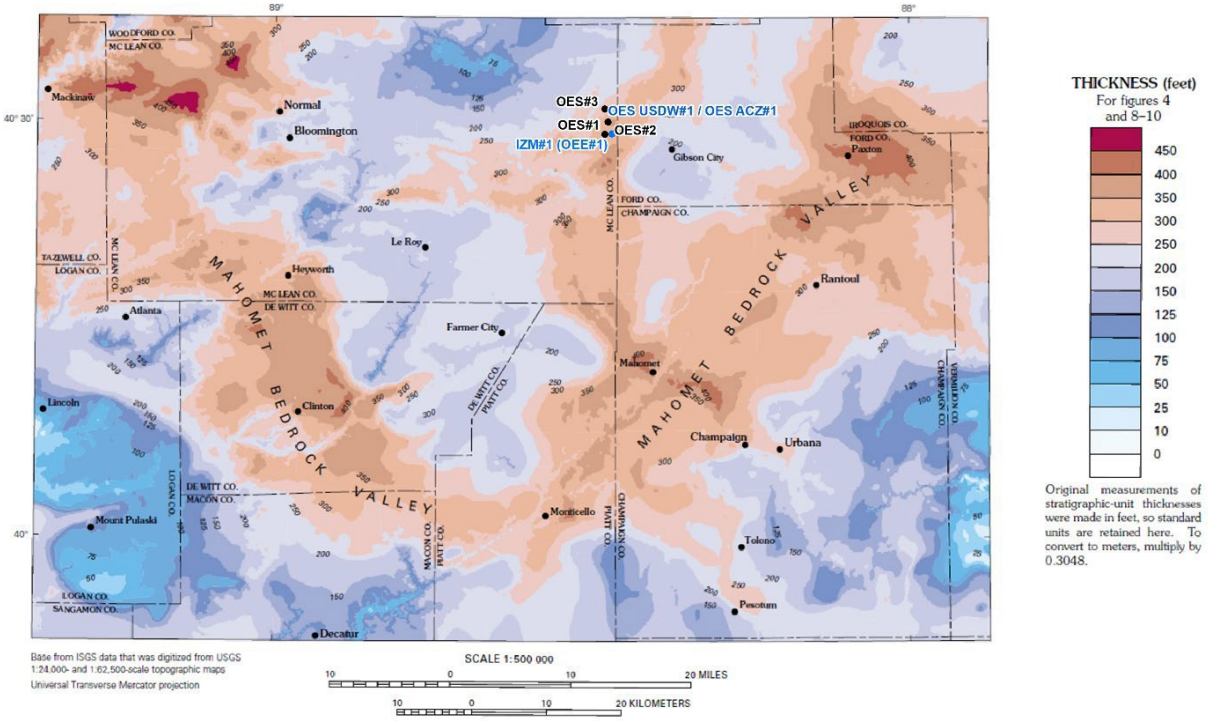

Figure 43. *Thickness of glacial sediments, including minor overlying sediments of nonglacial origin (modified from Soller et al., 1999). One Earth CCS project wells are included and labeled near the north-central portion of the image.*

Prior to glaciation, in east central Illinois, bedrock was uplifted several hundred million years ago and deeply incised to form the Mahomet Bedrock Valley (Locke et al., 2018).

The Mahomet-Teays River was part of a large drainage network that connected drainage from the Appalachian Mountains through the Mahomet Bedrock Valley westward towards the Ancient Mississippi River. The valley walls of the Mahomet Bedrock Valley were exposed at the land surface until the early part of the Illinois Episode, when it was finally filled in by deposits of glacial till, silt, clay, and sand and gravel (Kempton et al. 1991; Soller et al. 1999).

The glacial periods from youngest to oldest are: the Wisconsin and Hudson Episodes, Illinois Episodes, and pre-Illinois. Figure 44 illustrates, from surface to top of bedrock, the 1) shallow and surficial aquifers, 2) aquifers in the Upper Glasford Formation, 3) aquifers in the lower Glasford Formation, 4) aquifers in the Banner Formation, and 5) the Mahomet Aquifer identified in the glacial and post glacial sediments.

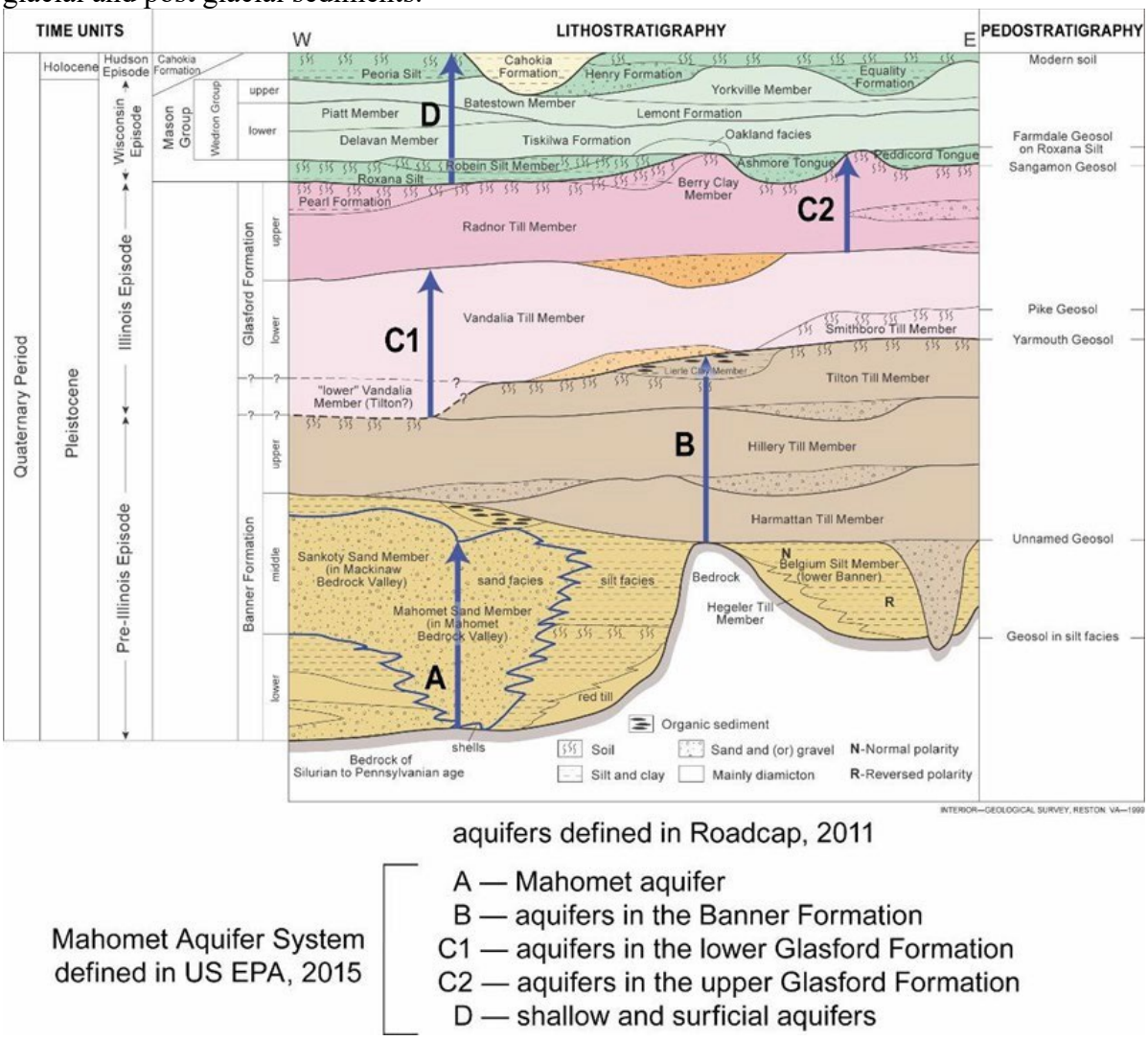

Figure 44. *Stratigraphic column and correlation of glacial deposits (Soller et al., 1999). Hydrogeologic framework recreated from Roadcap et al., 2011. The Sole Source Aquifer designation of the Mahomet aquifer, the Mahomet aquifer system (US EPA, 2015), includes all the hydrogeologic units of Roadcap et al., 2011. The Mahomet Sand Member and the Sankoty Sand Member of the Banner Formation are outlined in blue.*

The uppermost sediments of Quaternary Period in the project area are assigned to the Wisconsin and Hudson Episodes, a period starting ~60,000 years ago (Willman and Frye, 1970; Hansel and Johnson,1996; Johnson et al. 1997; Stiff and Hansel 2004). The shallow and surficial aquifers (Figure 45) can range in thickness from 25 up to 200 feet (8 to 61 m) thick. Thin, discontinuous sand and gravel deposits assigned to the Henry Formation and sand and gravel assigned to the Ashmore Tongue of the Henry Formation make up these aquifers. Additionally, some discontinuous sand and gravel deposits without any formal names are recognized in local mapping

efforts. Within the AoR these shallow sands and gravels are used as sources of drinking water for many households.

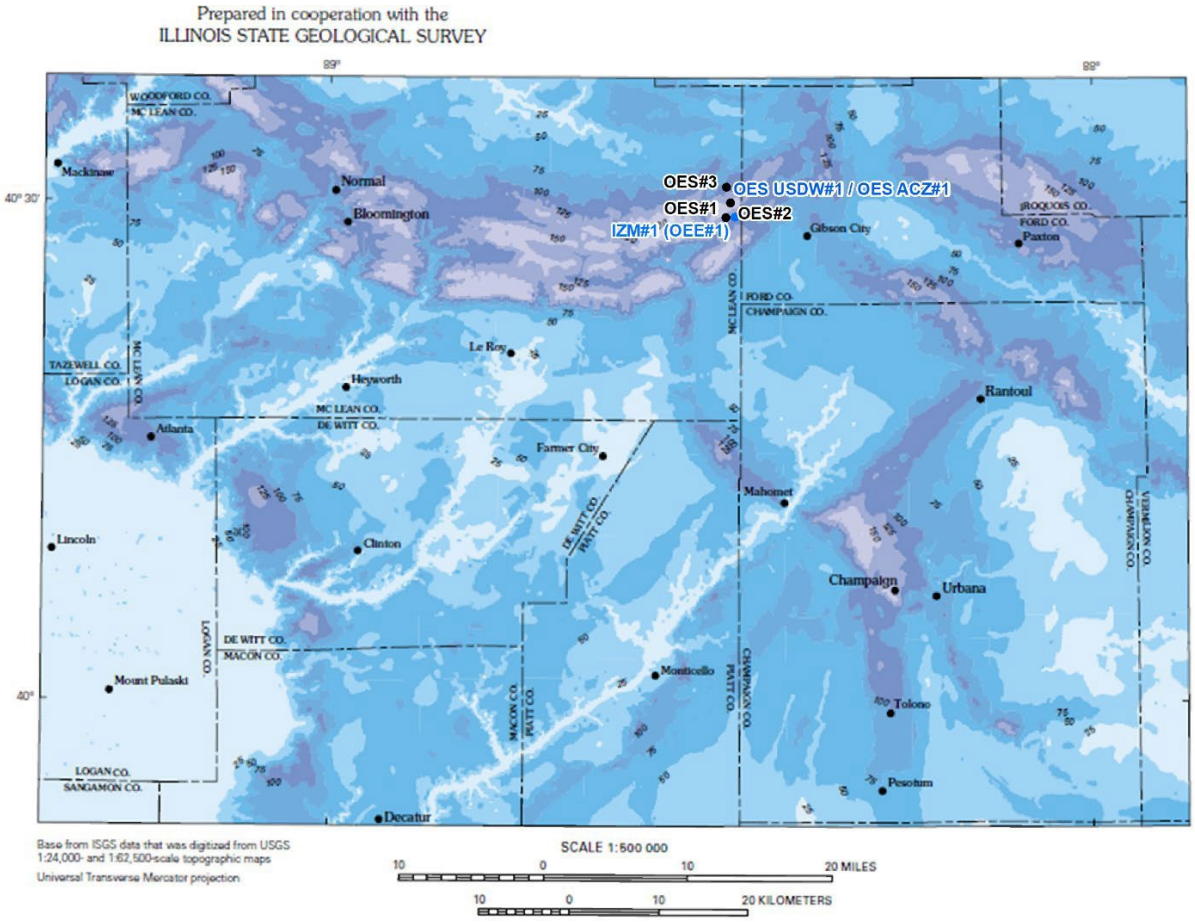

Figure 45. *Thickness of the Wedron and Mason Groups (Wisconsin Episode); includes minor thickness of the Cahokia Formation (Wisconsin and Hudson Episodes - modified from Soller et al., 1999). One Earth CCS project wells are included and labeled near the north-central portion of the image.*

Additionally, aquifers through the area are found in Illinoisian and pre-Illinoisian sediments. The sediments assigned to the Illinois Episode (~190,000 to ~130,000 years ago) include the Upper and Lower Glasford Formations (Figure 46), which can range in thickness from absent in modern river valleys to over 150 feet (46 m). The Glasford Formation sediments are discontinuous sands and gravels within or overlying the Vandalia Till Member or undifferentiated coarse-grained deposits within the Glasford itself.

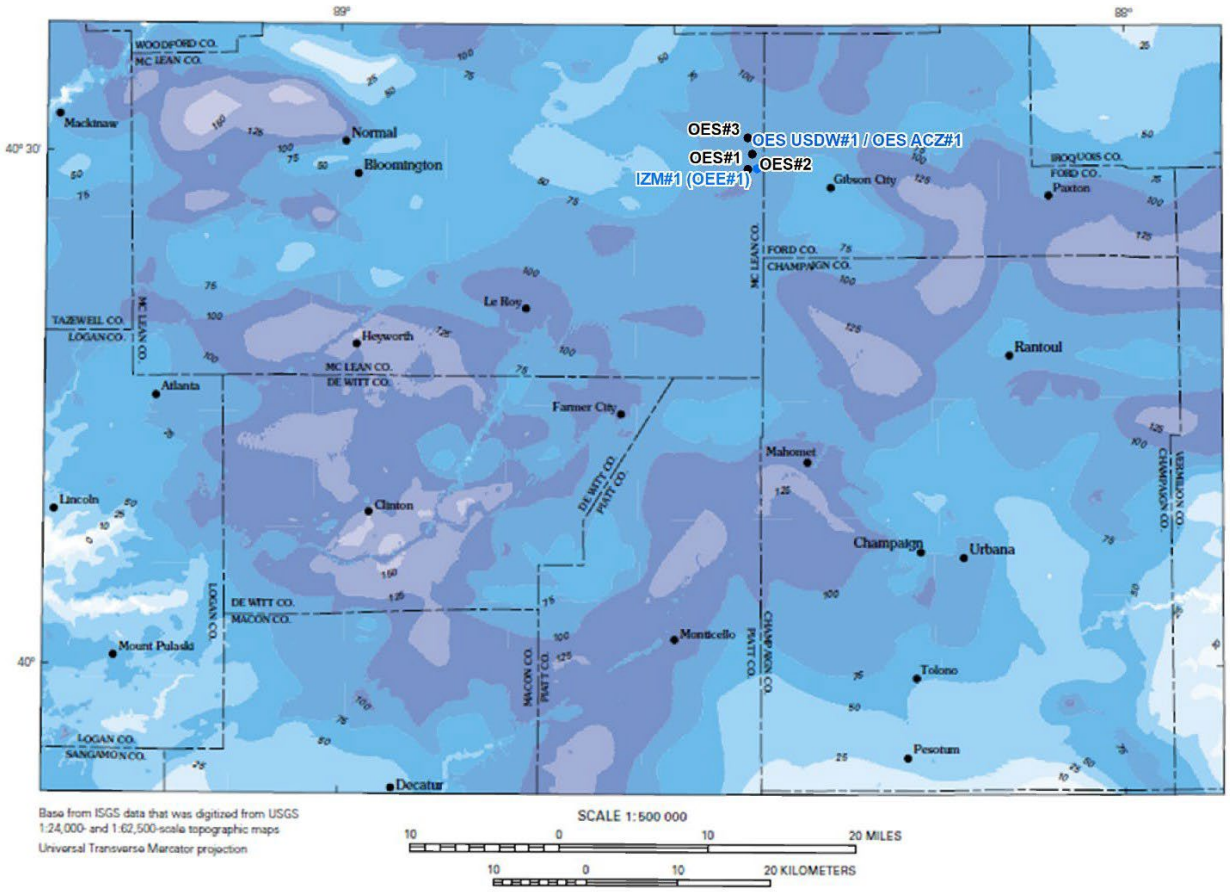

Figure 46. *Thickness of the Glasford Formation (Illinois Episode - modified from Soller et al., 1999). One Earth CCS project wells are included and labeled near the north-central portion of the image.*

The pre-Illinois Episode (~300,000 to ~130,000 years ago) was a period of multiple advances and meltings. The Upper, Middle, and Lower Banner Formation (Figure 47) can be absent due to erosion or up to 250 feet (76 m) thick through the region. The Mahomet Sand Member is the lowermost unit within the Banner Formation.

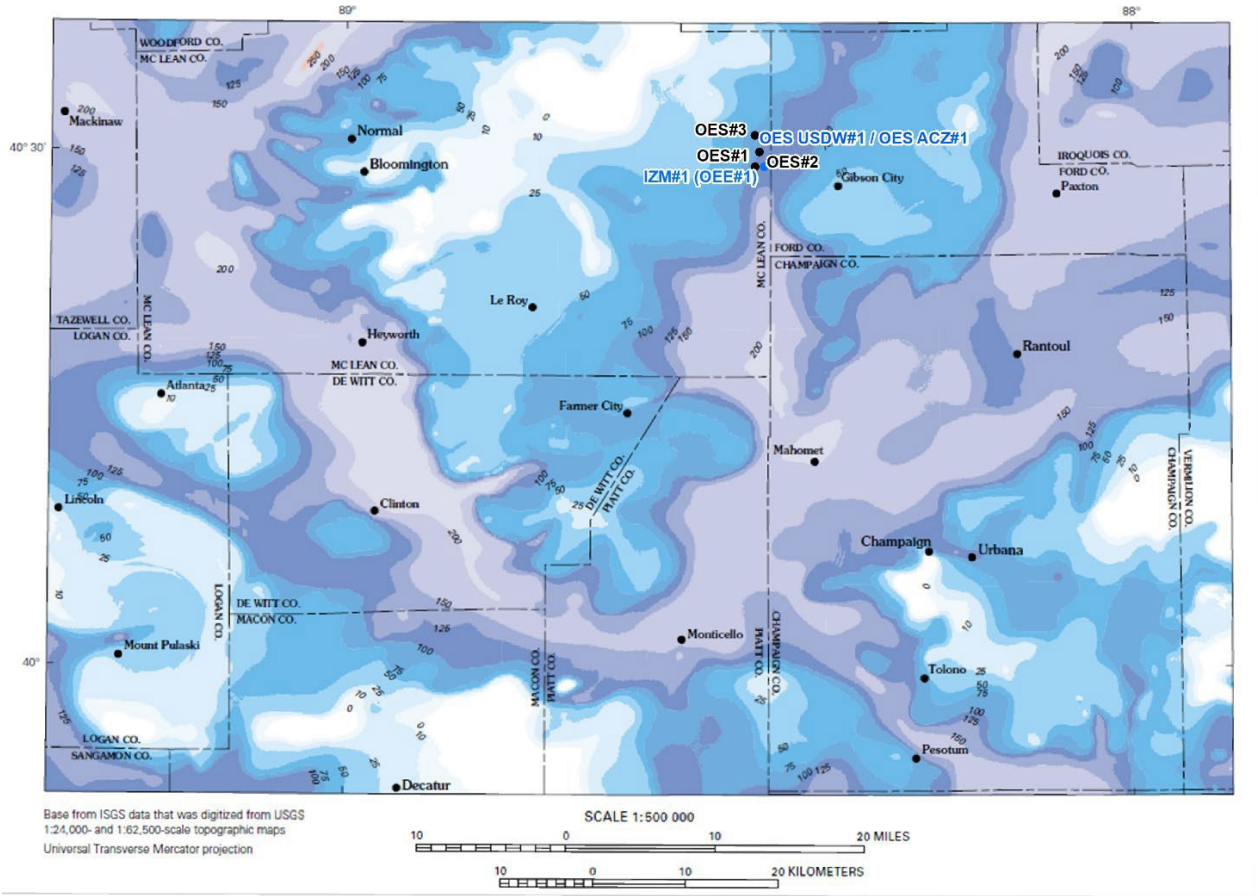

Figure 47. *Thickness of the Banner Formation (pre-Illinois Episode - modified from Soller et al., 1999). One Earth CCS project wells are included and labeled near the north-central portion of the image.*

Mahomet Aquifer

The Mahomet Aquifer extends across portions of 14 counties in east-central Illinois producing an average daily groundwater withdrawal rate estimated to be 210 million gallons a day (Roadcap et al., 2011) and providing an estimated "53 million gallons per day (mgd) of drinking water to approximately 120 public water supplies and thousands of rural wells" that serve over 500,000 people in the region (USEPA, 2015).

The One Earth Energy facility and proposed activity area are within the mapped boundary of the Sangamon River near Fisher Upstream Area watershed, Sugar Creek watershed, and Tributary to the Middle Fork Vermilion River watershed, which are adjacent to the Mahomet Sole Source Aquifer (SSA). The Project Review Area for the Mahomet SSA (Figure 48) consists of the designated SSA area plus these three adjacent watersheds that provide recharge to the Mahomet Aquifer System.

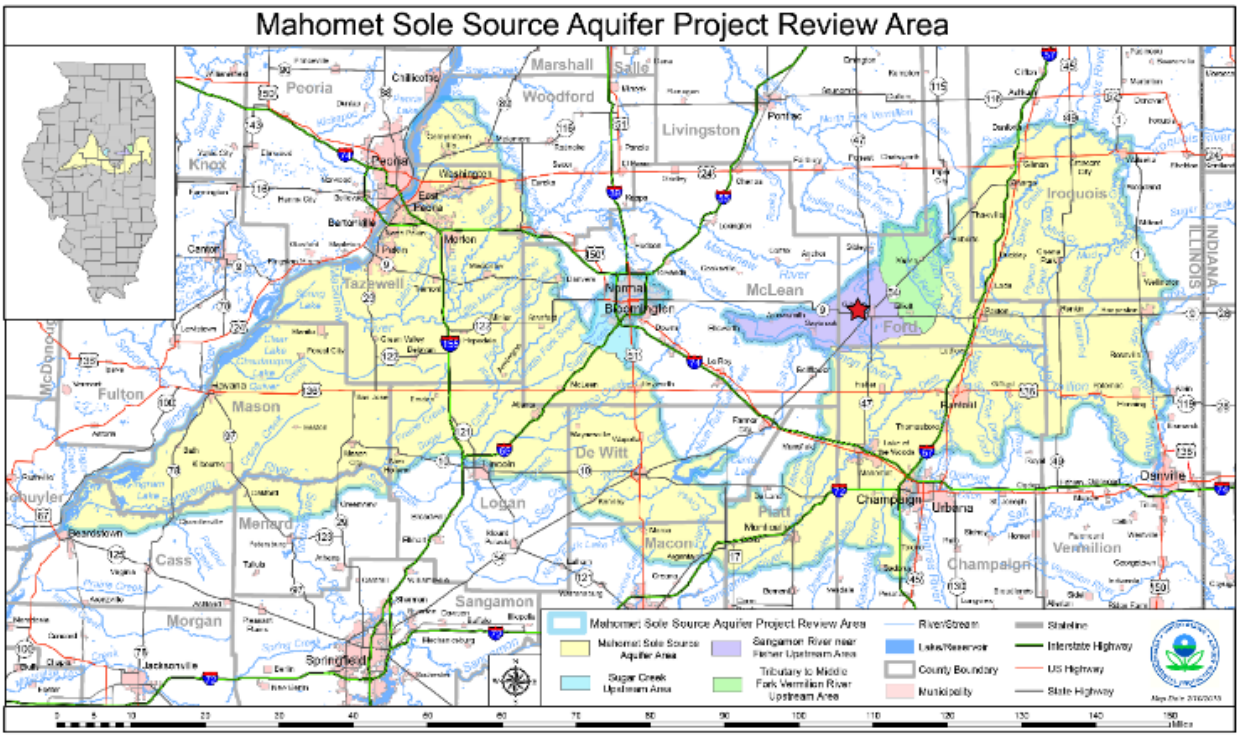

***Figure 48**. Location of One Earth Energy (red star) in relation to the Mahomet Sole Source Aquifer in yellow (USEPA).*

Bedrock Aquifers

A generalized geology of hydrostratigraphic units and non-aquifer units in east-central Illinois (Selkregg and Kempton 1958) is presented in Figure 49. Cambrian and Ordovician-age rocks are predominantly sandstones, Silurian through Mississippian-age rocks are predominantly carbonates, and Pennsylvanian-age rocks are shales, sandstones, and coal measures (Kelly et al 2018). The bedrock geology map of Champaign County and adjacent areas (Stumpf and Dey, 2012, modified from Kolata 2005) shows the regional bedrock change around the One Earth Sequestration project site.

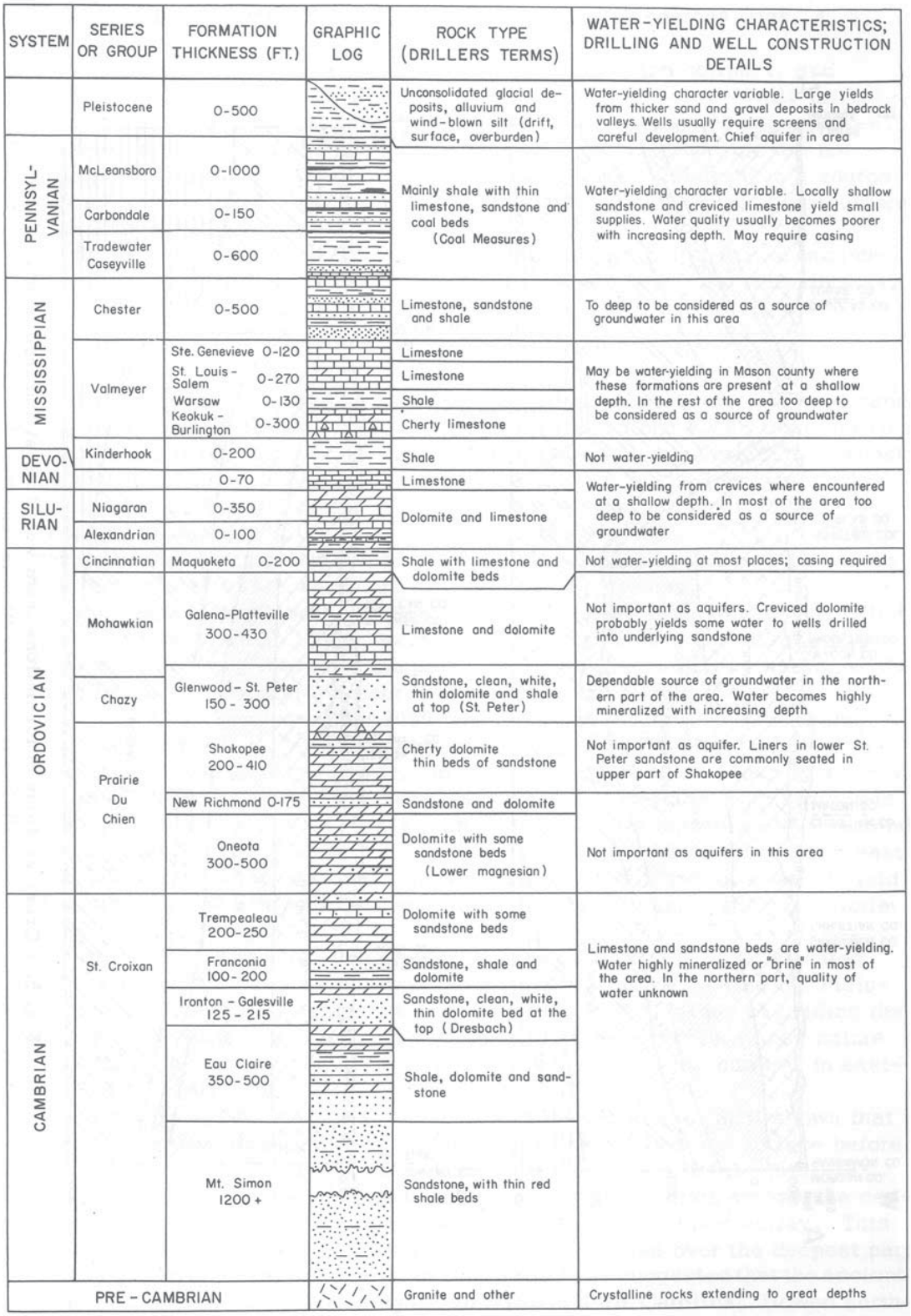

Figure 49. *Generalized geology of hydrostratigraphic units and non-aquifer units in east-central Illinois (Selkregg and Kempton 1958).*

Pennsylvanian

The Pennsylvanian rocks, in descending stratigraphic order, consist of the McLeansboro Group, the Carbondale Formation and Tradewater Formations. The Mattoon Formation, Shelburn-Patoka, Carbondale, and Tradewater Formations have been mapped in the region. Some of the shallow sandstones have the capacity to supply groundwater but the quality usually becomes poor with depth and these units are not generally used as a source of water. The Pennsylvanian formations are not present to the east due to erosion but are present throughout much of the region (Figure 50). Where present, the Pennsylvanian is between 270 to 325 feet (83 to 99 m) below surface and is between 300 to 450 feet (91 to 137 m) thick.

Mississippian

The Mississippian sediments are thin throughout the AoR with limited potential for consistent groundwater production. Regional mapping of the Mississippian aged deposits indicates that the sediments are eroded throughout most of project area except for Ford County and Champaign County. Two Mississippian aged limestone units which could potentially supply water, the Burlington-Keokuk and the Choteau, have been identified through recent correlation in the One Earth #1 well. The Burlington-Keokuk (which overlies the Choteau) and the Choteau occur between 710 feet (216 m) to approximately 750 feet (229 m) deep with a gross thickness of approximately 40 feet (12 m).

Devonian

Regional mapping has identified the presence of Devonian aged strata along the southwestern and southern boundary of Ford County into north central Champaign County. Within the AoR, the Devonian ranges between 800 and 1000 feet (244 to 305 m) deep to the west and northwest of the One Earth Energy #1 well. In the southeastern part of the AoR, the Devonian occurs at the bedrock surface, typically at depths of 210 to 250 feet (64 to 76 m). Further to the north (approximately 8-10 miles beyond the extent of the AoR) these rocks have been eroded away. In the One Earth #1 well the New Albany occurs from 753 to 903 feet (230 to 275 m) deep for a thickness of 149 feet (45 m). Groundwater production from the Devonian sediments is not favorable regionally, although several wells within the Gibson City municipal boundary in the southeastern AoR, and also south of Gibson City, penetrate up to 400 feet (122 m) deep and produce from the carbonates of the Silurian and Devonian.

Silurian

In the vicinity of Gibson City and through the southeastern portion of the AoR, the Silurian occurs near the surface of bedrock at depths of roughly 250 to 275 feet (76 to 83 m). West of Gibson City the Silurian is present at depths between 885 to 1020 feet (270 to 311 m), reaching a gross thickness of 520 to 610 feet (158 to 186 m) in the western portion of the AoR. Within the AoR, groundwater production in the Silurian occurs only in a few wells within Gibson City municipal boundary and south of Gibson City (see Devonian discussion above); outside of the Gibson City area, and at increased depths, strata of the Silurian are not a reliable source of drinking water.

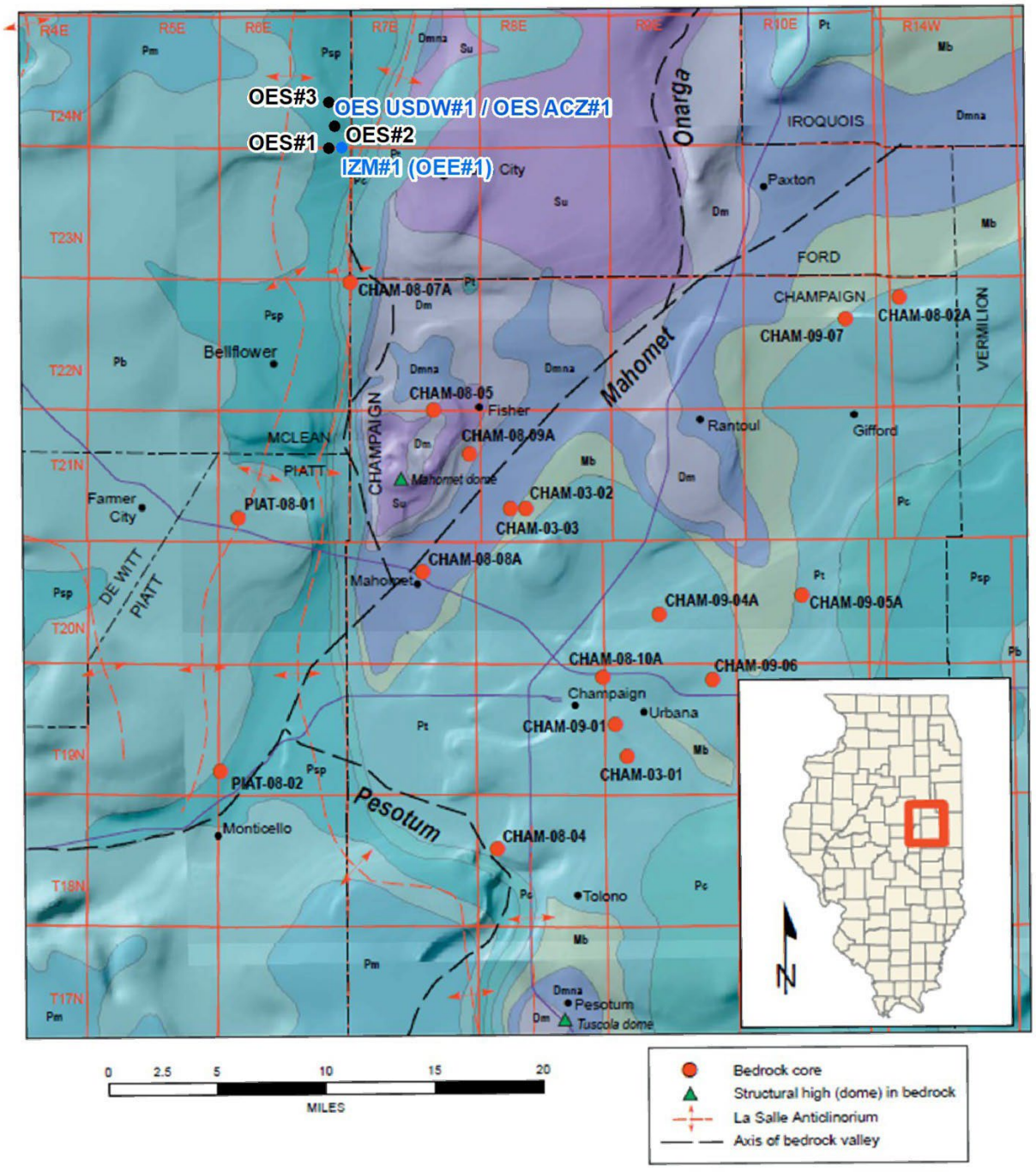

Figure 50. *Bedrock geology map of Champaign County and adjacent areas (modified from Stumpf and Dey, 2012, as modified from Kolata 2005) overlain on hill-shaded bedrock topographic bedrock surface. Bedrock unit mapped in the figure in descending age are the Pennsylvanian Mattoon Formation (Pm), Bond Formation (Pb), Shelburn-Patoka (Psp), Carbondale Formation (Pc), and Tradewater Formation (Pt), the Mississippian Borden Siltstone (Mb), the Devonian New Albany (Dmna) and Cedar Valley Limestone (Dm) and the Silurian Racine Dolomite (Su). One Earth CCS project wells are included and labeled in the northwest portion of the image.*

Ordovician – Galena/Trenton and Platteville

Within the One Earth #1 well the limestones and dolomites of the Galena and Platteville Formations reached a total thickness of 425 feet (130 m) occurring from 1792 to 2217 feet (546 to 676 m) deep. As summarized in Figure 49 some potential may exist for minor groundwater production, but the units are not considered a reliable aquifer. No wells within the AoR draw water from these formations.

Ordovician – St. Peter Sandstone

The Ordovician St. Peter and Cambrian Ironton-Galesville Sandstones are important aquifers in northern Illinois and in parts of Wisconsin, Iowa, and Minnesota (Wilson, 2011). The St. Peter Sandstone is a quartz-rich sandstone formation found throughout most of Illinois (Figure 51). The St. Peter Sandstone is an important source of drinking water in northern Illinois and Wisconsin where it is relatively shallow, but in central Illinois it is not sourced for groundwater mainly due to great depth; it is 2217 to 2449 feet (676 to 746 m) deep in the One Earth Energy #1 well. The City of Bloomington, McLean County, IL drilled two high-capacity wells into the St. Peter Sandstone to provide a secondary water source during drought to compliment surface water production from Lake Bloomington and Lake Evergreen. One Earth Energy #1 is approximately 25 miles (40 km) due east of the municipal boundary of Bloomington, IL.

Within Ford and McLean Counties the St. Peter Sandstone has been identified as the lowermost underground source of drinking water having TDS less than 10,000 mg/L. Drill stem test sampling was completed in the St. Peter Sandstone in the One Earth Energy #1 well to collect a representative water sample. The TDS concentration of the fluid retrieved from the St. Peter Sandstone was 1779 mg/L. Baseline gaseous CO_2 concentrations in USDWs or other formations along the wellbore are unavailable.

During drilling of OEE1 (to be IZM1), formation water samples were collected from the St. Peter Sandstone, the formation identified as the lowermost USDW (Table 10). USDWs within the AoR will be sampled during the drilling and Pre-Operational phases. Analytical results of baseline geochemical samples of USDWs will be shared with the Director.

Table 10. *Analytical Results for the Formation Water Sample Collected from the St. Peter Sandstone (Lowermost USDW).*

Date	Parameter	Value	Time	Units	Method
06-Jan-22	Sn	-0.022	44550.5592	mgL	EPA200.7
06-Jan-22	NO3_N	-0.02	44550.93774	mgL	EPA300.0
06-Jan-22	Pb	-0.019	44550.5592	mgL	EPA200.7
06-Jan-22	pH	8.051	44547.53152	SU	EPA150.1
06-Jan-22	S	31.8947	44550.5592	mgL	EPA200.7
06-Jan-22	Sb	-0.059	44550.5592	mgL	EPA200.7
06-Jan-22	Se	-0.13	44550.5592	mgL	EPA200.7
06-Jan-22	Si	3.96952	44550.5592	mgL	EPA200.7
06-Jan-22	P	-0.031	44550.5592	mgL	EPA200.7
06-Jan-22	SO4	81.99141	44550.93774	mgL	EPA300.0

06-Jan-22	Sr	1.68227	44550.5592	mgL	EPA200.7
06-Jan-22	TDS	1670	44551.39183	mgL	SM2540
06-Jan-22	Ti	0.004594	44550.5592	mgL	EPA200.7
06-Jan-22	Tl	-0.047	44550.5592	mgL	EPA200.7
06-Jan-22	V	-0.016	44550.5592	mgL	EPA200.7
06-Jan-22	Zn	0.007102	44550.5592	mgL	EPA200.7
06-Jan-22	Al	0.140661	44550.5592	mgL	EPA200.7
06-Jan-22	Fe	0.17983	44550.5592	mgL	EPA200.7
06-Jan-22	Ni	-0.021	44550.5592	mgL	EPA200.7
06-Jan-22	B	1.39639	44550.5592	mgL	EPA200.7
06-Jan-22	Li	0.247594	44550.5592	mgL	EPA200.7
06-Jan-22	Ba	0.039211	44550.5592	mgL	EPA200.7
06-Jan-22	Be	-0.00014	44550.5592	mgL	EPA200.7
06-Jan-22	Br	3.137641	44550.93774	mgL	EPA300.0
06-Jan-22	Ca	34.0873	44550.5592	mgL	EPA200.7
06-Jan-22	Cd	-0.0043	44550.5592	mgL	EPA200.7
06-Jan-22	Cl	762.6035	44551.06551	mgL	EPA300.0
06-Jan-22	Co	-0.0022	44550.5592	mgL	EPA200.7
06-Jan-22	Mo	0.16115	44550.5592	mgL	EPA200.7
06-Jan-22	Cu	-0.0016	44550.5592	mgL	EPA200.7
06-Jan-22	F	3.352888	44551.06551	mgL	EPA300.0
06-Jan-22	Alk_CaCO3lab	299.0215	44547.53152	mgL	SM2320B EPA 310.1 APHA 2320
06-Jan-22	K	17.5035	44550.5592	mgL	EPA200.7
06-Jan-22	As	-0.02	44550.5592	mgL	EPA200.7
06-Jan-22	Mg	20.0227	44550.5592	mgL	EPA200.7
06-Jan-22	Mn	0.225488	44550.5592	mgL	EPA200.7
06-Jan-22	Na	552.605	44550.5592	mgL	EPA200.7
06-Jan-22	Cr	-0.0016	44550.5592	mgL	EPA200.7
06-Jan-22	Sb	-0.059	44550.56164	mgL	EPA200.7
06-Jan-22	S	37.9472	44550.56164	mgL	EPA200.7
06-Jan-22	pH	7.899	44547.54287	SU	EPA150.1
06-Jan-22	Pb	-0.019	44550.56164	mgL	EPA200.7
06-Jan-22	P	0.03823	44550.56164	mgL	EPA200.7
06-Jan-22	Se	-0.13	44550.56164	mgL	EPA200.7
06-Jan-22	Ni	-0.021	44550.56164	mgL	EPA200.7
06-Jan-22	Ti	0.004252	44550.56164	mgL	EPA200.7
06-Jan-22	NO3_N	-0.02	44551.0144	mgL	EPA300.0
06-Jan-22	Si	4.32159	44550.56164	mgL	EPA200.7
06-Jan-22	Sn	-0.022	44550.56164	mgL	EPA200.7
06-Jan-22	SO4	89.04672	44551.0144	mgL	EPA300.0
06-Jan-22	TDS	1779	44551.39222	mgL	SM2540

06-Jan-22	Tl	-0.047	44550.56164	mgL	EPA200.7
06-Jan-22	V	-0.016	44550.56164	mgL	EPA200.7
06-Jan-22	Mo	0.086127	44550.56164	mgL	EPA200.7
06-Jan-22	Mn	0.412919	44550.56164	mgL	EPA200.7
06-Jan-22	Sr	1.54286	44550.56164	mgL	EPA200.7
06-Jan-22	Alk_CaCO3lab	297.904	44547.54287	mgL	SM2320B EPA 310.1 APHA 2320
06-Jan-22	Na	591.717	44550.56164	mgL	EPA200.7
06-Jan-22	Al	0.15882	44550.56164	mgL	EPA200.7
06-Jan-22	Zn	0.020982	44550.56164	mgL	EPA200.7
06-Jan-22	As	-0.02	44550.56164	mgL	EPA200.7
06-Jan-22	B	1.44419	44550.56164	mgL	EPA200.7
06-Jan-22	Ba	0.031884	44550.56164	mgL	EPA200.7
06-Jan-22	Be	-0.00014	44550.56164	mgL	EPA200.7
06-Jan-22	Br	3.335905	44551.0144	mgL	EPA300.0
06-Jan-22	Ca	36.577	44550.56164	mgL	EPA200.7
06-Jan-22	Cd	-0.0043	44550.56164	mgL	EPA200.7
06-Jan-22	Mg	17.7764	44550.56164	mgL	EPA200.7
06-Jan-22	Co	-0.0022	44550.56164	mgL	EPA200.7
06-Jan-22	Cr	-0.0016	44550.56164	mgL	EPA200.7
06-Jan-22	Cu	-0.0016	44550.56164	mgL	EPA200.7
06-Jan-22	F	3.15565	44551.14218	mgL	EPA300.0
06-Jan-22	Fe	0.764234	44550.56164	mgL	EPA200.7
06-Jan-22	K	17.3924	44550.56164	mgL	EPA200.7
06-Jan-22	Li	0.298947	44550.56164	mgL	EPA200.7
06-Jan-22	Cl	816.1013	44551.14218	mgL	EPA300.0

Panno et al. (2018) developed a map of TDS for the St. Peter Sandstone formation waters for the Illinois Basin (Figure 52) that is discussed further in the GEOCHEMISTRY section. This map indicates the St. Peter Sandstone is a USDW within much of the northern half of the Illinois Basin.

Cambrian – Ironton and Galesville Formation

The Cambrian Ironton-Galesville Sandstones are important sources of drinking water in northern Illinois, but for the One Earth Sequestration area the salinity of the formation water exceeds the 10,000 mg/L threshold for USDW. Calculations of salinity were run for the Ironton and Galesville Formations using formation temperature, apparent water resistivity and formation resistivity. The results indicate the average salinity of Ironton Formation water is 39,000 ppm, and Galesville Formation water is 36,000 ppm.

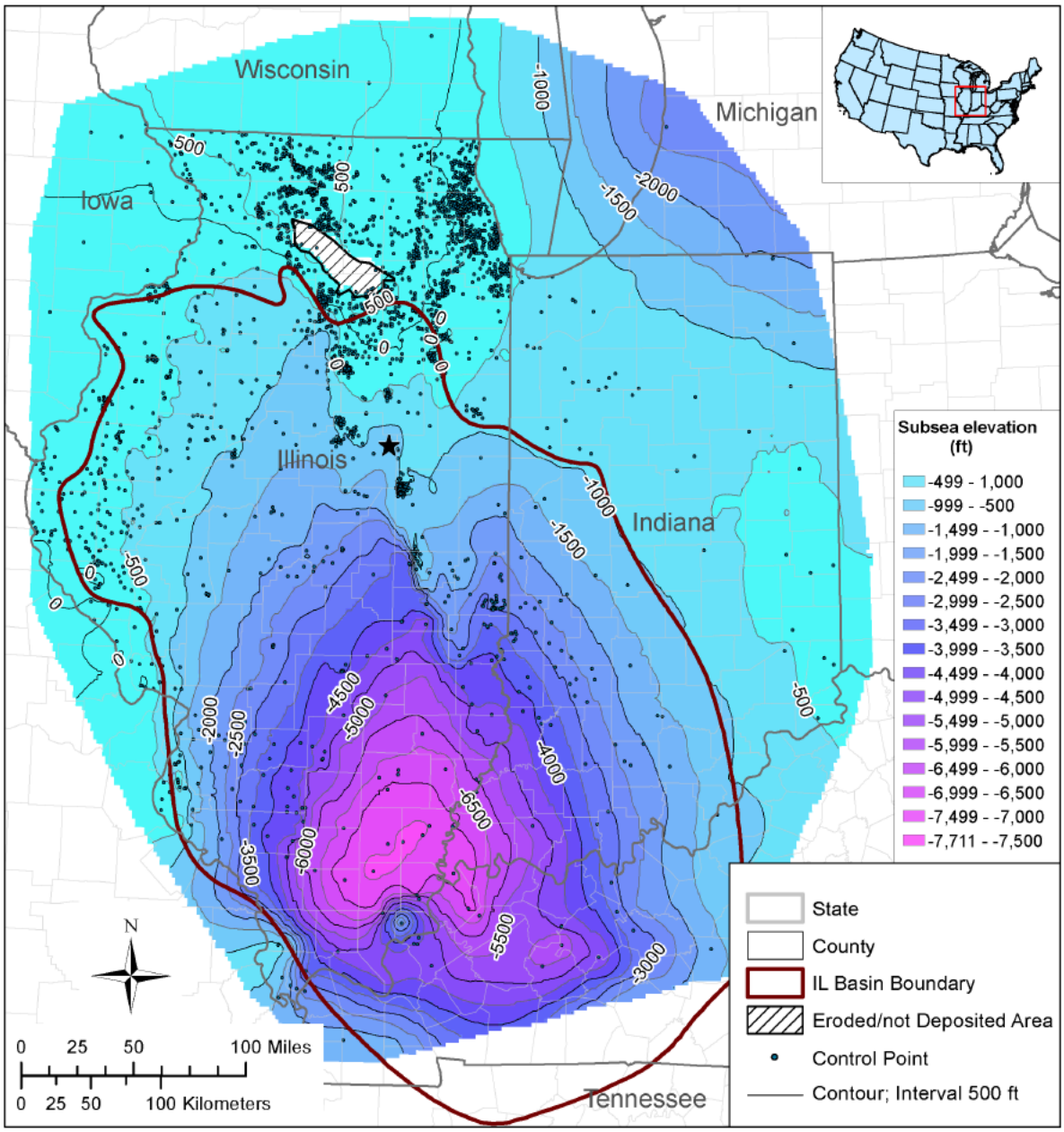

Figure 51. *Regional structure contour map of the St. Peter Sandstone. The black star is the location of the OES project site.*

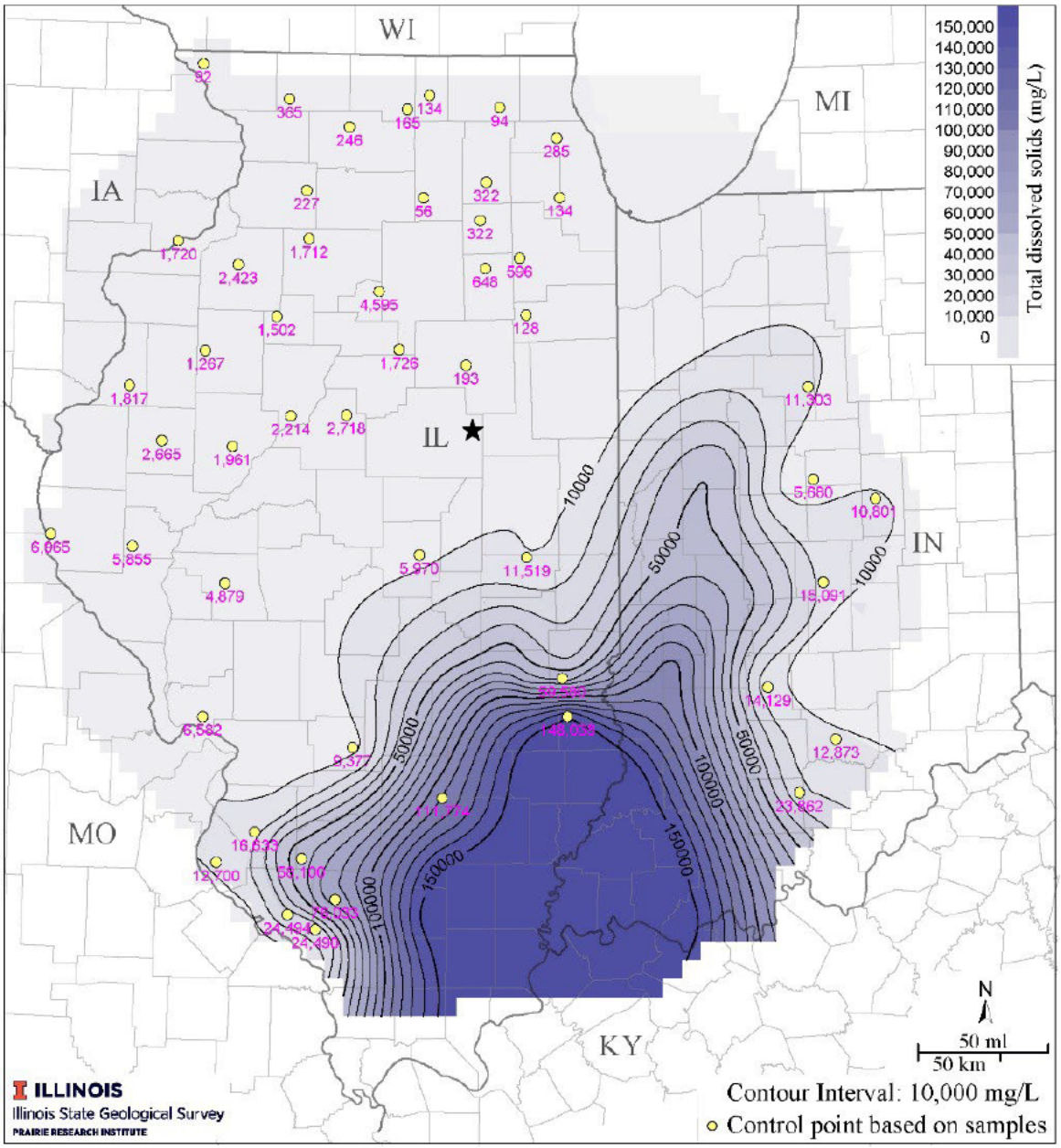

Figure 52. *Contour map of estimated total dissolved solids in St. Peter Sandstone formation waters (unpublished work by the ISGS, 2022). The black star is the location of the OES project site.*

Groundwater flow

Unconsolidated aquifers

A conceptual model (Figure 53) is a generalized representation of the different flow processes within the Mahomet Aquifer System which exhibits a wide range of hydraulic behaviors due to the complex geometry and composition of the glacial deposits, and the variable interconnections between the deposits, the land surface, and streams (Locke et al 2018).

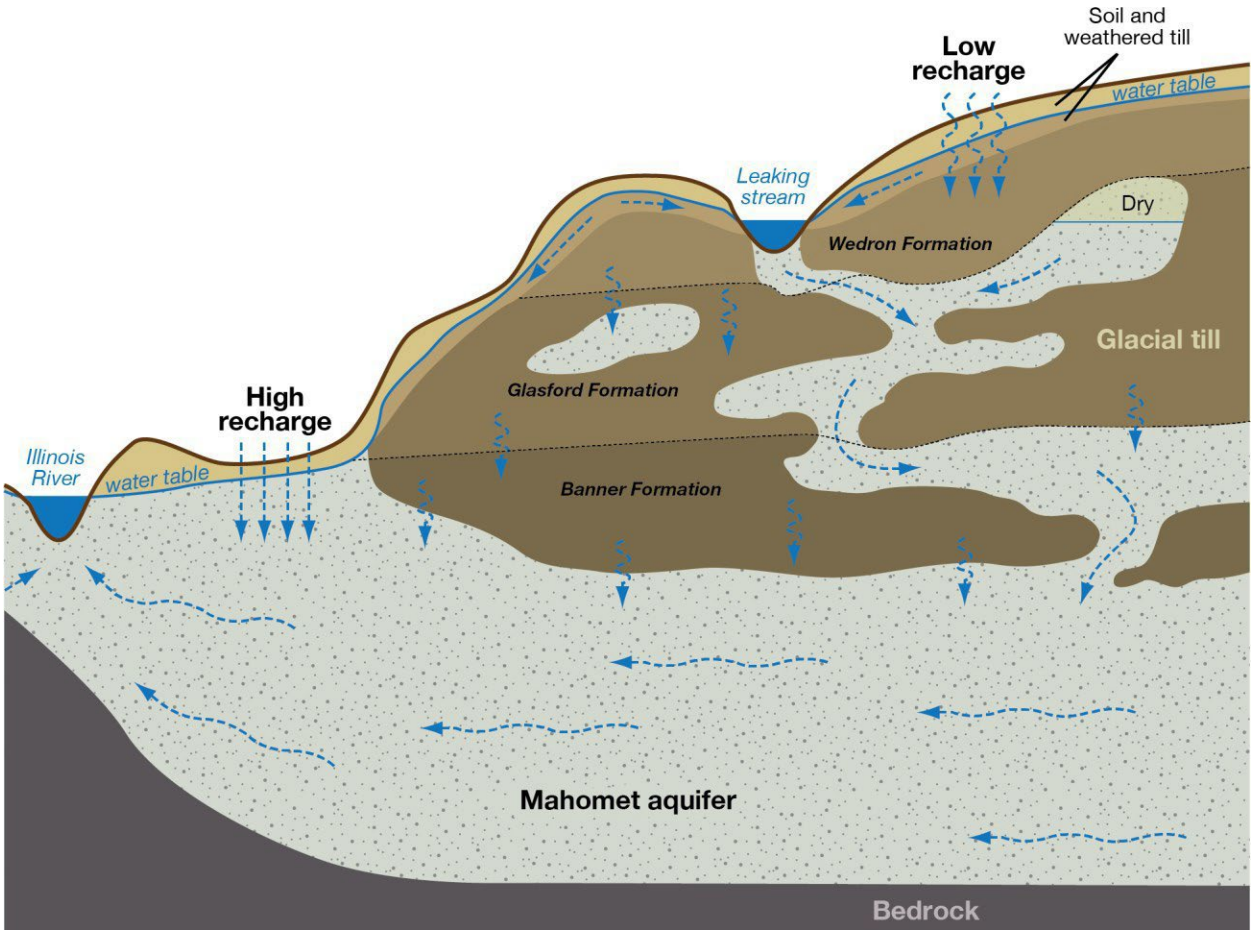

***Figure 53**. Conceptual model of flow in the Mahomet Aquifer System (Roadcap et al., 2011).*

The eastern section of the aquifer system is buried deeply under low permeability glacial till and lake sediments, which create confining conditions in the aquifer and greatly inhibit the rate of surface water recharge to the aquifers. Leaky stream segments have been found along the Sangamon River in Piatt County (Roadcap and Wilson, 2001), and connections likely occur along the Sangamon River north of Fisher and along Salt Creek near Rantoul (Roadcap et al., 2011).

Discussion on hydrologic conceptual model of flow in the Mahomet aquifer system was developed by Roadcap et al. (2011) and is summarized below.

Groundwater flow directions and areas of recharge and discharge for the eastern segment of the Mahomet aquifer were determined from a contour map of water level measurements from the 141 wells, to develop the potentiometric surface map (Figure 54). Two prominent features observed on the potentiometric surface map: a high in the potentiometric surface near Paxton in Ford County and a large cone of depression due to pumpage in Champaign-Urbana. Champaign-Urbana withdraws on average around 23 million gallons per day (mgd), resulting in water levels dropping to 100 feet (30 m) and a reversal of flow in Piatt and western Champaign Counties. Local precipitation and stream contribution balances out Champaign's groundwater withdrawal.

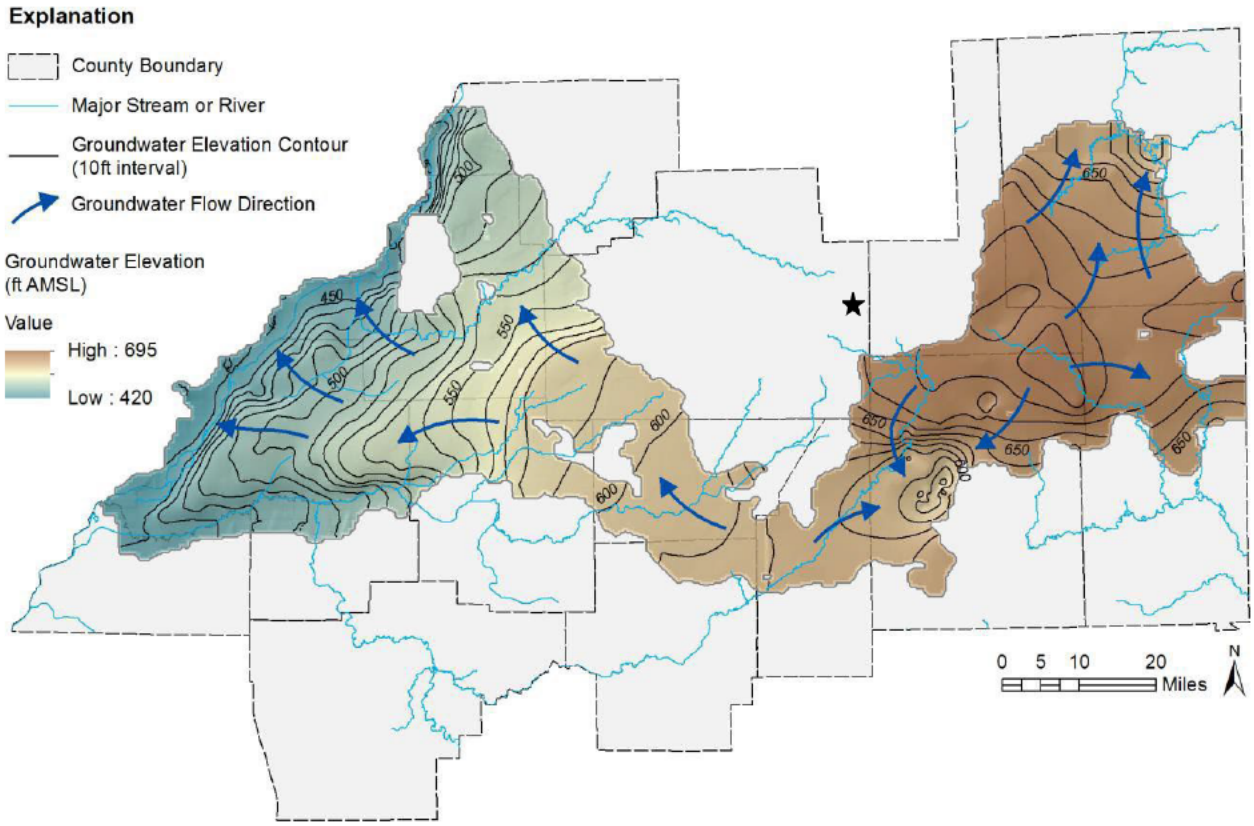

***Figure 54**. Composite potentiometric surface map of the Mahomet aquifer based on measurements from 1990 to 2009 (Roadcap et al., 2011). The black star is the location of the OES project site.*

Bedrock aquifers

The current major flow path in the Illinois Basin in Illinois is in a southerly-southeasterly direction (Kelly et al. 2018) toward the center of the Illinois Basin, becoming more sluggish and mineralized as it deepens (Cartwright, 1970, Panno et al., 1994, Siegel, 1989).

According to Kelly et al. (2018):

> "Pleistocene glaciation played a substantial role in altering hydrogeological and geochemical conditions of Paleozoic aquifers throughout the upper Midwest in the U.S., contributing large amounts of cold, dilute recharge that displaced in situ brines. The St. Peter Sandstone in central Illinois indicates that recharge during the Pleistocene and Holocene has come from multiple locations and sources, and that structural features,

primarily the LaSalle Anticlinal Belt but also possibly the Sandwich Fault Zone, are a major control on recharge and groundwater flow in the St. Peter Sandstone (Figure 55)."

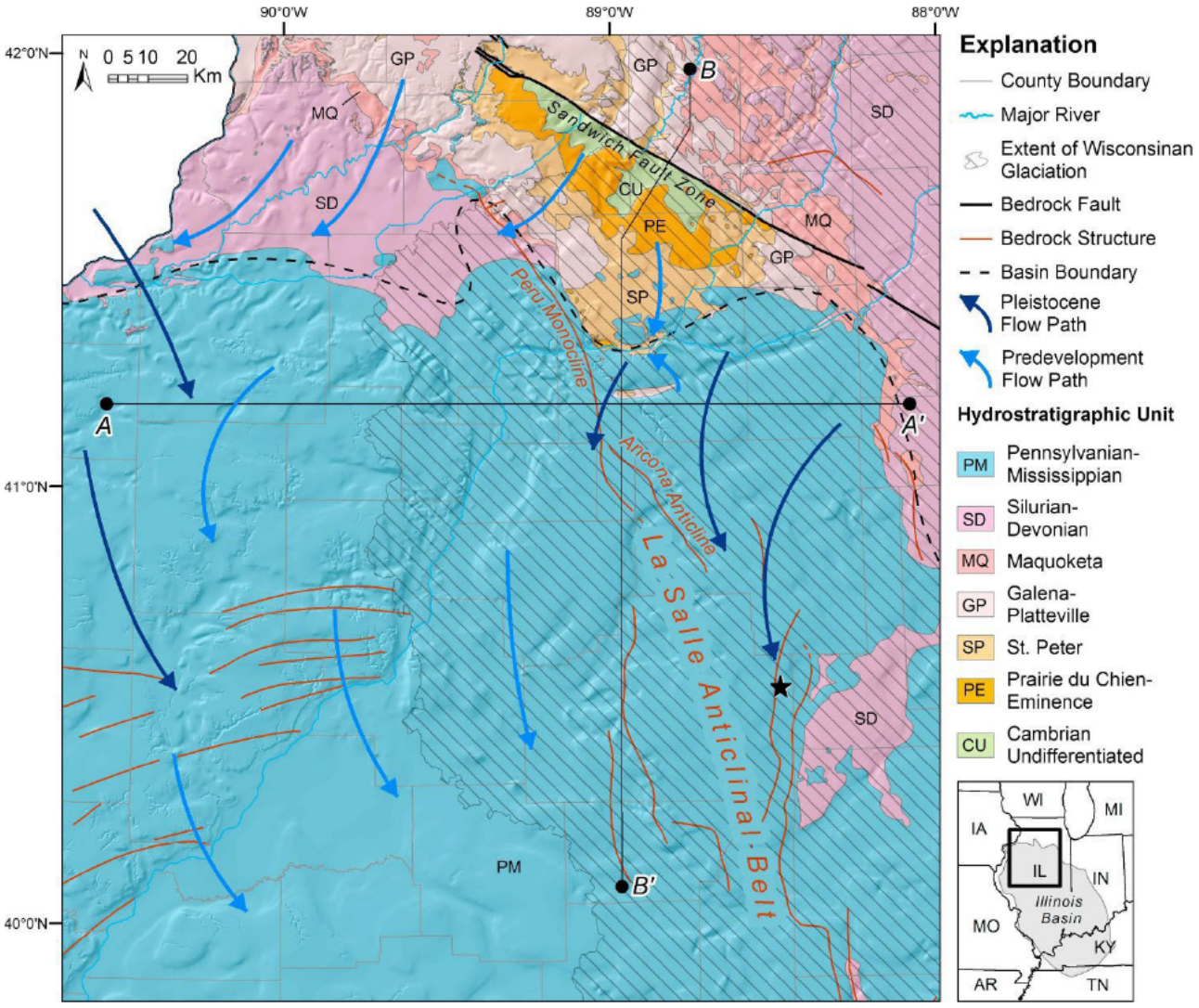

Figure 55. *Kelly et al. 2018 study region showing bedrock geology and structural features (modified from Kolata (2005). The inset map shows the study area located in the extend of the Illinois Basin. Cross-hatched area shows maximum extent of Wisconsin Glacial Episode. Dark blue arrows show inferred flow paths in the St. Peter Sandstone during the Pleistocene. Light blue arrows show predevelopment (1863) flow paths in the St. Peter Sandstone from Abrams et al. (2015). The black star is the location of the OES project site.*

Geochemistry [40 CFR 146.82(a)(6)]

Data Sources, Samples, and Analyses

The stratigraphic test well One Earth Energy OEE #1 provided data regarding fluid and rock composition for this project site. Fluid samples were collected at a depth of 2,230 feet (680 m) from the St. Peter Sandstone on December 17, 2021, and at a depth of 6,361feet (1,939 m) from the Mt. Simon Sandstone on January 26, 2022, during a drill stem test (DST). Produced fluid was collected at the well head and field parameters, including pH, temperature, density, and specific conductivity (SpC) were recorded on unfiltered fluid. Produced fluid was also filtered and

preserved for geochemistry analyses. The sample was analyzed for anions and cations using Ion Chromatography (IC) and Inductively Coupled Plasma-atomic Emission Spectrometry (ICP-AES), respectively. Total dissolved solid (TDS) and alkalinity were analyzed as described previously (Locke et al., 2013). The geochemistry parameters were selected based on our experiences in deep fluid monitoring for IBDP and ICCS projects.

Sidewall cores were collected for solid phase characterization. Forty samples collected between St. Peter Sandstone and Eau-Claire Formation were prepared and submitted to Schlumberger Reservoir Laboratories for XRD analysis with Bruker D8 Advance X-ray diffractometer to identify rock mineralogy. Seven samples from Precambrian formation were submitted to ISGS XRD/XRF Materials Characterization Laboratory for XRD analyses with Bruker D8 Advance X-ray diffractometer.

Rock cores and fluids were collected from the St. Peter Sandstone (USDW) and Mt. Simon Sandstone (storage formation) at the site characterization well (OEE #1). There is, in addition, considerable regional understanding of the geochemistry of fluids and lithology of most strata within the Illinois Basin from previous studies as well as CCS projects. There may be local variations in depositional fabrics, but there is high confidence in the bulk lithology and mineralogy of rock and geochemistry of formation fluids in injection zone, confining zone, and USDW in the Area of Review (AoR).

Fluid Geochemistry

The results of geochemistry analyses for fluid samples collected from St. Peter Sandstone and Mt. Simon Sandstone are listed in Table 10. The concentration of TDS of the fluid from St. Peter Sandstone was 1,779 mg/L, indicating that the water can be used as underground source of drinking water (USDW). The detection of dissolved iron indicates the presence of ferrous iron (Fe^{2+}) and thus suggests reducing conditions in the formation, which also indicates that the sample was properly preserved during sample collection at the well head (Shao et al. 2014). Metals of environmental concerns, including antimony, arsenic, beryllium, cadmium, chromium, lead, selenium, and thallium, were all below detection limits.

For the fluid collected from Mt. Simon Sandstone, the TDS was 165,500 mg/L, well above the TDS limit (10,000 mg/L) for USDW as defined by USEPA, indicating Mt. Simon Sandstone at One Earth CCS is suitable for geological storage of CO_2. This fluid is a Na-Ca-Cl type with Cl/Br ratio 170 which falls in the typical range (165±15) for groundwater originated from Mt. Simon (Panno et al., 2013).

Many fluid samples have been collected from the Mt. Simon Sandstone in the central Illinois Basin. To fulfil the requirements for Underground Injection Control (UIC) Class I or VI permits for the Illinois Basin – Decatur Project (IBDP) and Illinois – Industrial CCS (IL-ICCS) projects, the Illinois State Geological Survey has collected fluid samples since 2011 from both the Mt. Simon Sandstone and St. Peter Formation from these sites at Decatur, IL, about 50 miles southwest of One Earth Sequestration site. The geochemistry of the fluids collected from OEE #1 is consistent with that in the samples collected at Decatur sites. For example, chloride concentration in the fluid sample collected from Mt. Simon Sandstone in well OEE #1 falls in the general range of chloride concentrations (90,000 - 120,000 mg/L) measured for fluids from Mt. Simon Sandstone at Decatur

sites, indicating the representativeness of fluid chemistry for Mt. Simon Sandstone. The St. Peter Sandstone is the deepest USDW at the Decatur sites and fluid samples from this formation at IBDP had TDS values around 4,500 mg/L. This value is higher than measured at OEE #1 (Table 11) consistent with results of Panno at all (2018) indicating the salinity of St. Peter Formation trends lower as the formation becomes shallower to the north of Decatur as indicated by the St. Peter salinity contour map (Figure 47).

Table 11. *Analytical results for available deep fluid samples collected from Well OEE #1.*

Parameter	Unit	St. Peter	Mt. Simon
depth	ft	2230	6361
density	g/cm^3	0.9996	1.152
temperature	°C	19.9	15.4
pH	units	7.46	6.81
SpC	mS/cm	3.28	96.0
Alkalinity ($CaCO_3$)	mg/L	298	74.6
TDS	mg/L	1,779	165,500
Bromide	mg/L	3.3	595
Chloride	mg/L	816	101,137
Fluoride	mg/L	3.2	-40
Nitrate-N	mg/L	<0.02	<2
Sulfate	mg/L	89.0	578
Aluminum	mg/L	0.16	<0.93
Antimony	mg/L	<0.059	<1.5
Arsenic	mg/L	<0.02	0.27
Barium	mg/L	0.032	1.3
Beryllium	mg/L	<0.00014	0.0039
Boron	mg/L	1.4	15.2
Cadmium	mg/L	<0.0043	0.044
Calcium	mg/L	36.5	17,188
Chromium	mg/L	<0.0016	<0.016
Copper	mg/L	<0.0016	<0.04
Iron	mg/L	0.76	126
Lead	mg/L	<0.019	8.7
Magnesium	mg/L	17.8	2,187
Manganese	mg/L	0.41	47.0
Potassium	mg/L	17.4	1,281
Selenium	mg/L	<0.13	<1.3
Silicon	mg/L	4.3	4.6
Sodium	mg/L	592	39,848
Strontium	mg/L	1.5	525
Thallium	mg/L	<0.047	<1.2

Solid-Phase Geochemistry

XRD analysis results for 40 samples collected at different depths between St. Peter Sandstone and Eau-Claire Formation from OEE #1 are shown in Figure 56. The mineralogy of seven Precambrian samples is listed in Table 2. The one sample collected from St. Peter Sandstone contains 98% quartz and trace amount of dolomite and illite. Samples from the primary seal for this project, the Eau Claire Formation, consist of less quartz, but more K-feldspar and clay minerals, including illite, smectite, kaolinite, and chlorite. Near the top of this formation, the rock sample also contains plagioclase and a significant amount of dolomite. These results are consistent with previous studies for Eau Claire Formation (Neufelder et al., 2012; Carroll et al., 2013; Yoksoulian et al., 2014; Shao et al., 2020).

Regionally, the Mt. Simon Sandstone mineralogy has been characterized by numerous studies (Carroll et al., 2013; Freiburg et al., 2014; Yoksoulian et al., 2014; Davila et al., 2019; Shao et al., 2020) that indicate it is dominated by quartz (63-95%) with lesser amounts of feldspar (2-22%), authigenic clay, and detrital clay minerals (Freiburg et al., 2014). The clay-sized fraction of minerals present in the Mt. Simon Sandstone are a very small percentage (1–3% by volume). The comparison of the clay mineral components of the Mt. Simon Sandstone in central Illinois is consistent with that at the OEE# 1 well (Figure 57 a & b). The crossplot of spectral gamma ray of the Mt. Simon Sandstone indicates that the clay minerals are predominantly composed very fine mica, feldspars, and Illite in central Illinois. The similar crossplot of clay mineral at OEE #1 well shows that the most abundant clay-sized minerals are montmorillonite, Illite, and very fine mica.

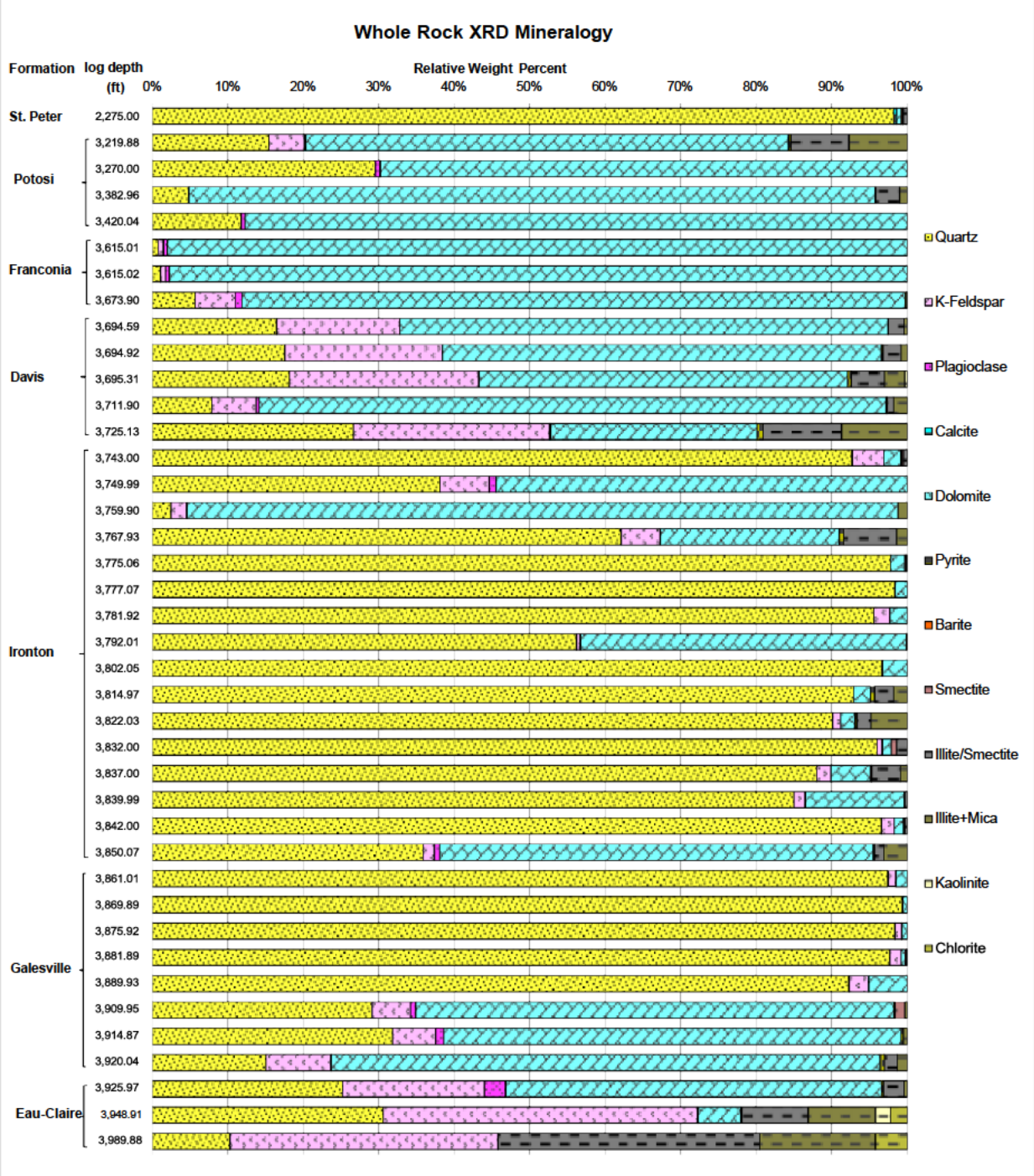

Figure 56. *XRD results for sidewall cores collected from OEE #1.*

a) b)

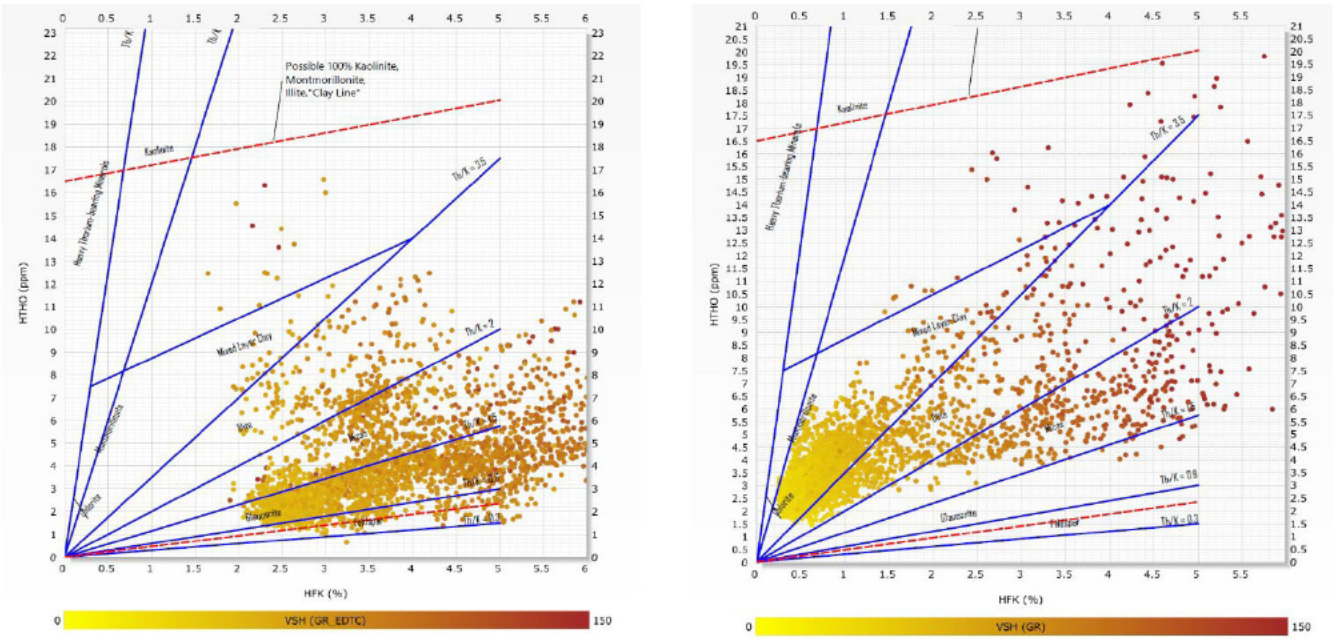

Figure 57*. Potassium/Thorium cross plots for the Mt. Simon Sandstone from CCS1 well in the central Illinois (a) and the OEE #1 well (b). Data are colored by GR value.*

XRD analyses for Precambrian rock were done for seven samples (Table 12). The major components of Precambrian rock are quartz (30-60%) and varying amounts of albite, microcline, orthoclase, and clay minerals. Muscovite is one of the major clay minerals in the seven Precambrian samples. Hematite, although of small amount (0.5-1.4%), was identified in all seven samples. In this region, the Argenta separates the Precambrian and Lower Mt. Simon, and CO_2 is not anticipated to contact Precambrian rock.

Table 12*. XRD results for samples collected from Precambrian basement at well OEE #1.*

Depth (ft)	Qtz	Albite	Micro	Ortho	Dolo	Kao	Musc	Hem
6920	58.9	0	0	0	0	20.3	19.4	1.4
6925	61.6	0	0	0	0	14.4	23	1
6995	38.3	0	33.2	0	0	0	27.7	0.9
7000	36	15	23.6	0	0	0	24.9	0.5
7020	30.6	0	39.8	0	0	0	28.6	1
7040	32.4	32	0	12.8	3.8	0	18.3	0.8
7070	32.5	23	22.9	0	0	0	20.8	0.7

Quartz – Qtz, Microcline – Micro, Orthoclase-Ortho, Dolomite-Dolo, Kaolinite-Kao, Muscovite-Musc, Hematite - Hem

Injection Zone Geochemistry

Results of XRD analyses for 42 Mt. Simon cores were received after our Class VI permit application was submitted in April 2023. The results are shown in Table 13. The XRD data indicate that these 42 samples contain 34-99% quartz, 1-60% feldspar, 0-7% clay minerals, and trace amount of other minerals (hematite, fluorapatite, pyrite, anatase, dolomite, calcite). For most of the samples, quartz is the dominant mineral phase with lesser amounts of feldspar, and small amounts of clay minerals. These results are consistent with the studies from the IBDP project as described in the narrative.

Table 13*. Whole rock minerology for samples from Mt. Simon Sandstone in OEE #1 well.*

Sample Number	Depth (ft)	Quartz	K-Feldspar	P-Feldspar	Illite+Mica	Calcite	Dolomite	Kaolinite	Chlorite	Anatase	Fluorapatite	Hematite	Pyrite	Total Clay *
3	6341.30	79.7	19.7	0†	0.4	0	0	0	0	0	0	0	0.1	0.4
4	6344.50	90.1	9.1	0	0.7	0	0	0	0	0	0	0	0	0.7
5	6349.12	74.7	24.3	0.2	0.4	0	0	0	0.4	0	0.1	0	0	0.8
6	6351.00	55.4	37.2	0.3	4.1	0	0	2.3	0.6	0	0.1	0.1	0	7.0
7	6355.08	84.3	13.3	0	2.2	0	0	0.2	0	0	0	0	0	2.4
8	6359.08	85.8	13.5	0.1	0.5	0	0	0.1	0	0	0	0	0	0.6
9	6360.15	79.3	19.9	0.1	0.6	0	0	0	0	0	0	0	0	0.6
10	6363.30	59.6	37.2	0.2	2.5	0	0	0.4	0	0	0	0.1	0	2.9
11	6365.00	61.9	36.3	0.2	1.1	0	0	0	0.3	0	0	0.1	0	1.4
12	6366.50	82.2	16.8	0.1	0.3	0	0	0	0.5	0	0	0	0	0.8
13	6368.50	69.6	28.5	0.2	0.6	0	0	0	1	0	0	0.1	0	1.6
14	6373.01	82.1	17.1	0.1	0.6	0	0	0	0	0	0.1	0.1	0	0.6
15	6374.80	95.7	4.1	0	0.2	0	0	0	0	0	0	0	0	0.2
16	6379.10	74.8	24.5	0.2	0.4	0	0	0	0	0	0.1	0.1	0	0.4
17	6380.50	86.2	13.4	0	0.3	0	0	0	0	0	0	0	0	0.3
1	6382.60	86.0	13.3	0.1	0.4	0	0	0	0	0	0	0	0	0.4
19	6384.06	82.0	15.8	0.1	1.1	0	0	0.5	0.2	0.1	0.2	0	0	1.8
20	6387.50	90.7	8.8	0.1	0.3	0	0	0	0	0	0	0	0	0.3
21	6389.50	95.0	4.8	0	0.2	0	0	0	0	0	0	0	0	0.2
22	6391.46	86.9	12.4	0.1	0.5	0	0	0	0	0.1	0	0	0	0.5
23	6393.10	95.8	4.0	0	0.2	0	0	0	0	0	0	0	0	0.2
52	6394.25	86.0	13.6	0.1	0.3	0	0	0	0	0	0	0	0	0.3
25	6396.40	85.9	13.4	0.1	0.5	0	0	0	0	0.1	0	0	0	0.5
26	6398.22	81.1	18.1	0.1	0.5	0	0	0	0	0	0	0	0	0.5
27	6405.45	81.3	17.6	0.1	0.9	0	0	0	0	0.1	0	0	0	0.9
28	6406.60	77.8	21.6	0.1	0.4	0	0	0	0	0	0	0	0	0.4
29	6409.67	59.2	37.6	0.1	2.3	0	0	0	0.6	0	0	0.2	0	2.9
30	6411.55	75.0	24.5	0.1	0.2	0	0	0	0	0	0	0.1	0	0.2
31	6412.55	81.7	17.4	0.1	0.6	0	0	0	0	0.1	0	0	0	0.6
32	6414.50	42.8	54	0.2	2.3	0	0	0	0.6	0	0	0.1	0	2.9
33	6432.15	81.7	17.9	0.1	0.3	0	0	0	0	0	0	0	0	0.3
34	6434.07	44.8	52.5	0.1	2.3	0	0	0	0	0	0.1	0.1	0	2.3
36	6440.16	58.6	39.8	0.2	1.1	0	0	0	0	0	0	0.3	0	1.1
37	6441.50	79.7	19.2	0.1	0.9	0	0	0	0	0.1	0	0.1	0	0.9

38	6443.98	89.4	10.3	0.1	0.2	0	0	0	0	0	0	0.1	0	0.2
39	6444.70	71.6	27.0	0.1	0.9	0	0	0	0.3	0	0	0.2	0	1.2
40	6445.60	34.1	60.3	0.2	4.1	0	0	0	1.0	0	0	0.3	0	5.1
41	6448.75	91.5	8.3	0.1	0	0	0	0	0	0	0	0.1	0	0
42	6449.38	81.7	18.0	0.1	0	0	0	0	0	0	0	0.2	0	0
18	6452.50	48.4	50.2	0.2	0.7	0	0	0	0	0	0.1	0.2	0	0.7
24	6462.49	72.8	21.6	0.2	3.8	0	0	0	0.8	0.2	0.2	0.5	0	4.6
43	6465.96	98.6	1.2	0.1	0	0	0	0	0	0	0	0.1	0	0

†: Zero values for a mineral mean that the mineral was not detected.
*: Total clay was calculated as the sum of illite+mica, kaolinite, and chlorite.

Geochemical Reactions and Modeling

To understand geochemical interaction of rock, brine, and CO_2 after CO_2 is injected into deep geologic formations, laboratory batch studies have been conducted with rock samples collected from Mt. Simon Sandstone and Eau Clare Formation at IBDP wells (Carroll et al., 2013; Yoksoulian et al., 2014; Berger et al. 2019; Shao et al., 2020). Batch experiments were conducted under relevant reservoir conditions to identify the reaction mechanisms, kinetics, and solid-phase products that are likely to occur when rock and brine are exposed to injected CO_2. The results of batch studies were also used to constrain the conceptual geochemical model, calibrate mean parameter values, and quantify parameter uncertainty in reactive-transport simulations.

Batch reactor experiments conducted with Mt. Simon Sandstone generally indicated limited dissolution of rock minerals (Carroll et al., 2013; Yoksoulian et al., 2014; Shao et al., 2020). The decrease of pH occurred quickly in these experiments after CO_2 was introduced into reaction systems as the result of CO_2 dissolution into the brine and dissociation of carbonic acid. Reaction of Mt. Simon sandstone from different depth intervals produced very similar results and can be characterized by an increase in dissolved TIC, Si, and Al after reaction, suggesting the dissolution of aluminosilicate minerals, such as feldspar and clay minerals. However, mineral dissolution was limited. For example, the mass of Al that dissolved from the solid phase into aqueous phase accounted for less than 0.3% of total Al in the rock samples. It is noteworthy that the liquid to solid ratios in batch experiments were much higher than aquifer conditions. It was expected that the amount of Al mobilized from sandstone samples into fluid would be less than 0.002% under aquifer conditions. In addition, results from XRD analyses indicated the bulk mineral composition remained unchanged for all sandstone samples after reaction (1-4 months), indicating that the influence of rock-brine-CO_2 interaction on bulk rock composition was negligible.

Batch experiments with Eau Clare shale indicated that dissolution of rock minerals occurred after CO_2 was introduced into the batch reactor. For experiments with crushed rock samples, mineral dissolution from Eau Clare samples were more significant than Mt. Simon sandstone samples (Carroll et al., 2013; Shao et al., 2020). This is likely due to the processing of rock samples to small fragments that increased the reactive surface area, thus facilitated mineral dissolution of Eau Clare rock. The Eau Claire Formation, however, is a highly laminated, fissile shale to silty shale with the shaliest section directly overlies the Mt. Simon Sandstone. Therefore, advective flow from the Mt. Simon Sandstone into the Eau Claire is expected to be insignificant (Roy et al 2014). Modeling of ionic diffusion into the Eau Claire has also shown this to be insignificant (Roy et al 2014).

With transmission electron microscopy (TEM) and energy dispersive spectroscopy (EDS), Carroll et al. (2013) observed the presence of Fe-rich clay minerals in both Mt. Simon Sandstone rock samples and Eau Clare rock samples. Numerical simulations with PHREEQC 2.17.0 geochemical code suggested that the geochemical alteration of the Mount Simon Sandstone and Eau Claire shale can be modeled by incongruent dissolution of annite, illite, K-feldspar, and formation of montmorillonite, amorphous silica, and kaolinite. However, the formation of these secondary minerals were not confirmed with available characterization techniques.

Mineral Trapping

Currently available literature on CCS generally indicates that mineral trapping capacity of sandstone saline aquifers is small. Laboratory and modeling studies for Mt. Simon Sandstone from the Illinois Basin suggest that the bulk of the mineralogy of the rock remained inert and brine compositions showed little alteration within the time scale of laboratory experiments (within a year) (Carroll et al., 2013; Yoksoulian et al., 2014; Berger et al., 2019). Yoksoulian et al. (2014) conducted batch experiments for up to 9 months and did not observe the precipitation of carbonate minerals. Numerical simulations with both TOUGHREACT and PHREEQC 2.17.0 geochemical codes indicate that calcite ($CaCO_3$) or siderite ($FeCO_3$) may precipitate as a result of feldspar dissolution which buffer pH, but it generally takes hundreds of years to see significant mineral trapping (Carroll et al., 2013; Berger et al., 2019).

The new XRD data for Mt. Simon core samples indicate that the mineralogical compositions of Mt. Simon core from OEE #1 are consistent with the data collected from IBDP. The cores in batch studies by Carroll et al. (2013), Yoksoulian et al. (2014), Davila et al. (2019), and Shao et al. (2020) contained 63-95% quartz, 2-22% feldspar, and 1-3% clay minerals. The mineral composition used by Carrol et al (2013) in their numerical modeling for geochemical reactions of Mt. Simon Sandstone was 72% quartz, 21% feldspar, and 7% clay minerals. These data are well within the ranges of corresponding minerals detected for One Earth project (Table 11). For confining zone, Eau-Claire formation, IBDP cores exhibit the similar mineralogical composition as OEE #1. For example, the core sample used by Shao et al (2020) was collected from Eau-Clair formation in IBDP VW2 well and contained 38% quartz, 37% K-feldspar, 21% illite, 3% dolomite, and 1% pyrite. This composition is similar to the rock sample collected from OEE #1 at depth 3948.91 ft, which contain 31% quartz, 36% K-feldspar, 18% illite, 6% dolomite, 2% kaolinite, and 2% chlorite (Figure 51). Therefore, the experimental studies conducted with IBDP core samples, as well as the numerical modeling studies are considered representative of One Earth project site.

Other Information

One Earth CCS will not actively monitor surface air or soil gas data. Baseline soil CO_2 flux and soil gas data are publicly available for a field site analogous to One Earth CCS at the Illinois Basin – Decatur Project (Carman 2019).

Site Suitability [40 CFR 146.83]

Summary

The proposed injection site meets the suitability requirements set forth at 40 CFR 146.83. The evaluation of the geologic setting of the proposed site indicates that the Mount Simon Sandstone at the site is sufficiently deep, sufficiently thick, and has the lateral continuity, porosity, and permeability required to store the proposed 90 million tonnes of CO_2.

The Eau Claire Formation at the site is of sufficient thickness, lateral continuity, and has low enough permeabilities and capillary entry pressures to serve as the primary confining zone. The site affords additional containment with several secondary confining zones within the Knox Group including the Franconia Formation, Oneota Dolomite, and Shakopee Dolomite. Both the Eau Claire Formation and Knox Group sealing intervals are present in the characterization well OEE #1 and are situated between the top of the injection reservoir and the St. Peter sandstone, the lowermost USDW.

No deep wells that penetrate the primary seal, except for OEE #1, are present within the AoR.

Seismic reflection data indicate that there are a few small normal faults penetrating the Eau Claire Formation in the northeast portion of the AoR, but these faults are located outside the expected extent of the CO_2 plume and are not projected to impact containment at this site. The small faults are predicted to be sealing based on the low throw of the faults and the mineralogy, Vshale content, and ductile nature of the Eau Claire Formation.

No potential conduits for CO_2 to migrate out of the Mount Simon reservoir are identified at the proposed storage site.

Capacity and Storage

The AoR and Corrective Action Plan show that the Mt. Simon Sandstone at the proposed storage location has the capacity and hydrogeologic characteristics necessary to store 90 million tonnes of CO_2. A dynamic model was used to simulate multiphase (brine and CO_2) flow in the subsurface. The model considered the reservoir geologic and hydrogeologic characteristics and includes three injection wells as a single system for a comprehensive representation of reservoir behavior. Two major CO_2 trapping mechanisms were modeled: structural/stratigraphic trapping and residual trapping. These processes allowed the prediction of CO_2 movement in terms of gas saturation and reservoir pressure change with time to delineate the Area of Review (AoR) and the corresponding tubing head pressure during and after injection. The model showed that in the post-injection phase and beyond, the pressure front dissipates rapidly, and the CO_2 plume is stable and confined to the injection reservoir.

Reservoir and Compatibility with the Injectate

Laboratory and modeling studies for the Mt. Simon Sandstone from the Illinois Basin suggest that there is minimal reactivity of the rock with brine and CO_2. Reaction experiments using Mt. Simon Sandstone suggest minor dissolution of aluminosilicate minerals, such as feldspar and clay minerals may occur, but the bulk of the mineralogy (i.e., quartz) is effectively inert. Results from XRD analyses indicated the bulk mineral composition remained unchanged for all sandstone

samples after reaction, indicating that the influence of rock-brine-CO_2 interaction on bulk rock composition was negligible. Numerical simulations indicate that some carbonate minerals may precipitate as a result of feldspar dissolution, but it would take hundreds of years to see significant mineral trapping.

Primary Seal

The Eau Claire Formation is the primary confining unit of the Mt. Simon Storage Complex at the One Earth Sequestration, LLC project site. The Eau Claire Formation is 534 feet (163 m) thick at OEE #1 and contains a succession of shale that is an effective seal because it is relatively ductile and has extremely low vertical permeabilities to restrict vertical movement of fluids. The thickness of the continuous shale interval in the Eau Claire Formation at OEE #1 is about 123 feet (37 m). Additional shale intervals in the Eau Claire above this shale package increase the sealing strata cumulative thickness to about 356 feet (108 m).

The Eau Claire Formation has been the subject of numerous investigations into sealing characteristics in the Illinois Basin, and it is the primary sealing strata for an existing carbon storage project at Decatur, IL. Advective flow from the Mt. Simon Sandstone into the Eau Claire is expected to be insignificant. Modeling of ionic diffusion into the Eau Claire has also shown this transport mechanism to be insignificant.

Secondary Confinement Strata

The Knox Group is a regionally extensive group predominantly of dolomite formations. The thick, dense intervals within the Knox Group, including the Franconia Formation, Oneota Dolomite, and Shakopee Dolomite would serve as secondary confining intervals.

Lowermost USDW

The St. Peter Formation is the lowermost USDW at the proposed storage site. At OEE #1 the top of the St. Peter is at 2,217 feet (676 m) and is 232 feet (71 m) thick.

Protection of Shallow USDWs

The Ordovician Maquoketa Shale Group is a laterally continuous impermeable confining layer situated above the St. Peter. The top of the Maquoketa is 1,598 feet (487 m) deep, and the formation is 194 feet (59 m) thick (Figure 1) in the OEE #1 well.

In addition, the Devonian-Mississippian New Albany Shale Group is a thick, impermeable, and laterally continuous shale formation At the OEE #1 location, the top of the New Albany is at 753 feet (230 m) MD and is 150 feet (45 m) thick.

Structural Integrity

From the analysis of 2D seismic data, a few small offset faults were identified within the northeastern portion of the AoR that transect the Mt. Simon Sandstone and the Eau Claire Formation. These faults are associated with the Osman Monocline, which is part of the regional LaSalle Anticlinorium, and are about 3.4 miles east of the predicted maximum extent of the CO_2 plume. The small faults are predicted to be sealing based on the low throw of the faults and the mineralogy and its Vshale content of the Eau Claire Formation. Because of this, as well as the

distance of the faults from the CO_2 plume, neither pressure nor containment will be compromised by the presence of these faults. Other small faults identified within the AoR only extend into the Argenta or lowermost Mt. Simon and do not reach the Eau Claire confining zone and will not impact the containment of the storage reservoir. No potential conduits for CO_2 to migrate out of the Mount Simon reservoir were identified at the proposed storage site.

Computational modeling predicts that reservoir pressure in the Mt. Simon Sandstone will decrease to below threshold pressure within seven years of the end of injection operations. Formation pressures will thereafter continue to steadily decrease toward the pre-injection static pressure.

AoR and Corrective Action

One Earth Sequestration, LLC has submitted the AoR and Corrective Action Plan (40 CFR 146.82(a)(13) and 40 CFR 146.84(b). Detailed documentation regarding the computational modeling (40 CFR 146.84(c)) has been submitted into the GSDT AoR and Corrective Action Module. This includes:

- Model domain
- Processes modeled
- Rock properties
- Boundary conditions
- Initial conditions
- Operational information
- Model output, and
- AoR pressure front delineation

The AoR and Corrective Action Plan provides a summary of the results of the modeling and AoR. There are no known wells within the AoR that require corrective action. The stratigraphic test well installed for this project is proposed for conversion to an in zone monitoring well.

AoR and Corrective Action GSDT Submissions
GSDT Module: AoR and Corrective Action ***Tab(s):*** All applicable tabs Please use the checkbox(es) to verify the following information was submitted to the GSDT: ☒ Tabulation of all wells within AoR that penetrate confining zone ***[40 CFR 146.82(a)(4)]*** ☒ AoR and Corrective Action Plan ***[40 CFR 146.82(a)(13) and 146.84(b)]*** ☒ Computational modeling details ***[40 CFR 146.84(c)]***

Financial Responsibility

The financial responsibility plan was uploaded to the GSDT. The plan includes a description of potential financial mechanisms for each phase. As required by 40 CFR 146.82(a)(14) and 40 CFR 146.85. The financial responsibility plan includes cost estimates for each phase.

The estimated costs of each of these activities include:

Table 14. *Estimated costs for site activities*

Activity		Total Cost ($)
Corrective Action		$0
Plugging Injection Wells (3 Injection wells @ $967.553/well)	TOTAL	$2,902,659
Post-Injection Site Care		$4,836,800
Site Closure		$3,950,000
Emergency and Remedial Response		$3,600,000
	Total	$15,289,459

The facility is owned and operated by One Earth Sequestration, LLC, and will provide financial assurance for the facility.

Financial Responsibility GSDT Submissions

GSDT Module: Financial Responsibility Demonstration
Tab(s): Cost Estimate tab and all applicable financial instrument tabs

Please use the checkbox(es) to verify the following information was submitted to the GSDT:
☒ Demonstration of financial responsibility ***[40 CFR 146.82(a)(14) and 146.85]***

Injection Well Construction (40 CFR 146.82(a)(12))

The injection wells will be constructed new to meet the requirements of 40 CFR 146.82.a.12 and 40 CFR 146.86. Proposed specifications and procedures for injection wells OES #1, OES #2, and OES #3 are described in the corresponding documents for Injection Well Design Plan for One Earth Sequestration, LLC [CONSTRUCTION DETAILS (40 CFR 146.86(a))].

Each INJECTION WELL PLAN document provides details on:

- Injection Well Operating Conditions
- Formation Conditions
- Open Hole Parameters
- Casing and Completion Tubing Specifications
- Minimum Logging Specifications for Well Construction
- Cement Specifications
- Wellhead Design Parameters
- Proposed Stimulation Program [40 CFR 146.82(a)(9)]

Selected elements of the INJECTION WELL PLAN are summarized as follows, using OES #1 as an example.

Proposed Stimulation Program [40 CFR 146.82(a)(9)]

The need for stimulation to enhance the injectivity potential of the Mount Simon Sandstone is not anticipated at this time. If it is determined that stimulation techniques are needed, a stimulation plan will be developed and submitted to EPA Region 5 for review and approval prior to conducting any stimulation.

Construction Procedures [40 CFR 146.82(a)(12)]

The injection well (Table 15, Figure 58) will be constructed to meet the requirements of 40 CFR 146.82.a.12 and 40 CFR 146.86.

Table 15. *Well construction open hole details for the OES #1 well.*

Name	Depth Interval (feet)	Open Hole Diameter (inches)	Comment	Drilling Mud Type & Weight (lb/gal)[1]	Pressure Gradient (psi/ft)	Maximum Deviation and Dog Leg Severity[2]
Surface	0 – 374	26	To bedrock	Fresh Spud Mud 8.6 – 9.0	0.433	>5° Deviation and <2° per 100 ft
Intermediate	374 – 4,046	17-1/2	To primary seal	Fresh Water Mud 8.8 – 9.0	0.433	>5° Deviation and <2° per 100 ft
Long	4,046 – 7,100	12-1/4	To bedrock	Fresh Water Mud 8.8 – 9.0	0.439	>5° Deviation and <2° per 100 ft

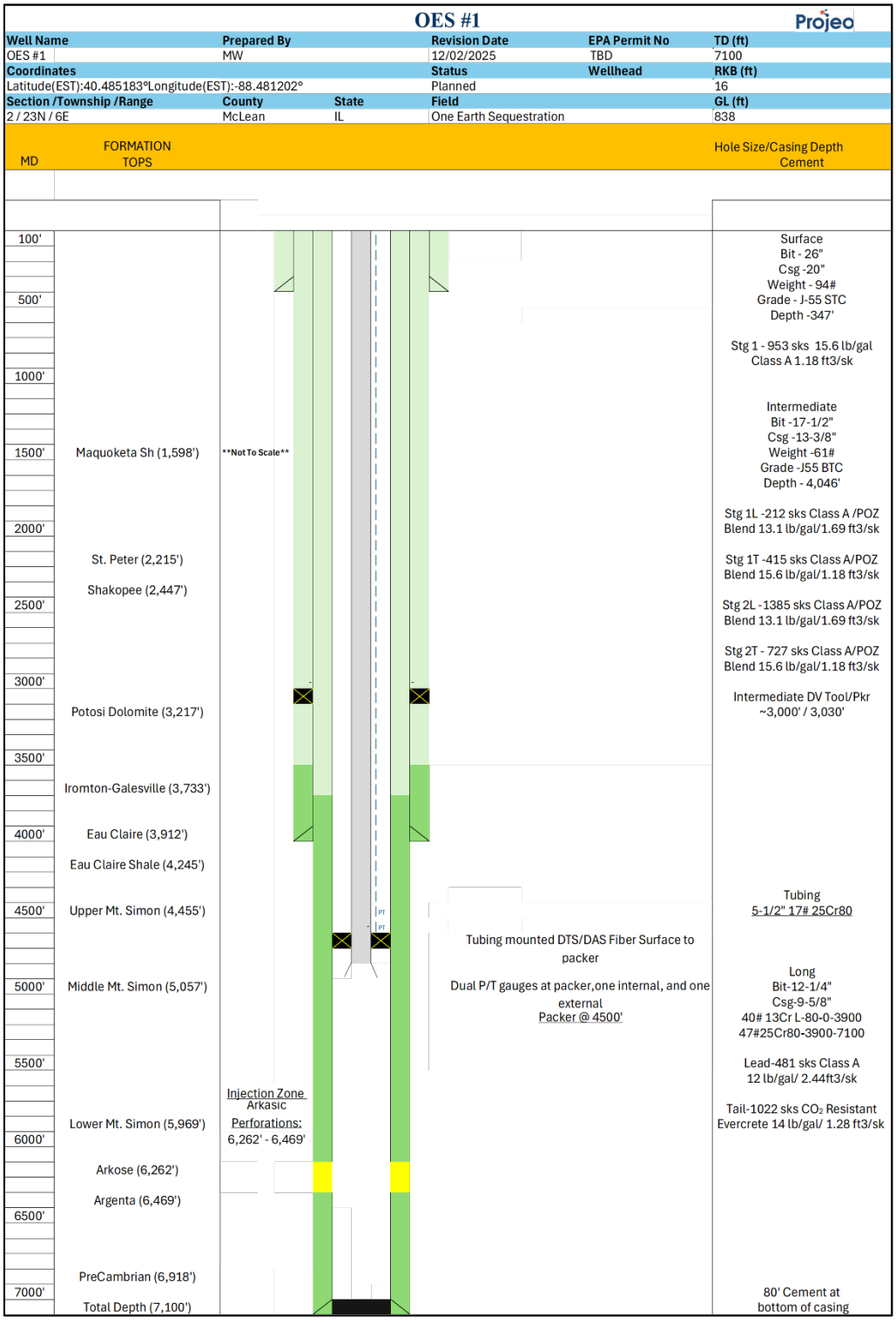

Figure 58. *Wellbore and completions schematic for OES #1 well.*

Casing and Completion Tubing Specifications

The proposed casing and tubing completion string specifications are provided in Table 16. The wellbore schematic is presented in Figure 58.

***Table 16**. Well casing and tubing specifications for the OES #1 well.*

Name	Depth Interval (feet)	Outside Diameter (inches)	Inside Diameter (inches)	Nominal Weight (lb/ft)	Material/Alloy	Design Coupling/Joint Yield (klbf)	Thermal Conductivity @ 77 ° F (BTU/ft.hr °F)	Tensile Strength (klbf)	Collapse Strength (psi)	Burst Strength (psi)
Surface[1]	0 - 347	20	19.124	94	J55	STC / 783	31	1,480	520	2,110
Intermediate[2]	0 - 4,046	13-3/8	12.515	61	J55	BTC / 1,025	31	962	1,540	3,090
Long[3] (chrome)	0 - 3,900	9-5/8	8.835	40	13 CR (API)	VAM21 / 916	31	916	3,090	5,750
Long[3] (chrome)	3,900 - 7,100	9-5/8	8.681	47	VM 25S CRA	VAM 21 / 1,086	16	1,086	4,750	6,870
Tubing[4]	0 - 4,500	5-1/2	4.839	17	VM 25S CRA	VAM TOP / 397	16	397	6,290	7,740

Note 1: After drilling a 26-inch hole to approximately 374 feet true vertical depth (TVD), a 20-inch, 94-ppf, J55 short-thread-coupling (STC) casing string will be set and cemented to the surface. The coupling outside diameter is approximately 21 inches. Based on available geologic data, setting the surface casing at approximately 347 feet is expected to place the shoe within bedrock, helping to protect shallow groundwater that may be used for domestic or commercial purposes. Centralizers will be installed on the first three joints and then on every third joint to the surface. Figure 1 shows the casing stress analysis for anticipated operating scenarios, and Table 5 provides the corresponding design data.

Note 2: After a shoe test or formation integrity test (FIT), a 17½-inch hole will be drilled to approximately 4,046 feet true vertical depth (TVD). A 13⅜-inch, 61-ppf, J55 buttress-thread-coupling (BTC) casing string will then be run and cemented to the surface. The coupling outside diameter is approximately 14⅜ inches. Centralizers will be installed on the first three joints and then on every third joint to the surface. Figure 2 shows the casing stress analysis for anticipated operating scenarios, and Table 6 provides the corresponding design data.

Note 3: After a shoe test or formation integrity test (FIT), a 12¼-inch hole will be drilled to approximately 7,100 feet true vertical depth (TVD), through the Mt. Simon Sandstone, where the long-string casing will be run and cemented. The coupling outside diameter is 10⅝ inches for L80 and 10.420 inches for VM 25S CRA. Centralizers will be installed on every joint from total depth to 200 feet above the injection interval, and on every third joint thereafter. Figure 3 shows the casing stress analysis for anticipated operating scenarios, and Table 7 provides the corresponding design data.

Note 4: The maximum allowable suspended weight, based on the specified yield strength of the injection tubing and the weakest tubular or connection, is 318,000 pounds. Figure 4 shows the tubing stress analysis for anticipated operating scenarios, and Table 8 provides the corresponding design data. The final tubing design will include profile nipples and latching devices suitable for downhole shut-in, testing, and well workovers. The packer will be a hydraulic-set mechanical packer with an HNBR sealing element and HNBR/Viton elastomers, with metallurgy of at least VM 25S CRA. Final vendor selection will occur during construction.

The annular completion fluid will be an inhibited $CaCl_2$ brine containing a corrosion inhibitor, scale inhibitor, oxygen scavenger, and biocide, with a density of approximately 8.8 lb/gal. Downhole instrumentation will include high-resolution tubing and annulus pressure gauges. Single-mode and multi-mode fiber-optic cable will be installed externally on the tubing for distributed temperature sensing (DTS) and distributed acoustic sensing (DAS).

Additional details and figures regarding casing stress analysis for anticipated operating scenarios are described in the INJECTION WELL PLAN.

Cement Specifications

The well will be fully cased, and all casing strings will be cemented back to ground level as detailed in Table 6 and illustrated in Figure 6. The long string will include a CO_2-resistant cement system such as EverCRETE. CO_2-resistant cement will be placed from total depth upward and tied back approximately 200 feet into the 13⅜-inch intermediate casing across the Eau Claire sealing formation. These CO_2-resistant cement systems are stable under highly acidic conditions, resistant to CO_2 and formation fluids, and capable of maintaining long-term integrity over the design life of the injection well.

The surface-casing cement system will provide isolation for shallow groundwater for the remainder of the well, and the intermediate string will serve as an additional barrier to prevent migration of CO_2 or formation fluids out of the injection zone. The final cementing program—including volumes, displacement rates, and placement technique (e.g., single-stage or two-stage)—will be refined using cement-design software with inputs from drilling operations such as caliper logs, fracture logs, and mud-loss data. A mud flush will be pumped ahead of all cement jobs to aid in borehole cleaning. The injection well will include approximately 80 feet of cement above the casing shoe to prevent the injected CO_2 from contacting the Precambrian granite basement.

Table 17. *Well cement specifications for OES #1 well.*

Name	Depth Interval (feet)	Access.	Stage 1 Lead	Stage 1 Tail	Stage 2 Lead	Stage 2 Tail
Surface	0 - 347	Float Shoe Float Collar Wiper Plug Centralizers	953 sacks (200 bbl) of 15.6 lb/gal Class A Cement (2% C-1 +1/8# C-30) yielding 1.18 ft^3/sack	n/a	n/a	n/a
Intermed.	0 - 4,046	Float Shoe Float Collar Wiper Plug Csg Pkr DV Tool Centralizers	212 sacks (64 bbl) of 13.1 lb/gal G/Poz Cement eXtreme blend with dry latex yielding 1.69 ft^3/sack	415 Sacks (87 bbl) of 15.6 lb/gal Class H Cement (0.8% C-17 + 1/8#C-30 + 2#C-42) yielding 1.18 ft^3/sack	1385 sacks (417 bbl) of 13.1 lb/gal 35/65 Poz/H Cement (6% C-20 + 0.8% C-17 + 0.2% C-13 + C-30) yielding 1.69 ft^3/sack	727 Sacks (153 bbl) of 15.6 lb/gal Class H Cement (0.8% C-17 + 1/8#C-30 + 2#C-42) yielding 1.18 ft^3/sack
Long	0 – 7,100	Float Shoe Float Collar Wiper Plug	481 sacks (209 bbl) of 12.7 lb/gal 35/65 Class A (D035, D020, D046, D167, D153, D079, D013) yielding 2.44 ft^3/sack	1022 Sacks (233 bbl) of 814.0 lb/gal EverCRETE CO_2 resistant (D206, D145A, D500, D177, D174) yielding 1.28 ft^3/sack	n/a	n/a

Pre-Operational Logging and Testing

The pre-operational formation testing program will be implemented to obtain an analysis of the chemical and physical characteristics of the injection zone and confining zone(s) and that meets the testing requirements of 40 CFR 146.87 and well construction requirements of 40 CFR 146.86. The preoperational testing program will include a combination of logging, coring, formation geohydrologic testing (e.g., a pump test and/or injectivity tests), and other activities during the drilling and construction of the CO_2 injection wells

The pre-operational testing program will determine or verify the depth, thickness, mineralogy,

lithology, porosity, permeability, and geomechanical information of the Mt. Simon Sandstone (CO_2 injection zone), the overlying Eau Claire Formation (confining zone), and other relevant geologic formations. In addition, formation fluid characteristics will be obtained from the Mt. Simon Sandstone injection wells (and in-zone and above zone monitoring wells) to establish baseline data against which future measurements may be compared after the start of injection operations. The results of the testing activities will be documented in a "Pre-operational Testing Narrative" report and submitted to the EPA after the well drilling and testing activities have been completed and before the start of CO_2 injection operations.

Baseline Gaseous CO_2 Conditions

Baseline gaseous CO_2 concentrations will be characterized during drilling and pre-operational activities, as applicable, in USDWs and other relevant formations encountered along the wellbore. These data will be collected prior to the commencement of injection to establish baseline conditions for comparison with operational and post-injection monitoring results.

After completing the characterization and testing, the borehole will be completed as an injection well. Mechanical integrity tests (e.g., wireline and pressure tests) will verify well construction and integrity.

The Pre-operational Logging and Testing Program Plan provides additional detail.

Pre-Operational Logging and Testing GSDT Submissions
GSDT Module: Pre-Operational Testing ***Tab(s):*** Welcome tab Please use the checkbox(es) to verify the following information was submitted to the GSDT: ☒ Proposed pre-operational testing program ***[40 CFR 146.82(a)(8) and 146.87]***

Well Operation

Injection operations will follow a defined sequence consistent with 40 C.F.R. §§ 146.82(a)(10), 146.88, and 146.90, as outlined below:

1. Pre-Injection Verification – Confirm mechanical integrity; verify and calibrate continuous monitoring instrumentation (pressure, rate/mass/volume, temperature, annulus pressure); and establish the required annulus–tubing differential pressure.

2. Startup – Activate surface equipment under no-flow conditions and introduce CO_2 gradually at low rates to confirm stable pressure behavior while remaining below the maximum allowable surface injection pressure (MASIP).

3. Normal Injection Operations – Maintain injection within the approved operating envelope; continuously record required operational parameters; and operate with alarms and automatic shutoff systems active.

4. Monitoring and Verification – Review operational data and conduct required sampling, plume- and pressure-front tracking, and mechanical-integrity testing in accordance with 40 C.F.R. § 146.90.

5. Operational Adjustments and Anomaly Response – Reduce injection rates or suspend injection if pressures approach limits and investigate and correct abnormal pressure behavior or indications of mechanical-integrity loss, consistent with the Emergency and Remedial Response Plan (ERRP). If a shutdown is triggered or monitoring indicates a potential loss of mechanical integrity, OES will immediately initiate an investigation to identify the nature, cause, and extent of the condition, implement corrective actions as appropriate in consultation with the Director, and demonstrate restoration of mechanical integrity prior to resuming injection.

6. Shutdown – Perform a controlled ramp-down; secure valves; verify stabilization of wellhead and annulus pressures; and document operating conditions.

Shutdown Triggers and Investigation Actions (40 C.F.R. § 146.88(f))
If a shutdown is triggered (automatic or manual), or if monitoring data indicate a potential loss of mechanical integrity, OES will immediately initiate an investigation to identify the nature, cause, and extent of the condition. Investigation actions include securing the well, monitoring wellhead and annulus pressure and temperature, reviewing operational and monitoring data to determine the root cause, and implementing corrective actions in consultation with the Director, as appropriate. Injection will not resume until mechanical integrity is restored and demonstrated to the Director's satisfaction. These actions will be implemented consistently with the approved Emergency and Remedial Response Plan (ERRP).

This procedure will be incorporated into the updated Well Operations section and finalized following installation and commissioning of as-built system components.

Proposed Operational Procedures and CO_2 Injectate

The injection operations will be implemented by the permit owner, One Earth Sequestration, LLC. under the permit, One Earth Sequestration, LLC will develop a storage hub near the One Earth Energy ethanol production facility in north-central Illinois.

Upon issuance of the UIC permits, One Earth Sequestration, LLC will begin the process of installing the injection wells and other project infrastructure as described in the permit application. Injection operations will begin once US EPA authorizes permission to operate, and the OEE ethanol plant capture, compression, and CO_2 transportation system is commissioned. The One Earth Energy facility is the intended initial source of CO_2. The operations plan is to expand the site to include CO_2 from other ethanol plants, ammonia production, and other compatible industrial sources. The project intends to begin with injection of approximately 0.5 million tonnes of CO_2 annually and then ramp up injection to 4.5 million tonnes of CO_2 annually. Injection will be, distributed across the three permitted injection wells, in accordance with the permit operating conditions for each respective well (Table 16). The project intends to store a total of up to 90 million tonnes of CO_2, injected over a period of approximately 20 years. Well operations and description of the proposed CO_2 injectate and its properties are described in this section below. Initial injection rates will range from 1,400 to 1,500 tonnes/day. Planned annual CO_2 injection for all wells could be up to 4,500,000 tonnes/year. At full operating capacity, expected daily injection, per well will ramp up to 4,225 tonnes/day depending on site geology and injectivity at each well location, and CO_2 availability. A flow meter will be installed to produce a direct reading of total volume per time of CO_2 being injected. Location will be after compression, but prior to well head.

While injection pressures and associated parameters are expected to stay constant for the lifetime of the injection project, injections rates may fluctuate due to maintenance at the ethanol plant and some variations in the pipeline delivered volumes. The injection system is designed to vary the number of wells in operation to accommodate thes fluctuations.

Proposed Injection Operations and Procedures (40 CFR 146.82(a)(10)

One Earth Sequestration, LLC proposed injection procedures for the project injection wells incorporates short-term maintenance, and inspection of the wells and surface equipment that the waste contacts, along with long-term operational monitoring and contingency planning for safe, responsible operations. One Earth Sequestration, LLC is committed to operating the wells to meet all applicable United States Environmental Protection Agency (US EPA) regulations for CO_2 injection wells. A detailed review of the monitoring program for the wells and surface equipment is provided in the Testing and Monitoring Plan.

The operation of all site wells includes continuous monitoring of injection flow rate, injection pressure, injection temperature, and annulus pressure using electronic temperature sensors at the wellhead, downhole temperature gauges near the packer, and the DTS fiber-optic system along the wellbore, with all measurements collected through the SCADA system and archived on digital drives and/or backup charts. Since the injection facility will operate 24 hours a day, 7 days a week, it will be continuously staffed by trained operators for injection well operations.

For the purposes of developing the injection modeling, a maximum surface top-hole pressure of 2,498 psia was used. The maximum surface injection pressure will be based on actual site conditions but will not exceed 90% of the fracture pressure.

A mechanical integrity testing program for each injection well will be implemented in accordance with the Testing and Monitoring Plan.

Operational Constraints – Maximum Allowable Surface Pressure

For purposes of injection modeling only, an assumed annulus pressure of 2,498 psia was used as an input parameter. Operational annulus pressure alarm and shutdown setpoints are implemented in SCADA in accordance with the Testing & Monitoring Plan (Table 15) and QASP (Table 11); those approved setpoints govern operational response triggers.. The proposed maximum surface injection pressures are based on the minimum operating pressure of the planned pipeline transporting CO_2 from the OES CO_2 compression facility to the injection wells. The outlet pressure of the compression facility (i.e., inlet pressure of the CO_2 pipeline) is designed to range between 2,250 psig and 2,300 psig. The pipeline is designed to maintain a minimum outlet pressure of 2,200 psi to ensure CO_2 is injected as a dense fluid (liquid or supercritical). The maximum surface injection pressure of the injection wells will range between 1700 psig and 2200 psig. Compression facility and pipeline design documents are available if needed.

The procedures are described in the Pre-Operational Testing Plan and includes:

- Conduct fall-off testing and injectivity testing
- Used these test results to calculate the maximum allowable injection pressure for each well.

The maximum (surface) injection pressure will not exceed 90% of the fracture pressure.

Operational Contingency Plans

Contingency plans will be in place to identify situations where potential plant and/or process upset conditions may occur and take appropriate measures which are protective to the local area and the environment by shutting in the wells and monitoring their pressure falloff. Operational contingency plans for all One Earth Sequestration, LLC injection wells include potential downtime periods when annual injection well testing, maintenance, well service, and stimulation occur. These plans include the following:

- Annual testing
- Monitoring downhole and on surface

With three permitted injection wells, two wells would normally be operational while one well is tested or serviced for maintenance.

The availability of multiple wells and adhering to proper operations practices, including regular well maintenance and service, will reduce most injection well down-time and should eliminate the unlikely occurrence of one or more wells being simultaneously unavailable for use. In the unlikely event that all wells are temporarily unavailable or are out of commission, the CO_2 from the One Earth Energy ethanol production will be vented to the atmosphere for that limited period until operations and injectivity is re-established. Delivery of CO_2 from other sources would be suspended. Additional detailed monitoring, and other contingency planning for potential events that may occur during well injection operations are provided in Testing and Monitoring Plan and in the Emergency and Remedial Response Plan.

Proposed Carbon Dioxide Stream [40 CFR 146.82(a)(7)(iii) and (iv)]

The One Earth Energy (OEE) CO_2 Capture Facility Feed Study and Class 4 Cost Estimate Final Report (Trimeric, 2022) provided the basis for the following discussion. The OEE plant in Gibson

City, Ford County Illinois makes ethanol through a corn fermentation process. For this project, the maximum ethanol production rate for this facility is 160 million gallons per year (MMgal/yr). Yeast ferments the corn mash to produce ethanol and produces carbon dioxide (CO_2) as a by-product at the same time. The CO_2 bubbles out of the mash and flows through a packed bed water scrubber to remove volatile organic compounds before the gas vents to the atmosphere. CO_2 will be captured after it has passed through the existing scrubber.

The nominal CO_2 production rate from the ethanol facility is estimated at 458,000 tonne (metric tons) per year based on 160 MMgal/yr of ethanol production. This is 1,290 tonne/day of CO_2 product based on operating 355 days/year. The nominal CO_2 feed gas rate entering the surface facilities (capture plant) is 25.6 MMSCFD.

Clarification of CO_2 Production vs. Injection Capacity

The 1,290 tonnes/day value reflects the CO_2 generated from fermentation at the One Earth Energy ethanol facility at the time of application. The larger injection rate of approximately 4,110 tonnes/day per well in Narrative Table 16 represents the total hub-scale injection capacity of the OES geologic storage site. The OES project is designed as a regional CO_2 storage hub, receiving:

- ~1,290 tonnes/day from the One Earth Energy plant, and
- up to ~2,820 tonnes/day from additional regional industrial sources.

As additional CO_2 sources are connected, total injected volumes across the three wells may reach the full permitted capacity of approximately 4.5 million tonnes per year.

The OES plant captures CO_2 from the ethanol facility and conditions it for pipeline sequestration through a series of compression, cooling, and dehydration steps. CO_2 vapor first enters the blower system, which increases suction pressure for the downstream screw compressors; the gas exits the blower at about 310°F, is cooled to 110°F in the desuperheater, and condensed water is removed in the precooler separator. Four parallel screw compressors (C-1 through C-4) then raise the pressure to 205 psig, heating the gas to roughly 200°F before it passes through the dryer beds and MS carbon dust filter (F-6) to remove moisture and particulates. The dried CO_2 flows to the reciprocating compressor (C-5), where the second stage boosts pressure to approximately 1,020–1,040 psig, followed by cooling in a desuperheater and final compression in the third stage to 2,250–2,500 psig. After cooling in the CO_2 aftercooler to about 105°F (adjustable by throttling cooling water), the CO_2 stream is ready for pipeline transport with a final moisture content of 0.732 ppmv.

The CO_2 capture facility will compress and dehydrate the feed gas to the conditions shown in Table 18. No contaminants beyond water vapor will be removed from the CO_2 other than any trace contaminants (such as trace alcohol species) that condense in the compression and cooling steps and are removed with the condensed water in the separators (compressor suction scrubbers). Proposed operational conditions for each injection well are shown in Table 16.

Table 18. *Injectate conditions*

CO_2 Product Specifications	
CO_2 Product Pressure (psig)	1,515
CO_2 Product Temperature (°F)	< 120 °F
CO_2 Moisture Content (lb/MMSCF) (ppmv)	≤ 10 lb/MMSCF (≤ 221 ppmv)

Source: *Salof CO_2 compression design basis (HMB Design CO_2, REV03) and OEE FEED process data (treated moisture limit: 221 ppmv).*

Moisture Specification Update

The <633 ppmv value reported in the original Narrative (Table 18) was a FEED-stage estimate based on preliminary dehydration assumptions. These preliminary values pre-dated the final Salof CO_2 compression and dehydration design and were conservatively high relative to expected operating conditions. The completed Salof Heat & Material Balance (HMB Design CO_2, Rev. 03) demonstrates that the treated CO_2 stream achieves an outlet moisture content of 0.723 ppmv. For regulatory and design purposes, this performance is expressed using the industry-standard dryness specification of ≤10 lb/MMscf, equivalent to approximately 211–221 ppmv, which is the threshold used for Class VI corrosion control and materials compatibility evaluations.

This engineered specification has been incorporated into the OES #1 Construction Plan and supersedes the earlier FEED placeholder. To ensure consistency across the Class VI application:

- Narrative Table 18 now reports the correct moisture specification of ≤10 lb/MMscf (~221 ppmv).
- A citation to the Salof HMB (Rev. 03) and Construction Plan design basis has been added as the source of the final moisture specification.

This update aligns the Narrative and Injection Well Plan with the final dehydration design and satisfies the injectate characterization requirements of 40 C.F.R. § 146.90(a). The proposed operational conditions are summarized in Table 19.

Table 19. *Proposed operational conditions.*

Parameters/Conditions	Limit or Permitted Value			Unit
	OES#1	OES#2	OES#3	
Maximum Injection Pressure				
Surface	1,710	1,850	1,825	psig
Downhole	3,780	3,962	3,932	psia
Average Injection Pressure				
Surface	1,130	1,160	1,160	psig
Downhole	3,161	3,181	2,137	psia
Maximum Injection Rate	4,225	4,225	4,225	Tonne/day
Average Injection Rate	4,110	4,110	4,110	Tonne/day
Maximum Injection Volume and/or Mass	30	30	30	Mt
Average Injection Volume and/or Mass	30	30	30	Mt
Average Annulus Pressure	1,230	1,260	1,260	psia
Annulus Pressure/Tubing Differential (minimum positive pressure differential between the annulus and the injection string)	100	100	100	psia

Testing and Monitoring

The Testing and Monitoring Plan describes how One Earth Sequestration, LLC will monitor the One Earth Sequestration, LLC site pursuant to 40 CFR 146.90. The data acquired by the monitoring and testing procedures will be used to demonstrate that injection wells are operating as planned, that the carbon dioxide plume and pressure front are evolving as predicted, and that there is no endangerment to underground sources of drinking water (USDW). Additionally, the monitoring and testing data will be used to validate and refine geological models and simulations used to forecast the distribution of the CO_2 within the storage zone, support AoR re-evaluations, and to demonstrate non-endangerment. Results of the testing and monitoring activities may trigger action according to the Emergency and Remedial Response Plan.

The Testing and Monitoring Plan will utilize direct and indirect monitoring technologies that will monitor:

- Injectate composition to demonstrate that it is consistent with the permit 40 CFR 146.90(a)
- Corrosion of well materials and components (40 CFR 146.90(c))
- To determine whether CO_2 or brine has migrated Above the Confining Zone (ACZ) (40 CFR 146.90(d))
- USDW groundwater quality (40 CFR 146.95(f)(3)(i))
- Well integrity over the injection phase of the project (40 CFR 146.89(c) and 146.90)
- Near well-bore environment using pressure fall-off testing (40 CFR 146.90(f))
- Injection rates and pressures and development of the CO_2 plume and pressure front in the storage formation over time (40 CFR 146.90(g))

Testing and Monitoring GSDT Submissions
GSDT Module: Project Plan Submissions ***Tab(s):*** Testing and Monitoring tab Please use the checkbox(es) to verify the following information was submitted to the GSDT: ☒ Testing and Monitoring Plan ***[40 CFR 146.82(a)(15) and 146.90]***

Injection Well Plugging

The Injection Well Plugging plan includes schematics and describes how the owner or operator will plug the injection well in accordance with the requirements at 40 CFR 146.92. All casing placed and used in the injection well will be cemented to surface and will not be retrievable at abandonment post-injection. After injection is complete and well pressure has stabilized, and upon approval and concurrence from US EPA, the well will be flushed with brine or fresh water to displace the injectate into the formation. The injection tubing and injection packer will be the only injection equipment remaining in the cased hole. Attempts will be made to remove the injection tubing and packer, however, if the packer cannot be released and/or removed from the cased hole, a wireline tubing cutter will be used to cutoff the tubing above the single packer. A series of balanced cement plugs will be used to fill the entire well with cement for final abandonment.

In order to address newly acquired information following pre-operational testing [40 CFR 146.82(c)(9)], One Earth Sequestration, LLC will submit amendments to US EPA, as needed, for the approved Injection Well Plugging Plan. The revised plan will highlight and explain changes that are needed to address modifications to the well's construction, as documented in the construction specifications or new information about subsurface geochemistry based on the results of pre-operational formation testing and the compatibility of well materials with subsurface fluids and the injectate.

Pending the granting of all approvals for the final plugging program, One Earth Sequestration, LLC will provide, in advance, a completed contact list for reporting to US EPA as part of process to plug and abandon the well and allow US EPA to either witness or oversee operations as needed to ensure compliance.

Injection Well Plugging GSDT Submissions
GSDT Module: Project Plan Submissions ***Tab(s):*** Injection Well Plugging tab Please use the checkbox(es) to verify the following information was submitted to the GSDT: ☒ Injection Well Plugging Plan ***[40 CFR 146.82(a)(16) and 146.92(b)]***

Post-Injection Site Care (PISC) and Site Closure

This Post-Injection Site Care and Site Closure (PISC) plan describes the activities that One Earth Sequestration, LLC will perform to meet the requirements of 40 CFR 146.93. One Earth Sequestration, LLC will monitor ground water quality and track the position of the carbon dioxide plume and pressure front after the end of injection operations. One Earth Sequestration, LLC may not cease post-injection monitoring until a demonstration of non-endangerment of USDWs has been approved by the UIC Program Director pursuant to 40 CFR 146.93(b)(3). Following approval for site closure, One Earth Sequestration, LLC will plug all monitoring wells, restore the site to its original condition, and submit a site closure report and associated documentation.

The PISC plan includes groundwater quality monitoring and plume and pressure front tracking during the post-injection phase. These, along with other activities described in the plan will meet the requirements of 40 CFR 146.93(b)(1). The results of all post-injection phase testing and monitoring will be submitted annually, within 60 days after the anniversary of the date on which injection ceased, as described under "Schedule for Submitting Post-Injection Monitoring Results," in the PISC plan.

A quality assurance and surveillance plan (QASP) for all testing and monitoring activities during the injection and post injection phases is provided in the Appendix to the Testing and Monitoring Plan.

PISC and Site Closure GSDT Submissions
GSDT Module: Project Plan Submissions ***Tab(s):*** PISC and Site Closure tab Please use the checkbox(es) to verify the following information was submitted to the GSDT: ☒ PISC and Site Closure Plan ***[40 CFR 146.82(a)(17) and 146.93(a)]***
GSDT Module: Alternative PISC Timeframe Demonstration ***Tab(s):*** All tabs (only if an alternative PISC timeframe is requested) Please use the checkbox(es) to verify the following information was submitted to the GSDT: ☒ Alternative PISC timeframe demonstration ***[40 CFR 146.82(a)(18) and 146.93(c)]***

Emergency and Remedial Response

The Emergency and Remedial Response (ERRP) plan is provided to meet the requirements of 40 CFR 146.94. The ERRP describes actions the owner/operator (One Earth Sequestration, LLC) will take at the One Earth Sequestration CO_2 storage site in the unlikely event of an emergency within the project Area of Review (AoR) during construction, operation, or post-injection site care. Unexpected events may include unplanned CO_2 release or detection of unexpected CO_2 movement or associated fluids in or from the injection zone. The plan demonstrates how One Earth Sequestration, LLC will comply with 40 CFR 146.94.
This ERRP describes actions that One Earth Sequestration, LLC shall take to address movement of the injection fluid or formation fluid in a manner that may endanger an underground source of drinking water (USDW) during the construction, operation, or post-injection site care periods.

If One Earth Sequestration, LLC obtains evidence that the injected CO_2 stream and/or associated pressure front may cause an endangerment to a USDW, One Earth Sequestration, LLC must perform the following actions:

1. Initiate shutdown plan for the injection well.
2. Take all steps reasonably necessary to identify and characterize any release.
3. Notify the permitting agency (UIC Program Director) of the emergency event within 24 hours.
4. Implement applicable portions of the approved ERRP.

Where the phrase “initiate shutdown plan” is used, the following protocol will be employed: One Earth Sequestration, LLC will immediately cease injection. However, in some circumstances, One Earth Sequestration, LLC will, in consultation with the UIC Program Director, determine whether gradual cessation of injection (using the parameters set forth in the Class VI permit) is appropriate.

If mechanical integrity is lost, the applicant will restore and demonstrate mechanical integrity to the satisfaction of the Director prior to resuming injection.
If mechanical integrity is lost, the applicant will notify the Director when injection can be expected to resume.

Emergency and Remedial Response GSDT Submissions
GSDT Module: Project Plan Submissions ***Tab(s):*** Emergency and Remedial Response tab Please use the checkbox(es) to verify the following information was submitted to the GSDT: ☒ Emergency and Remedial Response Plan ***[40 CFR 146.82(a)(19) and 146.94(a)]***

Injection Depth Waiver and Aquifer Exemption Expansion

No injection depth waivers will be requested in relation to the One Earth Sequestration, LLC project.

Injection Depth Waiver and Aquifer Exemption Expansion GSDT Submissions
GSDT Module: Injection Depth Waivers and Aquifer Exemption Expansions ***Tab(s):*** All applicable tabs Please use the checkbox(es) to verify the following information was submitted to the GSDT: ☐ Injection Depth Waiver supplemental report ***[40 CFR 146.82(d) and 146.95(a)]*** ☐ Aquifer exemption expansion request and data ***[40 CFR 146.4(d) and 144.7(d)]***

References

Abrams, D.B. et al., 2015. Changing Groundwater Levels in the Sandstone Aquifers of Northern Illinois and Southern Wisconsin: Impacts on Available Water Supply Contract Report 2015-02, Illinois State Water Survey, University of Illinois, Champaign, IL.

ASTM International, Standard Test Method for Determination of In-Situ Stress in Rock Using Hydraulic Fracturing Method. 2008: West Conshohocken, PA.

Atkinson, B.K., Subcritical crack growth in geological materials. Journal of Geophysical Research, 1984. 89(B6): p. 4077.

Bauer, R.A., M. Carney, and R.J. Finley, Overview of microseismic response to CO_2 injection into the Mt. Simon saline reservoir at the Illinois Basin-Decatur Project. International Journal of Greenhouse Gas Control, 2016. 54: p. 378-388.

Berger, P. M., Yoksoulian, L., Freiburg, J. T., Butler, S. K., & Roy, W. R. (2019). Carbon sequestration at the Illinois Basin-Decatur Project: experimental results and geochemical simulations of storage. *Environmental Earth Sciences*, *78*(22), 1-10.

Bond, G.D., Nickeson, P.A., Kominz, M.A., 1984. Breakup of a supercontinent between 635 Ma and 555 Ma: New evidence and implications for continental histories. Earth and Planetary Science Letters 70, p. 325-345.

Brown, E. and E. Hoek, Trends in Relationships between Measured In-Situ Stresses and Depth. International Journal of Rock Mechanics and Mining Sciences, 1978. 15: p. 211-215.

Buschbach, T. C., 1964, Cambrian and Ordovician strata of northeastern Illinois: Illinois State Geological Survey Report of Investigations 218, 90 p.

Carman, C. H., C. Blakley, C. Korose, R. A. Locke II, 2019. Illinois Basin – Decatur Project: Soil Carbon Dioxide Flux Monitoring. Circular 599, Illinois State Geological Survey."

Carroll, S., McNab, W., Dai, Z. and Torres, S. (2013) Reactivity of Mt. Simon sandstone and the Eau Claire shale under CO_2 storage conditions. Environ. Sci. Technol. 47, 252-261.

Cartwright, K., 1970, Groundwater discharge in Illinois basin as suggested by temperature anomalies, Water Resour. Res., 6 (3) (1970), pp. 912-918.

Cornet, F.H., Results from the In-Situ Stress Characterization Program, Phase 1: Geomechanical Tests Conducted in the FutureGen Stratigraphic Well (FGA#1). Battelle - Pacific Northwest Division: Richland, WA.

Daniel, R.F., and J.G., Kaldi, 2008. Evaluating seal capacity of caprocks and intraformational barriers for the geosequestration of CO_2. Paper-PESA Eastern Australian Basin Symposium III, Sydney, 14-17 September,2008.

Dávila, G., Dalton, L., Crandall, D.M., Garing, C., Werth, C.J. and Druhan, J.L. (2020) Reactive alteration of a Mt. Simon Sandstone due to CO_2-rich brine displacement. Geochimica et Cosmochimica Acta 271, 227-247.

Denny, F.B., W.J. Nelson, J.R. Breeden, and R.C. Lillie. 2020. Mines in the Illinois Portion of the Illinois-Kentucky Fluorspar District. Illinois State Geological Survey Circular 604, 73 p. and map.

Economides, M. and K. Nolte, Reservoir Stimulation. 2000: Wiley.

E. O. E. B. (n.d.-a). *Cincinnati Arch*. Brittanica. Retrieved June 2, 2023, from https://www.britannica.com/topic/Cincinnati-Arch.

E. O. E. B. (n.d.-b). *Nashville Dome*. Brittanica. Retrieved June 2, 2023, from https://www.britannica.com/place/Nashville-Dome.

Finley, R. (2005). An Assessment of Geological Carbon Sequestration Options in the Illinois Basin: Final Report to the United States Department of Energy, Contract: DE-FC26-03NT41994, 581p.

Fritz, R. D., Morgan, W. A., Longacre, S., Derby, J. R., and Sternbach, C. A., 2012. Introduction. In: J. R. Derby, R. D. Fritz, S. A. Longacre, W. A. Morgan, and C. A. Sternbach (eds.), The Great American carbonate bank: The geology and economic resources of the Cambrian–Ordovician Sauk Mega sequence of Laurentia: AAPG Memoir 98, p. 1-3.

Freiburg, J.T., Holland, M.E., Malone, D.H., and Malone, S.J. 2020. Detrital zircon geochronology of basal Cambrian strata in the deep Illinois Basin, USA: Evidence for the Paleoproterozoic-Cambrian tectonic and sedimentary evolution of central Laurentia. The Journal of Geology 128: 303-317.

Freiburg, J. T., and Leetaru, H.E. 2012, Controls on porosity development and the potential for CO_2 sequestration or wastewater disposal in the Cambrian Potosi Dolomite (Knox Group): Illinois Basin: Presented at the 41st Annual Eastern Section AAPG Meeting, Program Abstracts.

Freiburg, J.T., Leetaru, H.E., and Monson, C.C. 2015. The Argenta Formation: A newly recognized Cambrian stratigraphic unit in the Illinois basin. Geological Society of America Abstracts with Programs, 47(5): 86.

Freiburg, J.T., Morse, D.G., Leetaru, H.E., Hoss, R.P., and Yan, Q., 2014, A Depositional and Diagenetic Characterization of the Mount Simon Sandstone at the Illinois Basin–Decatur Project Carbon Capture and Storage Site, Decatur, Illinois, USA: Illinois State Geological Survey, Prairie Research Institute, University of Illinois, Circular 583, 59 p.

Freiburg, J.T., Ritzi, R.W., and Kehoe K.S., Depositional and diagenetic controls on anomalously high porosity within a deeply buried CO_2 storage reservoir—the Cambrian Mt. Simon Sandstone, Illinois Basin, USA, International Journal Greenhouse Gas Control, 55 (2016), pp. 42-54.

Frommelt, UIC Permic No. UIC-012-ADM, Illinois Environmental Protection Agency, UIC Form 4h, CCS Well #1 Completion Report Revised May 5, 2010, pp. 22. 2010.

Haimson, B.C. and F.H. Cornet, ISRM Suggested Methods for rock stress estimation—Part 3: hydraulic fracturing (HF) and/or hydraulic testing of pre-existing fractures (HTPF). International Journal of Rock Mechanics and Mining Sciences, 2003. 40(7–8): p. 1011-1020

Hangx, S.J.T., Spiers, C.J., 2009. Reaction of plagioclase feldspars with CO_2 under hydrothermal conditions. Chem. Geol. 265, 88–98.

Hansel, A. K., and W. H. Johnson, 1996, Wedron and Mason Groups: Lithostratigraphic reclassification of deposits of the Wisconsin Episode, Lake Michigan Lobe area: Illinois State Geological Survey, Bulletin 104, 116 p.

Hoholick, J.D., Metarko, T., Potter, P.E., 1984, Regional variations of porosity and cement: St. Peter and Mt. Simon Sandstones in Illinois Basin. The American Association of Petroleum Geologists Bulletin. V. 68, No. 6, P. 753-764.

Illinois Department of Natural Resources (IDNR). 1999b. *Upper Sangamon River Area Assessment, Volume 2: Water Resources.* Springfield, IL, 60 p.

Illinois State Geological Survey. *Drift Thickness Map of Illinois*. 2015. Prairie Research Institute, University of Illinois. Drift Thickness Map | Resources | UIUC.

Johnson, W. H., A. K. Hansel, E. A. Bettis, III, P. F. Karrow, G. J. Larson, T. V. Lowell, and A. F. Schneider, 1997, Late Quaternary temporal and event classifications, Great Lakes region, North America: Quaternary Research, v. 47, no. 1, p. 1–12.

Kaszuba, J.P., Navarre-Sitchler, A., Thyne, G., Chopping, C., Meuzelaar, T., 2011. Supercritical carbon dioxide and sulfur in the Madison limestone: a natural analogue in southwest Wyoming for geologic carbon–sulfur co-sequestration. Earth Planet. Sci. Lett. http://dx.doi.org/10.1016/j.epsl.2011.06.033.

Kelly, W.R., Panno, S.V., Hackley, K.C., Hadley, D.R., Mannix D.H.,2018, Paleohydrogeology of a Paleozoic sandstone aquifer within an intracratonic basin: Geochemical and structural controls, Journal of Hydrology, Volume 565, 2018, p 805-818, https://doi.org/10.1016/j.jhydrol.2018.09.004.

Kempton, J.P., W.H. Johnson, P.C. Heigold and K. Cartwright, 1991. Mahomet bedrock valley in east-central Illinois; topography, glacial drift stratigraphy, and hydrogeology. In Geology and Hydrogeology of the Teays -Mahomet Bedrock Valley System, W. N. Melhorn and J. P. Kempton. Boulder, CO, Ge ological Society of America Special Paper 258: 91-124.

Kolata, D. R., 2005, Bedrock geology of Illinois: Illinois State Geological Survey, Illinois Map 14, 1:500,000.

Kolata, D. R. and W. J Nelson, 1990. Tectonic history of the Illinois Basin. In: Leighton, M.W., Kolata, D. R., Oltz, D. F., Eidel, J. J. (eds.), Interior Cratonic Basins. AAPG Memoir 51, p. 263-285.

Kolata, D.R., and W.J. Nelson, 2010, Tectonic history. In D.R. Kolata and C.K. Nimz, eds., Geology of Illinois: Illinois State Geological Survey.

Lasemi, Y. and Z. Askari, 2014, Stratigraphy of the Cambo-Ordovician Knox succession in Illinois: US DOE Knox Project Cooperative Agreement No. DE-FE0002068, Topical Report No. FE0002068-12, 43 p.

Lasemi, Y., Askari Z. 2020. Stratigraphic variability, secondary porosity development, and correlation of the Cambrian Potosi Dolomite across the Illinois Basin. Geological Society of America Abstracts with Programs. Vol 52, No. 6.

Locke, R., Roadcap, G., Stumpf, A., Leetaru, H., Kelly, W., & Winkel, R. (2018). An Introductory Guide to the Mahomet Aquifer and Natural Gas Storage in East-Central Illinois. Prairie Research Institute, Champaign, IL, 18 p

Locke, R., Larssen, D., Salden, W., Patterson, C., Kirksey, J., Iranmanesh, A., Wimmer, B., & Krapac, I., 2013. Preinjection Reservoir Fluid Characterization at a CCS Demonstration Site: Illinois Basin – Decatur Project, USA. Energy Procedia. 37. P. 6424-6433. https://doi.org/10.1016/j.egypro.2013.06.572.

Lund Snee, J.-E. and M.D. Zoback, Multiscale variations of the crustal stress field throughout North America. Nature Communications, 2020. 11(1): p. 1951.

Magnenet, V., F.H. Cornet, and C. Fond, A Nontectonic Origin for the Present-Day Stress Field in the Paris Basin (France). Journal of Geophysical Research: Solid Earth, 2017. 122(11): p. 9313-9327.

McBride, J. H., 1998, Understanding basement tectonics of an interior cratonic basin: southern Illinois Basin, USA, Tectonophysics, Volume 293, Issues 1–2, p. 1-20.

McBride, J., Sargent, M., and Potter, C. (1997). Investigating possible earthquake-related structure beneath the southern Illinois basin from seismic reflection. Seismological Research Letters, 68:641–649.

McBride, John H., and Nelson, W. J. 1999, Style and origin of mid-Carboniferous deformation in the Illinois Basin, USA — Ancestral Rockies deformation? Tectonophysics, Volume 305, p. 249-273.

McClure, M., et al. A Collaborative Study on DFIT Interpretation: Integrating Modeling, Field Data, and Analytical Techniques. in SPE/AAPG/SEG Unconventional Resources Technology Conference. 2019.

Medina, Cristian & Mastalerz, Maria & Lahann, Richard & Rupp, John. (2020). A novel multitechnique approach used in the petrophysical characterization of the Maquoketa Group (Ordovician) in the southeastern portion of the Illinois Basin: Implications for seal efficiency for the geologic sequestration of CO_2. International Journal of Greenhouse Gas Control. 93. 10.1016/j.ijggc.2019.102883.

Medina, C., Rupp, J., Lahann, R., and Eldridge, J. 2019. "Evaluation of Caprock Integrity of the Upper Ordovician Units within the CarbonSAFE Prefeasibility Study Region, Subtask 4.3 – Geological Characterization". United States. https://www.osti.gov/servlets/purl/1524067. Topical report DOE-FE0029445-11.

Miao, X., Z. Lasemi, D.G. Mikulic, and M. Falter, 2016, Directory of Illinois mineral producers, and maps of extraction sites: Illinois State Geological Survey, Circular 584, 52 p.

Morales, R.H. and R.P. Marcinew. Fracturing of High-Permeability Formations: Mechanical Properties Correlations. in SPE Annual Technical Conference and Exhibition. 1993.

Morse, D. G. and Leetaru, H. E. 2005. Reservoir characterization and three-dimensional models of Mt. Simon gas storage fields in the Illinois Basin. *Illinois State Geological Survey Circular* 567.

Nelson, W. J. 1995. *Structural Features in Illinois*. Illinois State Geological Survey Bulletin 100, 144 p.

Nelson, W. J., 2010, Structural features. in D. R. Kolata & C. K. Nimz (eds), Geology of Illinois. Illinois State Geological Survey, pp. 90-104.

Neufelder, R.J., Bowen, B.B., Lahann, R.W., and Rupp, J.A., 2012. Lithologic, mineralogical, and petrophysical characteristics of the Eau Claire Formation: Complexities of a carbon storage system seal. Environmental Geosciences; 19: 81–104.

Panno, S.V., Askari, Z., Kelly, W.R., Parris, T.M. and K.C. Hackley. 2018. Recharge and Groundwater Flow Within an Intracratonic Basin, Midwestern United States. Groundwater, 56: 32-45. https://doi.org/10.1111/gwat.12545.

Panno, S.V., Hackley, K.C., Cartwright, K., Liu., C.L. 1994, Hydrochemistry of the Mahomet Bedrock Valley Aquifer, east-central Illinois: indicators of recharge and ground-water flow, Ground Water, 32 (4) (1994), pp. 591-604.

Piper, J. D. A., 2004. Discussion on "The making and unmaking of a supercontinent: Rodinia revisited" by J.G. Meert and T.H. Torsvik, Tectonophysics 375, p. 261-288. Tectonophysics 383, p. 91-97.

Pitman, J.K., Goldhaber, M.B., Spoetl, C., 1997, Reginal diagenetic patterns in the St. Peter Sandstone: implications for brine migration in the Illinois Basin. U.S. Geological Survey Bulletin 2094-A

Reesink, A.J.H., J.L. Best, J.T. Freiburg, N.D. Webb, C.C. Monson, and R.W. Ritzi. 2020. Interpreting pre-vegetation landscape dynamics: the Cambrian Lower Mount Simon Sandstone, Illinois, U.S.A. Journal of Sedimentary Research 90: 1614-1641.

Roadcap, G. S., Knapp, H. V., Wehrmann, H. A., & Larson, D. R. (2011). Meeting east-central Illinois water needs to 2050: Potential impacts on the Mahomet aquifer and surface reservoirs. Champaign, IL: Illinois State Water Survey Contract Report 2011-08, 188 p. http://hdl.handle.net/2142/39869.

Roadcap, G. S., & Wilson, S. D. (2001). The impact of emergency pumpage at the Decatur wellfields on the Mahomet aquifer: Model review and recommendations. Champaign, IL: Illinois State Water Survey Contract Report 2001-11, 68 p. http://www.sws.uiuc.edu/pubs/pubdetail.asp?CallNumber=ISWS+CR+2001%2D11

Roy, W. R., Mehnert, E., Berger, P. M., Damico, J. R. and Okwen, R. T. 2014. Transport modeling at multiple scales for the Illinois Basin – Decatur Project. Greenhouse Gases Science and Technology 4:645-661. doi:0.1002/ghg.1424.

Sarmadivaleh, A., Al-Yaseri, Z, and Iglauer, S., 2015. Influence of Temperature and Pressure on quartz-water-CO_2 contact angle and CO_2-water interfacial tension. Journal of Colloid and Interface Science, 441, 59-64.

Selkregg, L. F., and J. P. Kempton. 1958, Groundwater geology in east-central Illinois. Illinois State Geological Survey, Circular 248, 36 p.

Shao, H., Freiburg, J.T., Berger, P.M., Taylor, A.H., Cohen, H.F. and Locke, R.A. (2020) Mobilization of trace metals from caprock and formation rocks at the Illinois Basin – Decatur Project demonstration site under geological carbon dioxide sequestration conditions. Chemical Geology 550, 119758.

Shao, H., Kukkadapu, R.K., Krogstad, E.J., Newburn, M.K., Cantrell, K.J., 2014. Mobilization of metals from Eau Claire siltstone and the impact of oxygen under geological carbon dioxide sequestration conditions. Geochim. Cosmochim. Acta 141,
62–82.
Siegel, D.I., 1989. Geochemistry of the Cambrian-Ordovician aquifer system in the northern midwest, United States. Professional Paper 1405-D, U.S. Geological Survey, Reston, VA.

Soller, D. R., Price, S. D., Kempton, J. P., & Berg, R. C. (1999). Three-dimensional geologic maps of Quaternary sediments in east-central Illinois. Reston, VA: United States Geological Survey, Map I-2669. http://pubs.usgs.gov/i-maps/i-2669.

Sone, H. and M.D. Zoback, Time-dependent deformation of shale gas reservoir rocks and its long-term effect on the in-situ state of stress. International Journal of Rock Mechanics and Mining Sciences, 2014. 69: p. 120-132.

Stiff, B. J., and A. K. Hansel, 2004, Quaternary glaciations in Illinois, in J. Ehlers and P. Gibbard, eds., Quaternary glaciations—Extent and chronology, Part II: North America: New York, Elsevier, Developments in Quaternary Science, v. 2, p. 71–82.

Stover, C.W., B.G. Reagor, and S.T. Algermissen, 1979a, Seismicity map of the state of Illinois, U.S. Geological Survey Miscellaneous Field Studies Map, MF-1143.

Stumpf, A. J., & W.S. Dey, (eds.) (2012). Understanding the Mahomet aquifer: Geological, geophysical, and hydrogeological studies in Champaign County and adjacent areas. Champaign, IL: Illinois State Geological Survey, draft report to Illinois American Water, contract no. 2007-02899. http://hdl.handle.net/2142/95787.

Swann, D.H., and Willman, H.B. 1961, Megagroups in Illinois: American Association of Petroleum Geologists Bulletin, v. 45, p. 471-483; Illinois State Geological Survey Reprint 1961-N.

Swanson, B.F., 1981. A simple correlation between permeabilities and mercury capillary pressures. J. Pet. Technol. 33 (12), 2498–2504. https://doi.org/10.2118/8234-PA .

Texas World Operation, INC., 1995. Drilling and Completion Report Well No. 3 Cabot Corporation Tuscola Illinois. March 1995.

Thiercelin, M.J. and R.A. Plumb, A Core-Based Prediction of Lithologic Stress Contrasts in East Texas Formations. SPE Formation Evaluation, 1994. 9(4).

U.S. Environmental Protection Agency. (2015). Sole Source Aquifer designation of the Mahomet Aquifer System in east-central Illinois: Washington, DC, U.S. Environmental Protection Agency, Federal Register, 80(53), 14370–14371. https://federalregister.gov/a/2015-06365.

United States Geological Survey (USGS), 2020. Introduction to the National Seismic Hazard Maps: Frequency of Damaging Earthquake Shaking Around the U.S. (map). Retrieved from https://earthquake.usgs.gov/hazards/learn.

Willman, H. B., and J. C. Frye, 1970, Pleistocene stratigraphy of Illinois: Illinois State Geological Survey, Bulletin 94, 204 p.

Wilson, J. T. (2011). Water-Quality Assessment of the Cambrian-Ordovician Aquifer System in the Northern Midwest, United States (Scientific Investigations Report No. 2011–5229) (p. 154). Reston, VA: U.S. Geological Survey.

Wood, H.O., and F. Neumann, 1931, Modified Mercalli Intensity Scale of 1931: Bulletin of Seismological Society of America, v. 21. P. 278-283

Yielding, G., 2002, Shale gouge ratio--calibration by geohistory. in Koestler, A.G., Hunsdale, R. (Eds.), Hydrocarbon Seal Quantification, vol. 11. Norwegian Petroleum Society (NPF) Special Publications, Amsterdam, pp. 1–15.

Yoksoulian, L., Berger, P.M., Freiburg, J.T., and Butler, S.M, 2014. Geochemical investigations of CO_2-Brine-rock interactions of the Knox Group in the Illinois Basin, U.S. Department of Energy, Topical Report DOE/FE0002068-10, 58p.

Zhu, J., Parris, T. M., Bowersox, J. R., and Harris, D. C., 2013. Modeling CO_2–brine–rock interactions in the Knox Group: Implications of a deep carbon storage field test in western Kentucky, Applied Geochemistry, Volume 37, October 2013, Pages 29-42, ISSN 0883-2927, http://dx.doi.org/10.1016/j.apgeochem.2013.07.007.

Zoback, M.D., et al., Determination of stress orientation and magnitude in deep wells. International Journal of Rock Mechanics and Mining Sciences, 2003. 40(7-8).